Biochemical and Crystallographic Studies of the Escherichia Coli ß-Barrel Assembly Machine

Biochemical and Crystallographic Studies of the *Escherichia coli* β-Barrel Assembly Machine

A dissertation presented

by

David Westwood

to

The Department of Chemistry and Chemical Biology

in partial fulfillment of the requirements

for the degree of

Doctor of Philosophy

in the subject of

Chemistry

Harvard University

Cambridge, Massachusetts

July 2016

Dissertation advisor: Professor Daniel Kahne David Butler Westwood

Biochemical and Crystallographic Studies of the *Escherichia coli* β-barrel Assembly Machine

Abstract

Bacteria have developed resistance mechanisms to every class of antibiotics that has been created and combating the rise of multidrug-resistant bacteria—a major threat to public health—requires the continual development of novel antibacterial agents. Gram-negative bacteria are particularly difficult to target due to their dual-membrane cell envelope and highly impermeable outer membrane. Essential proteins at or near the cell surface of bacteria are therefore potential targets for novel antibiotic development. We sought to probe the mechanisms and structural details of two such essential bacterial proteins: the β-barrel assembly machine (Bam) of *Escherichia coli* and penicillin-binding protein 2 (PBP2) of *Staphylococcus aureus*.

Bam is a highly conserved five-protein complex that is situated in the outer membranes of Gram-negative bacteria, mitochondria, and chloroplasts. In *E. coli* the Bam complex performs the essential function of folding and inserting transmembrane β-barrel proteins into the cell's outer membrane. In Chapter 2, biochemical assays aimed at elucidating the process by which outer membrane proteins are delivered to Bam are described. We reconstituted the Bam complex and subcomplexes in vitro to examine the role of chaperone proteins in delivering unfolded outer membrane proteins to Bam. We demonstrated that two β-barrel protein substrates with large soluble periplasmic domains have the ability to fold on the complex independent of a chaperone.

In vitro biochemical experiments with the Bam complex cannot provide atomic-level mechanistic insight into how the complex binds, folds, and inserts transmembrane β-barrels into

the outer membrane. In Chapter 3, efforts toward obtaining a crystal structure of Bam are described. Structures of the five Bam proteins had been solved individually, but the structure of the Bam complex or a Bam subcomplex had not been reported. We successfully crystallized Bam subcomplexes and made progress toward obtaining a crystal structure of this macromolecular machine.

In Chapter 4, we report the use of a fluorescence displacement assay to identity putative small molecule inhibitors of the *S. aureus* PBP2 protein. PBP2 catalyzes the essential transglycosylation and transpeptidation steps in the synthesis of the bacterial cell wall and is therefore an attractive target for novel antibiotics. We report progress toward the cocrystallization of PBP2 with inhibitors identified using the fluorescence displacement assay.

Acknowledgements

There are many people without whom this work would have been impossible. I first want to thank my graduate advisor, Dan Kahne, for welcoming me into the lab and for fostering a healthy lab environment. His ability to open up to his students and his ability to get students to open up to him makes him a valuable mentor in all things, not only science. Your patience, tolerance, and optimism, even in the face of poor data, kept me going.

Thanks to the faculty who helped me enormously as I learned about the field of crystallography: my thesis committee members Drs. Stephen Harrison and Rachelle Gaudet, Dr. Catherine Drennan at MIT, and Dr. Jue Chen at Rockefeller. Every conversation about crystallography that we had gave me new paths to explore, be it new conditions to screen or new ways to handle my data.

Dr. Simon Jenni, Dr. Michael Oldham, and Dr. Michael Lazarus selflessly spent hours poring over my data in attempts to squeeze an additional tenth of an angstrom more resolution out of poor datasets or to think of paths toward completing a structure. I am also grateful to Lukas Bane for maintaining the crystallography infrastructure on the Cambridge campus and providing company while on trips to the beamline.

Thanks to Goran Malojcic, John Janetzko, and Mike Lazarus, for taking the time to show me how to set up crystal trays, pick crystals, shoot crystals, etc. Thanks especially to John, who for the last four or so years has handled all beamline scheduling on behalf of our lab and who took care of me at APS when I came down with the flu. To Christine Hagan and Suguru Okuda, thanks for carrying out the initial screening of the Bam complex and for introducing me to the system when I was a rotation student. And thanks to Tristan Owens, David Sherman, and Janine May, with

whom I was able to commiserate about the foibles of graduate school and the fickleness of crystallography.

I want to thank the Kahne lab as a whole and to take the time to acknowledge that our lab repels horrible people. Across the board, members of the Kahne lab are a helpful, thoughtful bunch. The lab would cease to function and its members would turn sour were it not for the work of Mike Quinn and Helen Corriero, who tirelessly tolerate wily new graduate students, embittered vets, and the scattered ways of the man at the helm.

I would not have made it through graduate school without the invaluable friends that I have made over the last six years. I am grateful to have met Noam Prywes, an incredibly easy person to live with and an incredibly easy person to talk to. As a correspondent, I must say that being able to talk about the three taboos—sex, religion, and politics—with one person is a rarity. Thanks to Kyle Strom, who showed me that chess is just as good of a game as go and whose home-brewed beers have no peer. Thanks to Emily Ricq, whose unerringly optimistic view toward the future serves as a valuable reminder to stay positive. And thanks to my future wife, Carolyn Brotherton, whose candidness, surreal sense of humor, fantastic cooking, and love have made my life orders of magnitude more exciting.

Finally, I want to thank my family. Though your words of encouragement, care packages, and missives came from 3,000 miles away, your influence was always close. To Laura, thanks for showing me what a balanced life looks like, for setting a supreme example for me as we grew up, and for being a friend. To my parents, Janet and Jim, thanks for brining my life into the world, for the unconditional love, and for reinforcing the idea that, no matter what, the glass is always half full.

Table of Contents

Abstract iii

Acknowledgements v

Table of Contents vii

Chapter 1: Introduction 1

1.1: Gram-negative bacteria and antibiotic resistance 2

1.2: Outer membrane biogenesis 4

1.3: Lipoprotein transport 6

1.4: Lipopolysaccharide transport to the OM 7

1.5: Outer membrane protein biogenesis 10

1.5.1: Transmembrane proteins 10

1.5.2: Transporting OMPs to the OM 11

1.5.3: Identification of the Bam complex 15

1.5.4: Structural studies of the Bam complex 17

1.6: References 23

Chapter 2: Reconstituting β-barrel Assembly in Vitro 38

2.1 The power of reconstituting Bam function in vitro 39

2.2: Initial overexpression, purification, and reconstitution of Bam activity 41

2.3: The Bam complex assembles BamA in vitro 42

2.4: The Bam complex assembles OmpA in vitro 44

2.5: Chaperones assist in the assembly of OmpA on Bam subcomplexes 48

2.6: Conclusion 51

2.7: Materials and Methods 52

2.7.1: Materials 52

2.7.2: Plasmid construction 52

2.7.3: Preparation of Competent Cells 54
2.7.4: Overexpression and purification of BamAB-His 54
2.7.5: Overexpression and purification of FLAG-ns-BamA 55
2.7.6: Overexpression and purification of BamCDE-His 56
2.7.7: Reconstruction of BamABCDE-His for biochemical experiments 57
2.7.8: Reconstruction of BamACDE-His for biochemical experiments 58
2.7.9: Preparation of Bam complex proteoliposomes 58
2.7.10: In vitro reconstitution of OMP folding 59
2.7.11: Overexpression and purification of FLAG-OmpA 59
2.7.12: Refolding of OMPs in Detergent 60
2.7.13: Overexpression and purification of His-ns-SurA 60
2.7.14: Overexpression and purification of ns-Skp-His 61
2.8: References 62
Chapter 3: Crystallization of the Bam Complex 66
3.1: Rationale for the crystallization of the Bam complex 67
3.2: Optimization of the purification of the Bam complex 69
3.2.1: Separation of folded from unfolded BamA 70
3.2.2: Purification of POTRA domain truncations of BamA 74
3.2.3: Purification of BamACDE 77
3.3: Screening of BamACDE crystallization conditions 80
3.4: Optimization of BamACDE crystals 85
3.4.1: Optimizing BamACDE crystals grown in ammonium dihydrogen phosphate 87
3.4.2: Optimizing BamACDE crystals grown in pentaerythritol propoxylate 92
3.5: Conclusion 93

3.6: Materials and Methods 96

3.6.1: Materials 96

3.6.2: Plasmid construction 96

3.6.3: Overexpression, purification and refolding of ns-BamA and POTRA truncations of ns-BamA 98

3.6.4: Overexpression and purification of BamCDE-His 99

3.6.5: Reconstruction of BamACDE-His for crystallographic studies 99

3.6.6: Limited proteolysis of the Bam Complex 100

3.6.7: Overexpression and purification of ns-SeMet-BamA 100

3.6.8: Lysine methylation of the Bam complex 101

3.6.9: Preparation of Bam complex bicelles 102

3.6.10: Crystallization 102

3.6.11: Collection and analysis of X-ray diffraction data 103

3.7: References 104

Chapter 4: Cocrystallization of *Staphylococcus aureus* PBP2 with Small Molecule Inhibitors 107

4.1: Introduction 108

4.2: Crystallization of PBP2 with putative PGT inhibitors 111

4.3: Conclusion 117

4.4: Materials and methods 118

4.4.1: Materials 118

4.4.2: Overexpression and purification of PBP2 118

4.4.3: Crystallization 119

4.4.4: Collection and analysis of X-ray diffraction data 120

4.5: References 121

Appendix I: Bam Lipoproteins Assemble BamA in Vitro 124

Chapter 1: Introduction

1.1: Gram-negative bacteria and antibiotic resistance

In 1884, Hans Christian Gram published a novel method for staining bacteria using the dye crystal violet. Although Gram was interested in identifying bacterially-infected lung tissue and not classifying bacteria, his staining technique led to the division of bacteria into two groups: Gram-negative and Gram-positive bacteria.[1] Electron micrographs obtained in the 1960s revealed marked structural differences between these two families of bacteria.[2]

A distinguishing feature of Gram-negative bacteria is the presence of a second lipid bilayer, the outer membrane (OM), which resides exterior to the cell's inner membrane (IM). The IM is a symmetric bilayer composed of phospholipids, while the OM is an asymmetric bilayer. The inner leaflet of the OM consists of phospholipids and the outer leaflet of the OM is composed of lipopolysaccharide (LPS), a hexa-acylated polysaccharide that acts as a permeability barrier, preventing easy access of small molecules into the interior of the cell.[3,4] An aqueous compartment known as the periplasm separates the IM from the OM and contains a thin layer of peptidoglycan (PG), a heavily-crosslinked polymer consisting of sugars and amino acids that is responsible for maintaining the integrity of the cell's shape during osmotic stress. Together, the IM, OM, and periplasm constitute the cell envelope. Gram-positive bacteria, as opposed to Gram-negative bacteria, have a single cell membrane that is composed of phospholipids and a thick, extracellular layer of peptidoglycan. Greater binding of crystal violet to the thick cell wall of Gram-negative bacteria causes the stain to be retained, while the layer of peptidoglycan in Gram-negative bacteria is too thin to retain the dye.[5]

The cell membrane of Gram-positive bacteria and the IM of Gram-negative bacteria contain transmembrane α-helical bundle proteins and membrane-associated lipoproteins, while the OM of Gram-negative bacteria contains membrane-associated lipoproteins and transmembrane β-barrel

proteins. Altogether, these proteins are responsible for the essential functions of maintaining the integrity of the cell's shape, assembling the membrane, transducing signals into the cell, transporting molecules into and out of the cell, and—importantly in the context of this research—folding and assembling transmembrane proteins.

Resistance mechanisms to all classes of clinically useful antibiotics have emerged, often within a decade of an antibiotic's development.[6-11] This arms race between bacteria and chemists requires the continual development of new classes of antibiotics. And while new antibiotics that target Gram-positive bacteria have been developed in recent years, the latest class of antibiotic to treat Gram-negative infections, the quinolones, was developed in the 1960s.[12] Although classifying bacteria based on their response to crystal violet is not a perfect system, understanding the structural differences between Gram-positive and Gram-negative bacteria helps to explain why the Gram-negatives are more resistant than their Gram-positive cousins. The greater number of membranes that separate a Gram-negative cell's exterior from its interior and the presence of LPS in the OM, which, through its extended polysaccharide exterior and its hydrophobic, membrane-bound core, creates a barrier to both hydrophobic and hydrophilic molecules. Additionally, LPS molecules in the OM are bridged with divalent cations, a feature that decreases the fluidity of the OM and reduces the membrane's permeability. Compared to a lipid membrane composed entirely of phospholipids, the outer membrane of Gram-negative bacteria is two orders of magnitude less permeable to small molecules, rendering antibiotics that effectively kill Gram-positive ineffective.[13,14]

Creating variants of existing antibiotics that can circumvent resistance mechanisms and identifying targets for new antibiotics are the two approaches for combating antibiotic resistance. Due to their proximity to the exterior of the cell and the greater ease by which small molecules can access their features, essential components in the outer membrane of Gram-negative bacteria

are well-suited as drug targets. Here, biochemical and structural studies of an essential *E. coli* outer membrane protein (OMP) complex, the β-barrel assembly machine (Bam) are described. The Bam complex is composed of five proteins, BamABCDE, which are responsible for the folding and insertion of transmembrane β-barrel proteins into the outer membrane of Gram-negative bacteria. Chapter 2 describes biochemical experiments that probe the roles of individual Bam proteins and Bam protein subcomplexes in the assembly of OMPs. Chapter 3 describes structural studies of the Bam complex. Finally, chapter 4 describes work toward the cocrystallization of an essential extracellular protein from *Staphylococcus aureus* with small molecule inhibitors. The latter system is outlined in the introduction to chapter 4. This chapter describes outer membrane biogenesis and the role of the Bam complex in the assembly of OMPs.

1.2: Outer membrane biogenesis

The assembly of outer membrane components presents a challenge to Gram-negative cells because there is no energy source in the periplasm, such as ATP, to drive biochemical processes. Instead, energy from the cytoplasm must be used to transport and to assemble lipoproteins, IM proteins (IMPs), OMPs, LPS, phospholipids, and the cell wall. Many of proteins that aid in these transport and assembly processes have been identified and biochemically characterized in recent years.[15-20] IMPs are assembled by a conserved α-helical bundle know as the secretion (Sec) machine, which is also responsible for the secretion of lipoproteins and nascent OMPs into the periplasm. Three pathways are at the heart of OM biogenesis: 1) the localization of lipoproteins (Lol) pathway is responsible for the maturation and transport of lipoproteins in the cell envelope, 2) the lipopolysaccharide transport pathway is responsible for the delivery and insertion of LPS into the OM, and 3) the β-barrel assembly machine carries out the final steps of OMP assembly in the OM (Figure 1.1). Despite progress in identification of the protein machinery involved in these three pathways, the mechanism by which phospholipids reach the OM remains a mystery.

The three pathways involved in OM biogenesis are described in more detail in the proceeding sections.

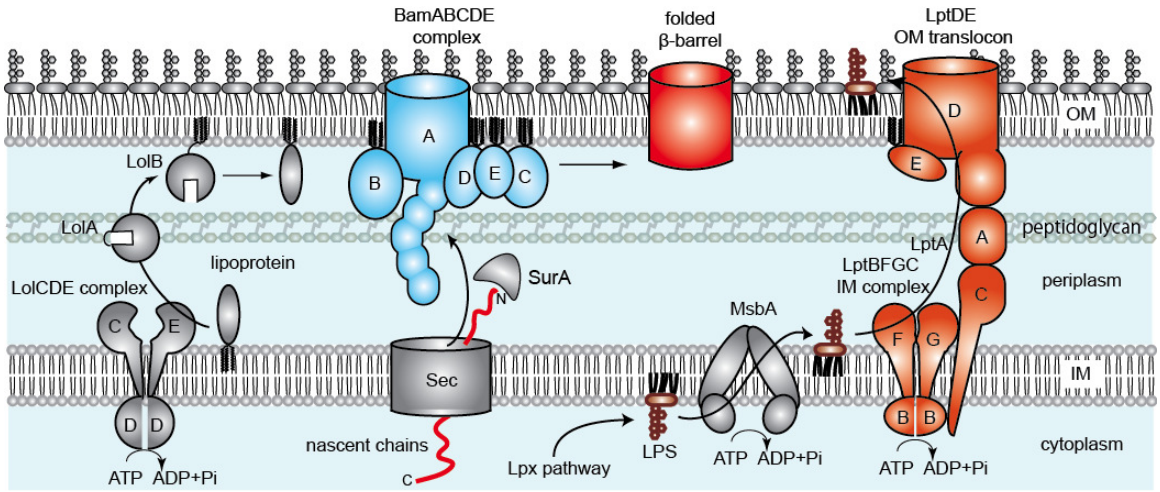

Figure 1.1. Three pathways are responsible for the biogenesis of lipoproteins, OMPs, and lipopolysaccharide. Lipoproteins and OMPs are synthesized ribosomally in the cytoplasm, directed to the cell envelope by an N-terminal signal sequence, and transported in an ATP-dependent fashion into the periplasm. Lipoproteins are lipidated and those destined for the OM are trafficked by LolA and inserted into the OM by LolB. After their transport through Sec, periplasmic chaperones receive nascent OMPs and deliver them to the Bam complex, which folds them and inserts them into the OM. The Lpt pathway transports LPS to the OM. MsbA transports LPS across the IM in an ATP-dependent fashion and the LptBCFG IM complex transfers the LPS to a periplasmic bridge composed of LptA. The outer membrane complex LptDE receives LPS from LptA and inserts it into the outer leaflet of the OM. Figure courtesy of Suguru Okuda.

1.3: Lipoprotein transport

All proteins that reside in the cell envelope—OMPs, IMPs, and soluble periplasmic proteins—are synthesized in the cytoplasm. Trafficking of these proteins to their final locations relies on an N-terminal signal sequence, which directs them to the secretory machinery, Sec. Lipoproteins are distinguished by a lipobox motif that immediately follows the N-terminal secretion signal sequence. Upon secretion into the periplasm, the lipobox motif binds with Lgt, a protein that covalently attaches diacylglycerol moiety to a cysteine residue just C-terminal to the signal sequence. LspA, a peptidase specific to the maturation of lipoproteins, cleaves the signal peptide on the lipoprotein peptidase and the now N-terminal cysteine residue is modified with three fatty acyl tails by the enzyme Lnt.[21,22]

The essential LolABCDE system is responsible for transporting mature lipoproteins from the outer leaflet of the inner membrane to the inner leaflet of the outer membrane. Upon cleavage of the N-terminal signal sequence and the appending of fatty acyl chains to the N-terminal cysteine residue, lipoproteins are ready to be directed to stay in the IM or to be transported to the OM. Lipoproteins that are to remain in the IM and those that are destined for the OM are distinguished by the two residues on the C-terminal side of the triacylated cysteine. In *E. coli*, the primary determinant of IM retention is the residue immediately C-terminal to the N-terminal cysteine.[23,24] Asp is nearly always the amino acid in this position in *E. coli.* The amino acid in the third position determines whether the protein remains in the IM or is directed to the OM. An Asn, Glu, Gln, or Asp residue in this position increases the propensity of the protein to remain in the IM, while a Lys or His in this position direct the lipoprotein to the OM.[25]

Removal of the lipoprotein from the IM is catalyzed in an ATP-dependent fashion by the protein complex LolCDE that form a 1:2:1 complex. LolC and LolE form a transmembrane α-helical heterodimer and the LolD dimer resides in the cytoplasm. LolD contains an ATP-binding

cassette, which is responsible for coupling ATP hydrolysis to the transport of lipoproteins across the periplasm.[26] Lipoproteins that are to be trafficked to the OM are transported via the soluble periplasmic chaperone protein LolA. The transfer of a lipoprotein to LolA is carried out by LolCDE in an ATP-dependent fashion. Transporting lipophilic molecules through the aqueous periplasm presents a challenge for cells, which must shield the fatty acyl tails of OM lipoproteins. The periplasmic protein LolA binds to the hydrophobic tails of transiting lipoproteins, thereby preventing the energetically unfavorable exposure of these tails to water and preventing the aggregation of lipoproteins. Once loaded onto LolA, the lipoprotein makes its way to the outer membrane protein LolB. LolB is a lipoprotein that, like LolA, contains a hydrophobic pocket for binding the acyl tails of a transiting lipoprotein. Finally, LolB releases the transiting lipoprotein into the inner leaflet of the OM. The transfer of a lipoprotein to LolA and the insertion of a lipoprotein into the OM by LolB must be energetically favorable, as there is no energy source in the periplasm.

1.4: Lipopolysaccharide transport to the OM

LPS synthesis occurs in the inner leaftlet on the IM and more than 100 genes are required for its biogenesis.[27] Many of these genes have been identified as viable targets for antibiotics since mature, correctly formed LPS is necessary to maintain the integrity of the OM and to ensure that the OM is impermeable to potentially deadly small molecules.[28] The biosynthetic pathway of LPS has been well studied and almost entirely reconstituted in vitro.[29,30] Once synthesized, the IM transmembrane protein MsbA flips LPS from the inner leaflet of the IM to the outer leaflet of the IM using the hydrolysis of ATP to drive the transport.[31-33] At this stage, LPS is much shorter than the form that is present in the OM upon maturation. O-antigen, a cytotoxic polymer of up to 200 sugars that ultimately presents itself to the cell's exterior, is appended to LPS in the periplasm.[34]

The transport of LPS from the IM to the OM depends on a seven-protein complex, LptABCDEFG, all of which are essential for the viability of *E. coli*. LptBCFG comprise a complex in the IM that is responsible for the initial stages of transport and are present in a 2:1:1:1 ratio. Upon flipping to the outer leaflet of the IM, LPS associates with the single-pass transmembrane protein LptC, which contains a periplasmic C-terminal domain that adopts a β-jellyroll fold, the interior of which shields the hydrophobic regions of LPS from the aqueous periplasm.[35,36] LptB forms a homodimer, which resides in the cytoplasm and contains two nucleotide binding domains at the dimer interface. The LptB dimer binds to the LptFG complex, a transmembrane α-helical dimer, via two coupling helices on LptFG.[37,38]

The energy released from the hydrolysis of ATP by LptB is used to shunt LPS from its binding site on LptC onto a periplasmic bridge composed of multiple molecules of LptA. Like LptC, LptA adopts a β-jellyroll fold to shield hydrophobic regions of LPS during its transit across the periplasm. LptA delivers LPS to the periplasmic, N-terminal domain of the OMP LptD, the C-terminus of which is a transmembrane β-barrel. LptA and LptC belong to the same OstA family as the N-terminal domain of LptD and structural studies of LptD indicate that its N-terminal domain also adopts a β-jellyroll fold.[39,40] Crystal structures of LptA reveal that the protein forms multimeric fibrils, with the β-jellyrolls of one LptA molecule aligning and forming contacts with the β-jellyroll folds of adjacent LptA proteins. These multimers form a continuous hydrophobic tunnel through which LPS makes its way to the OM (Figure 1.2). Creative biochemical assays revealed additional details of the intriguing periplasmic journey of LPS. Photocrosslinking studies by Okuda et al. determined that the Lpt proteins form a transenvelope bridge that connects the IM LptBCFG complex to the OM LptDE complex via LptA.[41] The unnatural amino acid *p*-benzoylphenylalanine (pBPA) was encoded at specific sites within LptA, LptC, and the N-terminal domain of LptD. UV-induced crosslinks formed between LptA and LptC, as well as between LptA and the N-terminal domain of LptD, supporting the model of a transenvelope Lpt

bridge.[42] Using a similar technique, Okuda et al. determined that LPS binds to the hydrophobic cores of LptA, LptC, and the N-terminal domain of LptD. These experiments demonstrated that multiple rounds of ATP hydrolysis by LptB are required for LPS transport onto LptA, suggesting that transit of LPS across the periplasm is driven by enzymatic activity in the cytoplasm. It is believed that LPS is transported in a continuous stream, where the hydrolysis of ATP by LptB pushes LPS through the transenvelope bridge.[35,43]

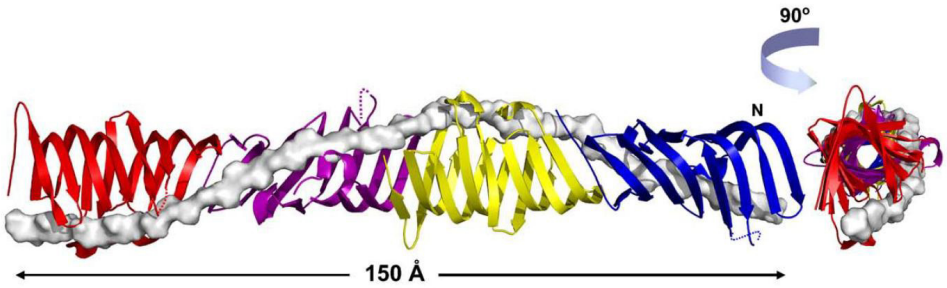

Figure 1.2. The crystal structure of LptA fibrils reveals an end-to-end assembly wherein neighboring β-jellyroll folds align, forming a continuous hydrophobic tunnel that aids in the transit of LPS from the inner membrane to the outer membrane. Figure from ref. 35

The final stage of LPS insertion into the OM is performed by LptDE, a 1:1 heterodimer. LptD is composed of an N-terminal periplasmic domain belonging to the OstA superfamily and that, like LptA and LptC, adopts a β-jellyroll fold. The C-terminal domain of LptD is a transmembrane β-barrel containing 26 anti-parallel β-strands. It is the largest transmembrane β-barrel protein identified to date.[44] LptE is a lipoprotein that is anchored to the inner leaflet of the OM. Proteolysis of purified LptD and LptE showed that LptD protects LptE from degradation, suggesting the LptE acts a plug to the LptD barrel.[45] Site-specific photocrosslinking experiments using pBPA provided more evidence for this hypothesis, with one crosslink forming between LptE and an extracellular loop of LptD.[46] Dong et al. reported the crystal structure of the LptDE complex in 2014, which confirmed this plug and barrel tertiary structure.[44] From this work, the

following mechanism of LPS transport across the periplasm has been proposed: LPS is directly transferred from LptC in the IM to LptA, which transfers LPS to the N-terminal domain of LptD. The LptDE complex then flip LPS to the outer leaflet of the OM without LPS ever entering the inner leaflet of the OM.[47]

1.5: Outer membrane protein biogenesis

The third pathway of cell envelope biogenesis is the synthesis, transport, and assembly of transmembrane β-barrel proteins that reside in the outer membrane. This section addresses common features of all transmembrane proteins, how OMPs are directed to the outer membrane, and past work on the protein complex responsible for folding and inserting OMPs into the outer membrane, the Bam complex.

1.5.1: Transmembrane proteins

In all living organisms, transmembrane proteins adopt either an α-helical bundle structure or a β-barrel structure.[48] Most transmembrane proteins are α-helical bundles, which are present in the cell membranes of eukaryotes and Gram-positive bacteria, as well as the IM of Gram-negative bacteria.[49,50] Transmembrane β-barrels, though less abundant than α-helical bundles, have also been conserved through higher organisms. They are present in the outer membranes of Gram-negative bacteria, chloroplasts, and mitochondria.[48] Just as α-helical bundle proteins are segregated from transmembrane β-barrel proteins, the protein machines that assemble transmembrane proteins are segregated in the cell. The protein machinery responsible for folding and inserting transmembrane α-helical bundles, Sec, is itself an α-helical protein that resides in the IM. Likewise, the protein machinery that carries out the folding and insertion of transmembrane β-barrel proteins is positioned in the membrane into which its substrates ultimately reside, the OM.

In their final, folded forms, the transmembrane regions of integral membrane proteins reside in a hydrophobic lipid bilayer. Exposing any hydrophilic moieties to this lipidic environment would incur a large energetic cost, so the transmembrane domains of integral membrane proteins must sequester polar amino acid side chains and their polar amide backbones from their hydrophobic surroundings. Transmembrane proteins solve the latter problem by forming hydrogen bonds internally along the length of the protein backbone or between distal regions of their transmembrane domains. In the case of α-helical bundle proteins, hydrogen bonds form between nearby residues to form α-helices, which are independently stable and assemble into bundles. In the case of beta-barrel proteins, hydrogen bonds form between distal residues in the form of β-sheets. Only when an extended β-sheet folds back on itself to form a cylinder will all hydrogen bonding partners be satisfied, which introduces a bit of a problem. If a β-barrel were to fold in a hydrophilic environment, the hydrophobic effect would dictate that the barrel would fold inside out, placing hydrophilic residues on the protein's surface. Likewise, a β-barrel cannot be inserted into the membrane unfolded since exposed unsatisfied hydrogen bonds would be too much of an energetic cost. It is therefore believed that the folding and insertion of transmembrane β-barrels is a coordinated process, though the mechanism by white this assembly process takes place has not been fully elucidated.

1.5.2: Transporting OMPs to the OM

All proteins that exist in the periplasmic space, the IM, or the OM, are initially synthesized on ribosomes in the cytoplasm. An N-terminal signal sequence directs these proteins to the secretory machinery, the Sec complex, which resides in the IM and is composed of the proteins SecAYEGDF. The transportation of all IMPs, periplasmic proteins, lipoproteins, and OMPs into the periplasm is performed by the Sec complex in an ATP-dependent fashion and SecA is the ATPase responsible for harnessing the energy of ATP hydrolysis.[51-53] IMPs are co-translationally targeted to the Sec machine via a nucleic acid-protein complex called signal recognition particle

(SRP), which binds to an IMP's signal sequence as it emerges from the ribosome and delivers the IMP-ribosome species to Sec. In contrast, OMPs are targeted to Sec post-translationally. A protein called trigger factor (TF) outcompetes SRP for binding the N-terminal secretion signal sequence and recruits the chaperone protein SecB to the OMP as it emerges from the ribosome.[54-59] SecB, like periplasmic chaperones of hydrophobic proteins, occludes the hydrophobic regions of unfolded OMPs from the cytoplasm.

The final, folded forms of IMPs and OMPs are energetically more stable than their unfolded forms, but the uncatalyzed folding of these proteins proceeds too slowly and is unable to be regulated by cells. Therefore, protein complexes aid in the assembly of transmembrane proteins. After IMPs are targeted to Sec, it is believed that individual α-helices assemble within the core of the transmembrane SecYEG complex, driven by the energy released during protein synthesis on the ribosome.[50,60] The α-helices are then secreted one-by-one into the IM through a lateral gate in Sec, where their hydrophobic exteriors interact more favorably with their hydrophobic surroundings than they would in an aqueous environment.[52] As the α-helices emerge from Sec, it is believed that they assemble with one another into bundles and release themselves from the Sec machinery. This entire process prevents hydrophilic sidechains or the polar backbone of an IMP from being exposed to water at any point in its transport and insertion into the IM.

OMPs are transported through the IM using the energy released from the ATPase activity of SecA.[61] Because they must transit the periplasm and are not assembled until reaching the OM, OMPs are released from Sec in an unfolded state. These proteins must remain in a folding-competent state, they cannot be allowed to misfold in the periplasm, and their aggregation must be prevented as they leave the Sec machinery, so periplasmic chaperone proteins assist in OMP delivery to the OM. Since no ATP is available in the periplasm, the protection of OMPs during their transit must be done in an energy-independent fashion.

Two pathways have been discovered that are responsible for chaperoning OMPs from their emergence from Sec to the OM. SurA, a periplasmic chaperone, is responsible for aiding in the transit of the majority of OMPs, while an alternative pathway involving the chaperones DegP and Skp has been shown to compensate for SurA activity when the gene encoding SurA is knocked out.[62] Two additional periplasmic proteins, FkpA and PpiD, have been implicated in OMP chaperoning as well. However, deletions of these proteins does no result in decreased levels of assembled OMPs, suggesting that their role in chaperoning may be very limited.[63,64]

Four domains comprise SurA, the most important chaperone involved in OMP transport. Its P1 domain and its N- and C-terminal domains form the core of the protein, exhibiting a hydrophobic groove that is believed to be responsible for binding the hydrophobic portions of OMPs. This core of SurA resembles the hydrophobic core of trigger factor, suggesting that the two proteins evolved to recognize similar features of unfolded, hydrophobic transmembrane proteins.[65] SurA's P2 domain is linked to its P1 domain via extended linkers. This domain exhibits peptidyl-prolyl isomerase (PPIase) activity in vitro.[66-69] The predominant OMPs of *E. coli* OmpA, OmpF, LamB, and OmpC, are chaperoned preferentially by SurA. When SurA is deleted from cells, the folded forms of these OMPs is reduced and cells exhibit membrane defects.[68,70]

In addition to the important role played by SurA in OMP transport, several biochemical experiments have implicated an additional protein, Skp, as a chaperone for OMPs, though its role is not fully understood. Skp is a trimeric protein that has been shown to bind unfolded OMPs.[71] In its folded state, the Skp trimer contains a large hydrophobic core large enough to envelop unfolded OMPs.[72] Likewise, Skp has been shown to crosslink to the Sec machinery, suggesting that it plays an early role in the protection of OMPs as they enter the periplasm.[73] Experiments involving the maturation of the OMP EspP have suggested that Skp and SurA collaborate to

transport EspP to the OM. EspP was shown to crosslink to Skp shortly after its emergence from Sec, while crosslinking at later timepoints resulted in an EspP-SurA crosslinked species.[74] Nevertheless, no experiments have been able to show a direct interaction between Skp and SurA.

Like SurA, FkpA exhibits both PPIase and chaperoning activity. Nevertheless, its role in chaperoning unfolded OMPs to the OM has been shown to be much less important for cells than that of SurA.[63,75] The deletion of FkpA by itself does not produce phenotypes consisted with flawed OMP assembly, but when FkpA is deleted in conjunction with SurA and two additional periplasmic chaperones, PpiD and PpiA, cells exhibit a greater sensitivity to antibiotics and do not grow as well as cells with single deletions of these genes. Together, these experiments suggest that FkpA is most relevant when cells are experiencing stress related to the accumulation of unfolded OMPs in the periplasm.

The presence of misfolded or aggregated proteins in the periplasm is toxic to cells, so *E. coli* and other Gram-negative bacteria have evolved stress responses to degrade and to isolate these toxic species. The σ^E stress response is responsible for upregulating the expression of periplasmic chaperones when cell envelope stress develops.[76-79] The expression of DegP, which displays proteolytic activity and chaperoning activity, is enhanced when unfolded proteins in the periplasm cause the cell stress. DegP is hexameric when unbound to an unfolded OMP and adopts a cage-like structure consisting of 12 or 24 monomers when bound to an unfolded OMP.[80,81] Upon entering the cage structure of DegP, an unfolded OMP is quickly degraded, after which the DegP complex disassembles.[82] When in its hexameric form, DegP exhibits no protease activity. Although the protease activity of DegP suggests that the protein would not serve as a good molecular chaperone for unfolded OMPs, cryo-EM studies have shown that an unfolded protein can reside within a DegP 12-mer without being degraded.[81]

1.5.3: Identification of the Bam complex

After OMPs have been chaperoned to the OM, the β-barrel assembly machine, Bam, receives its unfolded substrates, folds them, and inserts them into the OM. The discovery of this complex occurred fairly recently and was in large part delayed due to the historical difficulty of identifying any OMPs. The majority of OMPs were first identified by fractionation experiments—outer membrane fragments were isolated from cells and the most abundant OMPs were identified quite readily. These include OmpA, OmpF, LamB, and OmpC. Less abundant OMPs avoided detection.

When the search for the machinery responsible for the assembly of OMPs in *E. coli* began, only one outer membrane β-barrel protein, LptD, and one lipoprotein, LolB, had been identified as essential components of the OM.[83-85] LptD, which carries out the final step of LPS transport to the OM, was discovered through genetic selections for proteins whose absence caused permeability defects in the outer membrane. Depletion experiments of LptD indicated that it was essential, which implied that the outer membrane protein or protein complex responsible for assembling LptD was also essential.[17,86] Using the nucleotide sequence of Toc75, a transmembrane β-barrel present in the outer membrane of chloroplasts that had been implicated in protein import, a search was performed for homologues in bacteria. A gene in *Neisseria meningitides*, ultimately termed BamA, showed significant homology to Toc75 and was subsequently shown to have a role in transmembrane β-barrel assembly.[87-90] Homology searches for the other chloroplastic membrane proteins implicated in β-barrel protein assembly did not turn up any additional matches in bacteria, suggesting that only BamA has been conserved.

To search for additional proteins involved in the assembly of outer membrane proteins, a strain of *E. coli* expressing a defective copy of LptD was used to elicit mutations in membrane protein assembly-associated genes that would correct the defective LptD.[91-93] Specifically, the cells

expressed the gene *lptD4213*, a variant of the LPS transporter that causes *E. coli* to have a leaky OM. This strain was grown in the presence of small molecule toxins that would kill the cells if they reached their targets in the periplasm. This approach, termed "chemical conditionality" had been used by Jacob and Monod in their studies of the *lac* operon.[94] The result of this work by Ruiz et al. was the identification of a mutation in BamB, an OM lipoprotein, that restored the OM's permeability barrier. Because small molecules can rely on alternative means of entering cells, it is possible to elicit diverse genetic mutations in the components affecting membrane permeability.

The identification of BamB inspired affinity purifications in the hopes of revealing additional factors involved in the assembly of OMPs. BamB was determined not to be essential for *E. coli*, but as stated earlier, it was suspected that an essential protein central to OMP assembly existed. The results of these affinity purifications revealed that BamB associates with the 88.5 kDa outer membrane β-barrel protein BamA, which interacts with the lipoproteins BamC, BamD, and BameE.[18,19,92] Additionally, affinity purifications in which a polyhistidine tag was placed on any one of the five components resulted in pulling down the entire five-protein complex. In addition, the complex can be run on a protein gel using blue native gel electrophoresis without dissociation of the complex.

Depletion experiments showed that BamA and BamD are necessary for cell viability, while single deletions of BamB, BamC, and BamE cause defects in the assembly of OMPs and elicit the σ^E stress response without causing cell death.[19,20,95,96] The essentiality of BamA and BamD suggest that these two proteins are largely responsible for the catalytic activity of the Bam complex. BamB, BamC, and BamE likely play accessory roles, perhaps in the selection of OMPs for assembly or as regulators of OMP assembly, though their in vivo functions are still unclear.

Together, BamABCDE comprise the essential OM complex responsible for transmembrane β-barrel assembly in the OM of Gram-negative bacteria.

1.5.4: Structural studies of the Bam complex

BamA belongs to the Omp85 superfamily of transmembrane β-barrel proteins, a family that includes the BamA homologues present in chloroplasts and mitochondria, as well as β-sheet autotransporters, such as the OMP FhaC. This superfamily is distinguished by the presence of soluble polypeptide transport associated (POTRA) domains and a transmembrane β-barrel domain. In the case of *E. coli* BamA, there are five periplasmic POTRA domains on the protein's N-terminus and a 16-strand β-barrel on the C-terminus. To determine how the four Bam lipoproteins associate with BamA, pull-down experiments were performed using POTRA domain deletions of BamA.[97] These studies showed that BamB associates with POTRA domains P2-5, since deletions of those domains from BamA prevent copurification of BamB. When P5 is deleted from BamA, BamD, BamC, and BamE fail to copurify with BamA, suggesting that the three lipoproteins coordinate with BamA at that site. Single deletions of BamC or BamE do not prevent the copurification of BamD with BamA, but depletion experiments of BamD cause BamC and BamE not to associate with BamA, suggesting that BamD coordinates directly with P5 of BamA and acts as an intermediary in the coordination of BamC and BamE to the complex.[20] POTRA domains 2-5 have been shown to be essential in *E. coli*, but because BamB is nonessential and the other three lipoproteins associate with BamA through P5, POTRA domains 2-4 likely play an essential role in the assembly of OMPs.[97]

Kim et al. published the first two structures of BamA POTRA domains 1-4 that contained a fragment of P5. The structure suggests roles for these domains of BamA in OMP assembly. Each POTRA domain consists of about 75 residues, which are arranged into two anti-parallel α-helices that stack onto a three-stranded β-sheet. Each POTRA domain contains a hydrophobic core at the

interface of the α-helices and β-strand. In the crystal structure, the crystallized fragment of P5 folds back to P3 and extends the three-stranded β-sheet of P3 by an additional β-strand. Kim el al. interpreted this finding as evidence of a possible mechanism of Bam's recognition of OMP substrates, a process that has been termed β-augmentation.[98] This mechanism has been observed in the machinery that senses unfolded OMPs that arise during cell envelope stress.[99] Additionally, both the β-augmentation observed in the BamA POTRA domain crystal structure and the β-augmentation between unfolded OMPs and their sensors rely only on β-sheet secondary structure, with no readily identifiable selection for a specific sequence. This is not surprising in the case of BamA, which is known to handle dozens of OMP substrates. Finally, the two structures published by Kim et al. showed two distinct conformations of the POTRA domains, with one structure displaying a linear arrangement of the POTRA domains and the other exhibiting a pronounced bend in the linker region between P2 and P3. Because the Bam complex likely manipulates its substrates on a large scale—the final β-strand must be coordinated with the first β-strand in order to complete the β-barrel—perhaps this flexible linker in the POTRA domains facilitates large-scale movements of OMPs during the folding process.

More recently, Noinaj et al. published two structures of BamA: one from *Neisseria gonorrhoeae* containing all five POTRA domains and another from *Haemophilus ducreyi* lacking P1-3 (Figure 1.3).[100] The crystal structures showed that the interior of the BamA β-barrel is nearly empty with a volume of ~13,000 $Å^3$. Extracellular loops form a dome-like structure on the extracellular face of BamA in both structures, which may prevent the influx or efflux of small molecules. Though the two structures bear many similarities, they also exhibit several differences. In the *N. gonorrheoaea* structure, P5 sits closer to the BamA β-barrel and interacts with several periplasmic loops, while the three POTRA domains of the *H. decreyi* structure swing away from the β-barrel of BamA. In the latter structure, there are no interactions between P5 and periplasmic loops of BamA. These differences are consistent with the model of OMP assembly via large-scale

motions of the BamA POTRA domains, with particular flexibility in the POTRA domains. Another difference between the two structures is the orientation of a long, extracellular loop L6, which contains a conserved VRGF motif that has been shown to play a role in OMP assembly.[101] In both structures, the L6 loop stretches into the lumen of the BamA β-barrel and interacts with β-strands 14-16 roughly 18 Å away from the periplasmic face of the OM. Mutagenic studies of the VRGF motif indicate that the motif is not essential for β-barrel assembly, but mutations in the loop result in growth defects and fewer colonies than wild-type BamA. Finally, the *H. ducreyi* shows a closed β-barrel with eight hydrogen bonds stabilizing the interaction between strands 1 and 16, where the β-barrel closes. In the *N. gonorrheoaea* structure, on the other hand, the C-terminal β-strand is bent back into the β-barrel, forming only two hydrogen bonds with the N-terminal strand. This is an unprecedented fold and a v-shaped gap created on the periplasmic face where the two strands meet suggests a mechanism whereby β-hairpins of a folding OMP emerge into the OM through a lateral gate in the BamA β-barrel, in a similar fashion to the gating mechanism that has been demonstrated in the Sec machine.

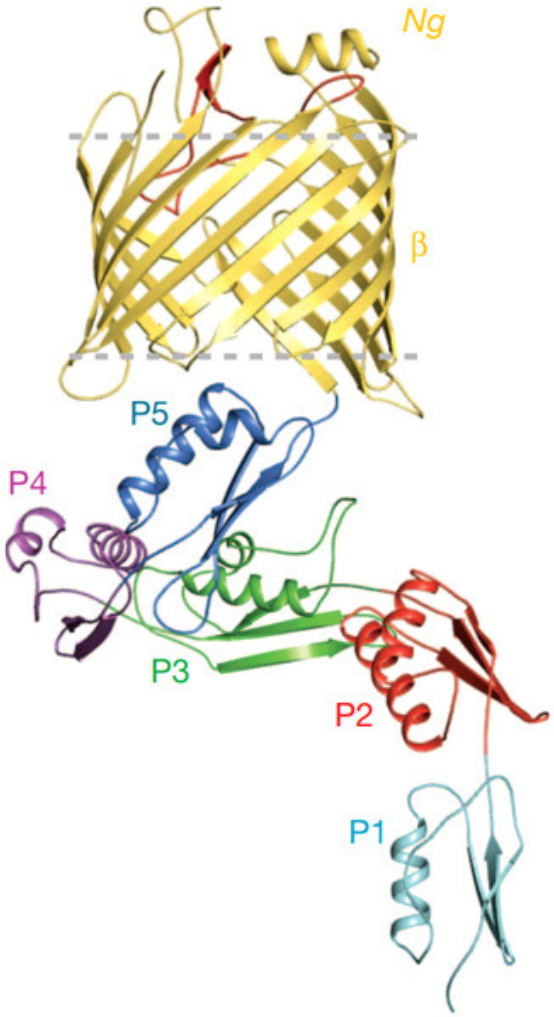

Figure 1.3. The structure of BamA from *N. gonorrheoaea*. POTRA domains 1-5 are labeled P1-5, the β-barrel domain is labeled "β," and the location of the OM is indicated with grey dotted lines. Figure adapted from ref. 100

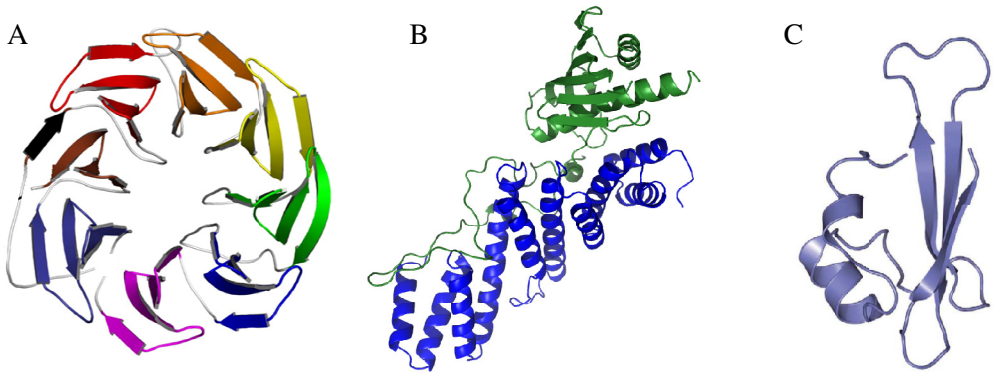

Figure 1.4. A. The structure of BamB is colored blue to red from the N-terminus to the C-terminus. The structure consists of an eight-bladed β-propeller. (pdb: 3prw) **B.** The structures of BamC (green) and BamD (blue) in complex with one another. BamC consists of two globular domains and displays an extended loop that interacts along the length of BamD. BamD consists of five TPR domains, suggesting a role in binding unfolded OMPs. (pdb: 3tgo) **C.** BamE is a globular protein whose role in OMP assembly is poorly understood. (pdb: 2kxx).

X-ray crystal structures of the soluble domains of the four Bam lipoproteins have also been reported, but the individual structures are not particularly informative about the roles of the lipoproteins in OMP assembly (Figure 1.4).[102-104] BamB is a 39.8 kDa, eight-bladed β-propeller, the β-strands of which have been implicated in binding OMPs via β-augmentation.[105-108] Other than those simple features, very little is understood of its role in OMP assembly. Kim et al. reported a crystal structure of BamC, a 34.3 kDa protein, in complex with BamD, a 25.8 kDa protein. The structure revealed that BamC consists of two globular domains and an extended loop that interacts along the length of BamD. BamD consists of ten α-helices that form five tetracopeptide repeats (TPRs).[104,105] TPR domains are implicated in mediating protein-protein interactions and it has been proposed that a pocket formed by the first three TPRs of BamD may

serve as a binding site for unfolded OMPs as they reach the Bam complex. The extended loop of BamC partially occludes this pocket of BamD, which suggests that BamC could play a regulatory role, controlling which substrates interact with BamD. Lastly, BamE is a small globular protein with a mass of 10.3 kDa. In BamE, two α-helices pack against a three-sheet β-strand. Other than these simple features, the role of BamE in OMP assembly is not understood.

While the studies presented in this thesis were being conducted, two crystal structures of the four-protein BamACDE complex were reported by Gu et al. and Bakelar et al.[109,110] These structures demonstrate the orientation that the Bam lipoproteins adopt with respect to the BamA barrel and suggest a model for how OMP assembly occurs in vivo. This structure and its mechanistic implications are discussed more extensively in the concluding remarks of Chapter 3.

1.6: References

1. Austrian, Robert. "The Gram stain and the etiology of lobar pneumonia, an historical note." *Bacteriological reviews* 24.3 (1960): 261.

2. Bladen, Howard A., and Stephan E. Mergenhagen. "Ultrastructure of *Veillonella* and morphological correlation of an outer membrane with particles associated with endotoxic activity." *Journal of bacteriology* 88.5 (1964): 1482-1492.

3. Mühlradt, Peter F., and Jochen R. Golecki. "Asymmetrical distribution and artifactual reorientation of lipopolysaccharide in the outer membrane bilayer of *Salmonella typhimurium*." *European Journal of Biochemistry* 51.2 (1975): 343-352.

4. Kamio, Yoshiyuki, and Hiroshi Nikaido. "Outer membrane of *Salmonella typhimurium*: accessibility of phospholipid head groups to phospholipase c and cyanogen bromide activated dextran in the external medium." *Biochemistry* 15.12 (1976): 2561-2570.

5. Beveridge, Terry J. "Use of the Gram stain in microbiology." *Biotechnic & Histochemistry* 76.3 (2001): 111-118.

6. Boucher, Helen W., et al. "Bad bugs, no drugs: no ESKAPE! An update from the Infectious Diseases Society of America." *Clinical Infectious Diseases* 48.1 (2009): 1-12.

7. Peleg, Anton Y., and David C. Hooper. "Hospital-acquired infections due to gram-negative bacteria." *New England Journal of Medicine* 362.19 (2010): 1804-1813.

8.Taubes, Gary. "The bacteria fight back." *Science* 321.5887 (2008): 356-361.

9. Rice, Louis B. "Federal funding for the study of antimicrobial resistance in nosocomial pathogens: no ESKAPE." *Journal of Infectious Diseases* 197.8 (2008): 1079-1081.

10. Li, Jian, et al. "Colistin: the re-emerging antibiotic for multidrug-resistant Gram-negative bacterial infections." *The Lancet infectious diseases* 6.9 (2006): 589-601.

11. Mauldin, Patrick D., et al. "Attributable hospital cost and length of stay associated with health care-associated infections caused by antibiotic-resistant gram-negative bacteria." *Antimicrobial agents and chemotherapy* 54.1 (2010): 109-115.

12. Lesher, George Y., et al. "1, 8-Naphthyridine derivatives. A new class of chemotherapeutic agents." *Journal of Medicinal Chemistry* 5.5 (1962): 1063-1065.

13. Plesiat, Patrick, and Hiroshi Nikaido. "Outer membranes of Gram-negative bacteria are permeable to steroid probes." *Molecular microbiology* 6.10 (1992): 1323-1333.

14. Plesiat, Patrick, et al. "Use of steroids to monitor alterations in the outer membrane of *Pseudomonas aeruginosa*." *Journal of bacteriology* 179.22 (1997): 7004-7010.

15. Ruiz, Natividad, et al. "Identification of two inner-membrane proteins required for the transport of lipopolysaccharide to the outer membrane of *Escherichia coli*." *Proceedings of the National Academy of Sciences* 105.14 (2008): 5537-5542.

16. Hagan, Christine L., and Daniel Kahne. "The reconstituted *Escherichia coli* Bam complex catalyzes multiple rounds of β-barrel assembly." *Biochemistry* 50.35 (2011): 7444-7446.

17. Wu, Tao, et al. "Identification of a protein complex that assembles lipopolysaccharide in the outer membrane of *Escherichia coli*." *Proceedings of the National Academy of Sciences* 103.31 (2006): 11754-11759.

18. Wu, Tao, et al. "Identification of a multicomponent complex required for outer membrane biogenesis in *Escherichia coli*." *Cell* 121.2 (2005): 235-245.

19. Sklar, Joseph G., et al. "Lipoprotein SmpA is a component of the YaeT complex that assembles outer membrane proteins in *Escherichia coli*." *Proceedings of the National Academy of Sciences* 104.15 (2007): 6400-6405.

20. Malinverni, Juliana C., et al. "YfiO stabilizes the YaeT complex and is essential for outer membrane protein assembly in *Escherichia coli*." *Molecular microbiology* 61.1 (2006): 151-164.

21. Zwizinski, C., and W. Wickner. "Purification and characterization of leader (signal) peptidase from *Escherichia coli*." *Journal of Biological Chemistry* 255.16 (1980): 7973-7977.

22. Tokuda, Hajime. "Biogenesis of outer membranes in Gram-negative bacteria." *Bioscience, biotechnology, and biochemistry* 73.3 (2009): 465-473.

23. Gennity, Joseph M., and M. Inouye. "The protein sequence responsible for lipoprotein membrane localization in *Escherichia coli* exhibits remarkable specificity." *Journal of Biological Chemistry* 266.25 (1991): 16458-16464.

24. Yamaguchi, Kyoji, Fujio Yu, and Masayori Inouye. "A single amino acid determinant of the membrane localization of lipoproteins in *E. coli*." *Cell* 53.3 (1988): 423-432.

25. Terada, Makiko, et al. "Lipoprotein sorting signals evaluated as the LolA-dependent release of lipoproteins from the cytoplasmic membrane of *Escherichia coli*." *Journal of biological chemistry* 276.50 (2001): 47690-47694.

26. Masuda, Kazuhiro, Shin-ichi Matsuyama, and Hajime Tokuda. "Elucidation of the function of lipoprotein-sorting signals that determine membrane localization." *Proceedings of the National Academy of Sciences* 99.11 (2002): 7390-7395.

27. Raetz, Christian RH, et al. "Lipid A modification systems in gram-negative bacteria." *Annual review of biochemistry* 76 (2007): 295.

28. Onishi, H. Russel, et al. "Antibacterial agents that inhibit lipid A biosynthesis." *Science* 274.5289 (1996): 980.

29. Brozek, K. A., Ch E. Bulawa, and C. R. Raetz. "Biosynthesis of lipid A precursors in *Escherichia coli*. A membrane-bound enzyme that transfers a palmitoyl residue from a glycerophospholipid to lipid X." *Journal of Biological Chemistry* 262.11 (1987): 5170-5179.

30. Raetz, Christian RH. "Biochemistry of endotoxins." *Annual review of biochemistry* 59.1 (1990): 129-170.

31. Doerrler, William T., Henry S. Gibbons, and Christian RH Raetz. "MsbA-dependent translocation of lipids across the inner membrane of *Escherichia coli*." *Journal of Biological Chemistry* 279.43 (2004): 45102-45109.

32. Ward, Andrew, et al. "Flexibility in the ABC transporter MsbA: Alternating access with a twist." *Proceedings of the National Academy of Sciences* 104.48 (2007): 19005-19010.

33. Doerrler, William T., and Christian RH Raetz. "ATPase activity of the MsbA lipid flippase of *Escherichia coli*." *Journal of Biological Chemistry* 277.39 (2002): 36697-36705.

34. Abeyrathne, Priyanka D., et al. "Functional characterization of WaaL, a ligase associated with linking O-antigen polysaccharide to the core of *Pseudomonas aeruginosa* lipopolysaccharide." *Journal of bacteriology* 187.9 (2005): 3002-3012.

35. Suits, Michael DL, et al. "Novel structure of the conserved gram-negative lipopolysaccharide transport protein A and mutagenesis analysis." *Journal of molecular biology* 380.3 (2008): 476-488.

36. Tran, An X., Changjiang Dong, and Chris Whitfield. "Structure and functional analysis of LptC, a conserved membrane protein involved in the lipopolysaccharide export pathway in *Escherichia coli*." *Journal of Biological Chemistry* 285.43 (2010): 33529-33539.

37. Gronenberg, Luisa S., and Daniel Kahne. "Development of an activity assay for discovery of inhibitors of lipopolysaccharide transport." *Journal of the American Chemical Society* 132.8 (2010): 2518-2519.

38. Sherman, David J., et al. "Validation of inhibitors of an ABC transporter required to transport lipopolysaccharide to the cell surface in *Escherichia coli*." *Bioorganic & medicinal chemistry* 21.16 (2013): 4846-4851.

39. Polissi, Alessandra, and Paola Sperandeo. "The lipopolysaccharide export pathway in *Escherichia coli*: structure, organization and regulated assembly of the Lpt machinery." *Marine drugs* 12.2 (2014): 1023-1042.

40. Botos, Istvan, et al. "Structural and Functional Characterization of the LPS Transporter LptDE from Gram-Negative Pathogens." *Structure* (2016).

41. Okuda, Suguru, Elizaveta Freinkman, and Daniel Kahne. "Cytoplasmic ATP hydrolysis powers transport of lipopolysaccharide across the periplasm in *E. coli*." *Science* 338.6111 (2012): 1214-1217.

42. Freinkman, Elizaveta, et al. "Regulated assembly of the transenvelope protein complex required for lipopolysaccharide export." *Biochemistry* 51.24 (2012): 4800-4806.

43. Sherman, David J., et al. "Decoupling catalytic activity from biological function of the ATPase that powers lipopolysaccharide transport." *Proceedings of the National Academy of Sciences* 111.13 (2014): 4982-4987.

44. Dong, Haohao, et al. "Structural basis for outer membrane lipopolysaccharide insertion." *Nature* 511.7507 (2014): 52-56.

45. Chng, Shu-Sin, et al. "Characterization of the two-protein complex in *Escherichia coli* responsible for lipopolysaccharide assembly at the outer membrane." *Proceedings of the National Academy of Sciences* 107.12 (2010): 5363-5368.

46. Freinkman, Elizaveta, Shu-Sin Chng, and Daniel Kahne. "The complex that inserts lipopolysaccharide into the bacterial outer membrane forms a two-protein plug-and-barrel." *Proceedings of the National Academy of Sciences* 108.6 (2011): 2486-2491.

47. Bishop, Russell E. "Structural biology: Lipopolysaccharide rolls out the barrel." *Nature* 511.7507 (2014): 37-38.

48. Hagan, Christine L., Thomas J. Silhavy, and Daniel Kahne. "β-Barrel membrane protein assembly by the Bam complex." *Annual review of biochemistry* 80 (2011): 189-210.

49. Rapoport, Tom A. "Protein translocation across the eukaryotic endoplasmic reticulum and bacterial plasma membranes." *Nature* 450.7170 (2007): 663-669.

50. Driessen, Arnold JM, and Nico Nouwen. "Protein translocation across the bacterial cytoplasmic membrane." *Annu. Rev. Biochem.* 77 (2008): 643-667.

51. Heijne, Gunnar. "Signal peptides." *eLS* (1990).

52. Van den Berg, Bert, et al. "X-ray structure of a protein-conducting channel." *Nature* 427.6969 (2004): 36-44.

53. a Nijeholt, Jelger A. Lycklama, and Arnold JM Driessen. "The bacterial Sec-translocase: structure and mechanism." *Phil. Trans. R. Soc. B* 367.1592 (2012): 1016-1028.

54. Ferbitz, Lars, et al. "Trigger factor in complex with the ribosome forms a molecular cradle for nascent proteins." *Nature* 431.7008 (2004): 590-596.

55. Hoffmann, Anja, Bernd Bukau, and Günter Kramer. "Structure and function of the molecular chaperone Trigger Factor." *Biochimica et Biophysica Acta (BBA)-Molecular Cell Research* 1803.6 (2010): 650-661.

56. Valent, Quido A., et al. "Early events in preprotein recognition in *E. coli*: interaction of SRP and trigger factor with nascent polypeptides." *The EMBO journal* 14.22 (1995): 5494.

57. Beck, Konstanze, et al. "Discrimination between SRP-and SecA/SecB-dependent substrates involves selective recognition of nascent chains by SRP and trigger factor." *The EMBO journal* 19.1 (2000): 134-143.

58. Crooke, Elliott, and William Wickner. "Trigger factor: a soluble protein that folds pro-OmpA into a membrane-assembly-competent form." *Proceedings of the National Academy of Sciences* 84.15 (1987): 5216-5220.

59. Valent, Quido A., et al. "Nascent membrane and presecretory proteins synthesized in *Escherichia coli* associate with signal recognition particle and trigger factor." *Molecular microbiology* 25.1 (1997): 53-64.

60. Luirink, Joen, et al. "Biogenesis of inner membrane proteins in *Escherichia coli*." *Annu. Rev. Microbiol.* 59 (2005): 329-355.

61. Zimmer, Jochen, Yunsun Nam, and Tom A. Rapoport. "Structure of a complex of the ATPase SecA and the protein-translocation channel." *Nature* 455.7215 (2008): 936-943.

62. Sklar, Joseph G., et al. "Defining the roles of the periplasmic chaperones SurA, Skp, and DegP in *Escherichia coli*." *Genes & development* 21.19 (2007): 2473-2484.

63. Ramm, Kathrin, and Andreas PluÈckthun. "High enzymatic activity and chaperone function are mechanistically related features of the dimeric *E. coli* peptidyl-prolyl-isomerase FkpA." *Journal of molecular biology* 310.2 (2001): 485-498.

64. Horne, Shelley M., and Kevin D. Young. "*Escherichia coli* and other species of the *Enterobacteriaceae* encode a protein similar to the family of Mip-like FK506-binding proteins." *Archives of microbiology* 163.5 (1995): 357-365.

65. Oh, Eugene, et al. "Selective ribosome profiling reveals the cotranslational chaperone action of trigger factor in vivo." *Cell* 147.6 (2011): 1295-1308.

66. Behrens, Susanne, et al. "The SurA periplasmic PPIase lacking its parvulin domains functions in vivo and has chaperone activity." *The EMBO journal* 20.1-2 (2001): 285-294.

67. Tormo, A., M. Almiron, and R. Kolter. "surA, an *Escherichia coli* gene essential for survival in stationary phase." *Journal of bacteriology* 172.8 (1990): 4339-4347.

68. Lazar, Sara W., and Roberto Kolter. "SurA assists the folding of *Escherichia coli* outer membrane proteins." *Journal of bacteriology* 178.6 (1996): 1770-1773.

69. Bitto, Eduard, and David B. McKay. "Crystallographic structure of SurA, a molecular chaperone that facilitates folding of outer membrane porins." *Structure* 10.11 (2002): 1489-1498.

70. Rouvière, Pierre E., and Carol A. Gross. "SurA, a periplasmic protein with peptidyl-prolyl isomerase activity, participates in the assembly of outer membrane porins." *Genes & development* 10.24 (1996): 3170-3182.

71. Bulieris, Paula V., et al. "Folding and insertion of the outer membrane protein OmpA is assisted by the chaperone Skp and by lipopolysaccharide." *Journal of Biological Chemistry* 278.11 (2003): 9092-9099.

72. Walton, Troy A., and Marcelo C. Sousa. "Crystal structure of Skp, a prefoldin-like chaperone that protects soluble and membrane proteins from aggregation." *Molecular cell* 15.3 (2004): 367-374.

73. Schäfer, Ute, Konstanze Beck, and Matthias Müller. "Skp, a molecular chaperone of gram-negative bacteria, is required for the formation of soluble periplasmic intermediates of outer membrane proteins." *Journal of Biological Chemistry* 274.35 (1999): 24567-24574.

74. Ieva, Raffaele, and Harris D. Bernstein. "Interaction of an autotransporter passenger domain with BamA during its translocation across the bacterial outer membrane." *Proceedings of the National Academy of Sciences* 106.45 (2009): 19120-19125.

75. Saul, F. A., et al. "Structural and functional studies of FkpA from *Escherichia coli*, a cis/trans peptidyl-prolyl isomerase with chaperone activity." *Journal of molecular biology* 335.2 (2004): 595-608.

76. Dartigalongue, Claire, Dominique Missiakas, and Satish Raina. "Characterization of the *Escherichia coli* σ_E Regulon." *Journal of Biological Chemistry* 276.24 (2001): 20866-20875.

77. Rezuchova, Bronislava, et al. "New members of the *Escherichia coli* σ_E regulon identified by a two-plasmid system." *FEMS microbiology letters* 225.1 (2003): 1-7.

78. Rhodius, Virgil A., et al. "Conserved and variable functions of the σ_E stress response in related genomes." *PLOS biol* 4.1 (2005): e2.

79. Kabir, Md Shahinur, et al. "Cell lysis directed by σ_E in early stationary phase and effect of induction of the rpoE gene on global gene expression in *Escherichia coli*." *Microbiology* 151.8 (2005): 2721-2735.

80. Krojer, Tobias, et al. "Crystal structure of DegP (HtrA) reveals a new protease-chaperone machine." *Nature* 416.6879 (2002): 455-459.

81. Krojer, Tobias, et al. "Structural basis for the regulated protease and chaperone function of DegP." *Nature* 453.7197 (2008): 885-890.

82. Kim, Seokhee, Robert A. Grant, and Robert T. Sauer. "Covalent linkage of distinct substrate degrons controls assembly and disassembly of DegP proteolytic cages." *Cell* 145.1 (2011): 67-78.

83. Sampson, Barbara A., Rajeev Misra, and Spencer A. Benson. "Identification and characterization of a new gene of *Escherichia coli* K-12 involved in outer membrane permeability." *Genetics* 122.3 (1989): 491-501.

84. Matsuyama, Shin-ichi, Naoko Yokota, and Hajime Tokuda. "A novel outer membrane lipoprotein, LolB (HemM), involved in the LolA (p20)-dependent localization of lipoproteins to the outer membrane of *Escherichia coli*." *The EMBO journal* 16.23 (1997): 6947-6955.

85. Braun, Martin, and Thomas J. Silhavy. "Imp/OstA is required for cell envelope biogenesis in *Escherichia coli*." *Molecular microbiology* 45.5 (2002): 1289-1302.

86. Bos, Martine P., et al. "Identification of an outer membrane protein required for the transport of lipopolysaccharide to the bacterial cell surface." *Proceedings of the National Academy of Sciences of the United States of America* 101.25 (2004): 9417-9422.

87. Voulhoux, Romé, et al. "Role of a highly conserved bacterial protein in outer membrane protein assembly." *Science* 299.5604 (2003): 262-265.

88. Pardee, Arthur B., François Jacob, and Jacques Monod. "The genetic control and cytoplasmic expression of “inducibility” in the synthesis of β-galactosidase by *E. coli*." *Journal of Molecular Biology* 1.2 (1959): 165-178.

89. Reumann, Sigrun, Jennifer Davila-Aponte, and Kenneth Keegstra. "The evolutionary origin of the protein-translocating channel of chloroplastic envelope membranes: identification of a cyanobacterial homolog." *Proceedings of the National Academy of Sciences* 96.2 (1999): 784-789.

90. Hsu, Shih-Chi, and Kentaro Inoue. "Two evolutionarily conserved essential beta-barrel proteins in the chloroplast outer envelope membrane." *Biosci Trends* 3.5 (2009): 168-178.

91. Eggert, Ulrike S., et al. "Genetic basis for activity differences between vancomycin and glycolipid derivatives of vancomycin." *Science* 294.5541 (2001): 361-364.

92. Ruiz, Natividad, et al. "Chemical conditionality: A geneticstrategy to probe organelle assembly." *Cell* 121.2 (2005): 307-317.

93. Ruiz, Natividad, et al. "Probing the barrier function of the outer membrane with chemical conditionality." *ACS chemical biology* 1.6 (2006): 385-395.

94. Jacob, François, and Jacques Monod. "Genetic repression, allosteric inhibition, and cellular differentiation." *Cytodifferentiation and macromolecular synthesis.* Vol. 21. Academic Press New York, 1963. 30-64.

95. Wu, Tao, et al. "Identification of a multicomponent complex required for outer membrane biogenesis in *Escherichia coli*." *Cell* 121.2 (2005): 235-245.

96. Onufryk, Christina, et al. "Characterization of six lipoproteins in the σ_E regulon." *Journal of bacteriology* 187.13 (2005): 4552-4561.

97. Kim, Seokhee, et al. "Structure and function of an essential component of the outer membrane protein assembly machine." *Science* 317.5840 (2007): 961-964.

98. Harrison, Stephen C. "Peptide–surface association: the case of PDZ and PTB domains." *Cell* 86.3 (1996): 341-343.

99. Walsh, Nathan P., et al. "OMP peptide signals initiate the envelope-stress response by activating DegS protease via relief of inhibition mediated by its PDZ domain." *Cell* 113.1 (2003): 61-71.

100. Noinaj, Nicholas, et al. "Structural insight into the biogenesis of β-barrel membrane proteins." *Nature* 501.7467 (2013): 385-390.

101. Leonard-Rivera, Margaret, and Rajeev Misra. "Conserved residues of the putative L6 loop of *Escherichia coli* BamA play a critical role in the assembly of β-barrel outer membrane proteins, including that of BamA itself." *Journal of bacteriology* 194.17 (2012): 4662-4668.

102. Kim, Kelly H., et al. "Structural characterization of *Escherichia coli* BamE, a lipoprotein component of the β-barrel assembly machinery complex." *Biochemistry* 50.6 (2011): 1081-1090.

103. Kim, Kelly H., and Mark Paetzel. "Crystal structure of *Escherichia coli* BamB, a lipoprotein component of the β-barrel assembly machinery complex." *Journal of molecular biology* 406.5 (2011): 667-678.

104. Kim, Kelly H., Suraaj Aulakh, and Mark Paetzel. "Crystal structure of β-barrel assembly machinery BamCD protein complex." *Journal of Biological Chemistry* 286.45 (2011): 39116-39121.

105. Knowles, Timothy J., et al. "Membrane protein architects: the role of the BAM complex in outer membrane protein assembly." *Nature Reviews Microbiology* 7.3 (2009): 206-214.

106. Danese, Paul N., and Thomas J. Silhavy. "Targeting and assembly of periplasmic and outer-membrane proteins in *Escherichia coli.*" *Annual review of genetics* 32.1 (1998): 59-94.

107. Tokuda, Hajime, and Shin-ichi Matsuyama. "Sorting of lipoproteins to the outer membrane in *E. coli*." *Biochimica et Biophysica Acta (BBA)-Molecular Cell Research* 1693.1 (2004): 5-13.

108. Ruiz, Natividad, Daniel Kahne, and Thomas J. Silhavy. "Advances in understanding bacterial outer-membrane biogenesis." *Nature Reviews Microbiology* 4.1 (2006): 57-66.

109. Bakelar, Jeremy, Susan K. Buchanan, and Nicholas Noinaj. "The structure of the β-barrel assembly machinery complex." *Science* 351.6269 (2016): 180-186.

110. Gu, Yinghong, et al. "Structural basis of outer membrane protein insertion by the BAM complex." *Nature* 531.7592 (2016): 64-69.

Chapter 2: Reconstituting β-barrel Assembly in Vitro

2.1 The power of reconstituting Bam function in vitro

Due to the essentiality of BamA and BamD in the assembly of transmembrane β-barrel proteins, studying the function of the Bam complex in vivo presents challenges. Deletions of either essential component breaks the OMP-folding machine, leading to cell death, while deletions of BamB, C, or E result in impaired OMP assembly and the induction of the σ^E stress response.[1-4] Similarly, in vivo experiments have not been able to elucidate fully the role of periplasmic chaperones in the delivery of OMPs to the OM. SurA has been shown to crosslink BamA in vivo in a BamB-dependent fashion.[5] A SurA and BamB double deletion strain of *E. coli* exhibits severe growth defects and since single deletions of either protein cause similarly reduced rates of OMP assembly, it is presumed that the two proteins may play comparable roles in the pathway.[6] Although it is possible to assess levels of OMP assembly in vivo by fractionating cells and isolating OMPs from the outer membrane, it is not possible to determine the roles of individual Bam components due to the pleiotropic effects of deletions or depletions of any of the Bam proteins. An in vitro reconstitution of OMP assembly by the Bam complex gives the researcher total control over the components in an assembly reaction. Through in vitro reconstitution experiments, it is possible to identify the minimal components of OMP assembly, which in theory could include cell envelope proteins that do not associate stably with any of the five Bam proteins. Additionally, an in vitro reconstitution of Bam activity can be used to probe the roles of individual Bam proteins in the folding and insertion of OMPs.

2.2: Initial overexpression, purification, and reconstitution of Bam activity

The overexpression and purification of BamABCDE was first reported by Kim et al. in 2007.[7] The strategy for obtaining good yields of the complex relied on the knowledge that BamB associates with BamA at a distinct location from that of BamCDE. BamB associates with POTRA domains P2-5 of BamA, and BamC, BamD, and BamE coordinate BamA through P5-BamD interactions.[4] BamA and BamB were expressed in a single strain of *E. coli*, cells were lysed, and

pelleted membrane fractions were dissolved in detergent. A second strain of *E. coli* overexpressed BamCDE-His, which was purified from the OM in the same manner as BamAB. The two solutions of Bam proteins were mixed and a polyhistidine tag on the C-terminus of BamE was used to pull down the whole complex using nickel affinity chromatography. Amino acid contents of the complex were determined quantitatively, indicating that the complex was comprised of BamABCDE in a 1:1:1:1:1 molar ratio. In addition, the complex was shown to form a stable assembly that runs on a blue native electrophoretic gel as a single band.

Acquiring a high yield of Bam proteins from overexpression strains enabled efforts to reconstitute Bam activity in vitro, which was first reported by Hagan et al. in 2010.[8] Prior to Bam's in vitro reconstitution, the minimal components of OMP assembly were unknown. The in vitro reconstitution of Bam had to address several challenges. First, the absence of periplasmic components necessary for Bam activity or the loss of activity upon removing Bam from its native environment could easily prevent any OMP formation at all. Second, the propensity of β-barrels to aggregate in aqueous environment also posed a challenge for the detection of a correctly folded OMP substrate. The in vitro assay for OMP assembly relied on techniques that had been developed to reconstitute the activities of other transmembrane proteins, such as the IM Sec machinery.[9-13] Purified Bam complexes dissolved in detergent micelles were rapidly diluted in the presence of *E. coli* phospholipids, a process that reduces the detergent concentration below its critical micelle concentration and forces the dissolved proteins into phospholipid liposomes.[14] These liposomes were exposed to an unfolded substrate and the Bam complex assembles them into the liposomes. Importantly, the substrate must access the assembly machinery before it aggregates, a problem that was solved by dissolved OMP substrates in an 8 M solution of urea. Alternatively, urea-denatured OMPs could be incubated with a periplasmic chaperone prior to its addition to the proteoliposomes to probe the roles of these chaperone proteins.

The first reported OMP to be assembled using the in vitro reconstitution was OmpT, an enzymatic β-barrel that exhibits proteolytic activity when folded into a membrane (Figure 2.1).[8] OmpT was chosen because even if the majority of the OMP aggregated or failed to fold on Bam, it was possible to detect small amounts of its folded form by virtue of its enzymatic activity. OmpT recognizes peptides that contain several consecutive basic amino acids and a fluorogenic peptide substrate had been developed to monitor OmpT activity.[15] Proteoliposomes containing the full BamABCDE complex or Bam subcomplexes BamAB or BamACDE were prepared. OmpT was preincubated with the periplasmic chaperone SurA, exposed to the proteoliposomes, and OmpT activity was monitored by fluorescence. The experiment showed that OmpT folded on all of the complexes, but when faced with empty liposomes, OmpT self-insertion occurred at a negligible rate. The BamAB complex, perhaps not too surprisingly, folded OmpT at the slowest rate, BamACDE folded the substrate slightly faster, and the full Bam complex assembled OmpT at the greatest rate. In the case of OmpT, the minimal components for successful assembly were thus BamA and SurA. The Bam proteoliposomes were also found to act catalytically by showing a greater extent of OmpT folding when additional amounts of SurA-OmpT were added to the folding reactions, demonstrating turnover. While it is not known what proportion of Bam complexes in the proteoliposomes are active, work with a reconstitution of the Sec machinery showed that roughly 15% of the reconstituted complexes were active.[16]

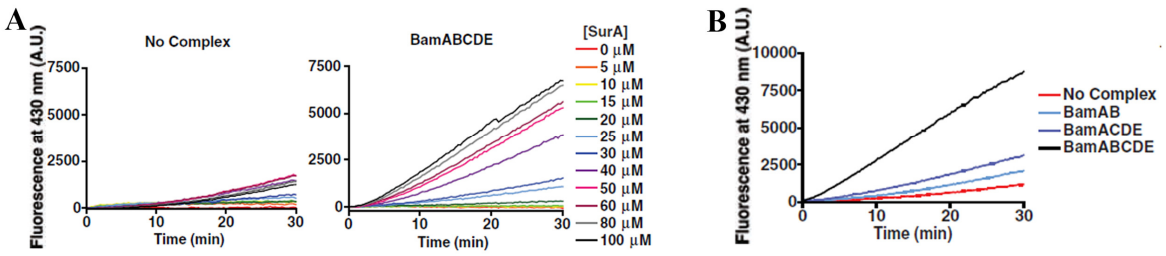

Figure 2.1. OmpT assembly by the Bam complex in vitro. **A.** SurA has a positive effect on OmpT assembly only when the Bam complex is present. **B.** The full Bam complex assembles OmpT much more efficiently than Bam subcomplexes. Figure adapted from ref. 8.

Not all OMPs are enzymes with a well-developed activity assay, so an alternative means of detecting OMPs folded in vitro was desired. Transmembrane β-barrel proteins retain a folded β-barrel in the presence of many denaturants, which allowed for a gel-based folding assay to be developed. Boiling a β-barrel in SDS sample buffer denatures the protein entirely, but SDS by itself cannot disrupt the β-barrel, a property called heat-modifiability. Therefore, semi-native SDS-PAGE allowed for the separation of folded from unfolded forms of an OMP by virtue of their folding state. The folded form of an OMP is more compact than its unfolded form, usually resulting in its faster passage through a polyacrylamide gel. Immunoblotting of refolding reactions allowed for semi-quantitative measurements of the extent of OMP assembly from in vitro folding reactions.

2.3: The Bam complex assembles BamA in vitro

The Bam complex is responsible for the folding of outer membrane β-barrel proteins and because BamA is itself a β-barrel, the complex has the rare property of being a machine that assembles itself. This has been further demonstrated in depletion studies of the Bam complex, which showed that Bam complexes already present in the OM assemble the β-barrels of additional BamA

proteins.[17] The two other dominant machines in *E. coli* that are known to assemble themselves are the secretory machinery of the IM and the ribosome. Although the ribosome has long been understood as a ribozyme, ribosomal proteins are necessary for efficient protein synthesis by interacting with intermediate forms of RNA during polypeptide extension.[18-21] In the case of SecAYEG, the SecA translocon has been specifically implicated in the assembly of transmembrane α-helical proteins.[22] The self-assembly properties of these systems present a chicken and egg problem and raise questions about the first forms of the systems and how they evolved to their current forms. Addressing these questions by studying the proteins' activities in vivo is difficult due to the proteins' essentiality. To study the roles of individual Bam components in BamA assembly, we were therefore interested in reconstituting the assembly of BamA in vitro.

The Bam complex or Bam subcomplexes were incorporated into liposomes and a urea-denatured FLAG-tagged BamA substrate was incubated in 8 M urea, TBS pH 8.0, or 50 μM SurA for ten minutes prior to exposure to the liposomes (Figure 2.2).[23] After 60 minutes, the reactions were quenched with SDS sample buffer and reaction products were separated on semi-native SDS-PAGE. Immunoblotting with α-FLAG-HRP antibodies showed that the BamABCDE, BamAB, and BamACDE complexes successfully fold and assemble BamA, but rely on the substrate remaining in an unfolded, unaggregated folding-competent state. Unlike OmpT, BamA does not require a chaperone to fold in vitro, but incubation of BamA with the periplasmic chaperone SurA or with urea is able to keep BamA in a folding-competent state. Likewise, increased concentrations of SurA did not affect the final levels of folded FLAG-BamA.

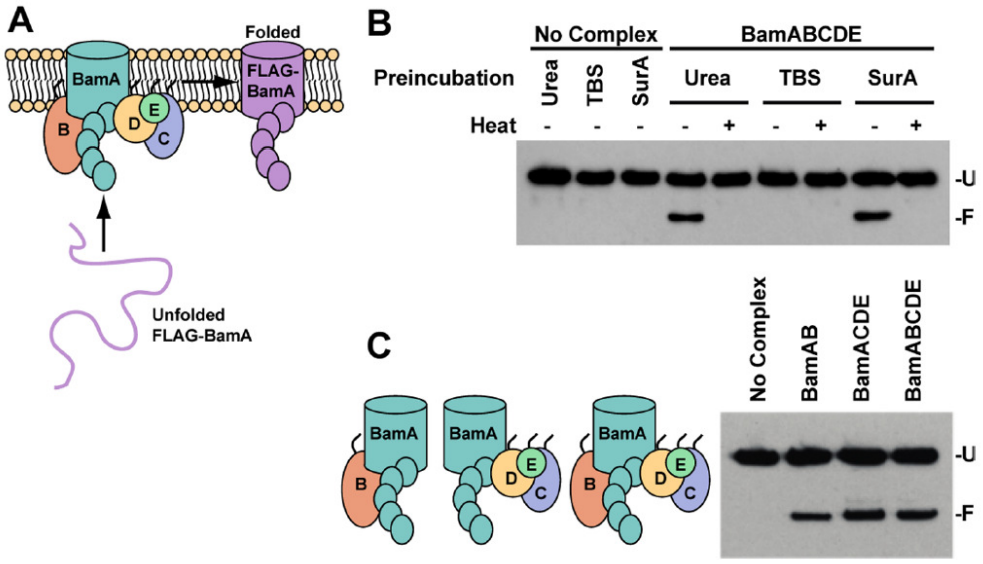

Figure 2.2. The Bam complex assembles BamA in vitro **A.** A schematic overview of the experimental design. Unfolded FLAG-tagged substrate is fed to Bam complexes, which are situated in phospholipid liposomes. **B.** An α-FLAG blot. Urea and SurA equally maintain the folding competency of BamA, while TBS does not. **C.** Bam subcomplexes lacking Bam lipoproteins are able to incorporate BamA into proteoliposomes. (U, unfolded FLAG-BamA; F, folded FLAG-BamA). Figure from ref. 23.

2.4: The Bam complex assembles OmpA in vitro

The result that BamA does not require a molecular chaperone for its assembly in the in vitro reconstitution led us to believe that the periplasmic POTRA domains of BamA could play a role in the protein's assembly. OMPs are secreted into the periplasm from their N- to C-termini, which would could allow the POTRA domains of BamA, which are at the protein's N-terminus, to fold independently as they enter the intermembrane space. We hypothesized that a large soluble domain on BamA or other OMPs could act to shield hydrophobic regions of the OMP from the aqueous periplasm and keep the protein in a folding-competent state. Having reconstituted the assembly of OmpT and BamA, we were also interested in how generalizable the in vitro

reconstitution was to the assembly of other OMPs. There were several types of OMPs to consider: 1) those with and without soluble periplasmic domains; 2) multimeric OMPs, which frequently assemble into trimers in the membrane and could be expected to have different requirements for proper folding and insertion into the OM; and 3) LptDE, which due to its large size and the presence of LptE inside LptD's β-barrel could require a higher degree of Bam protein coordination. Likewise, LptD and BamA are the only essential OMPs, so LptD's assembly pathway is of particular interest.

Two trimetric OMPs, LamB and OmpF, were screened for in vitro assembly, but no folding was observed. This could be due to special requirements of periplasmic components that were not present in the reconstitution or perhaps the high curvature of liposomes, which could interfere with the correct assembly of an OMP trimer.

OmpA, a 35 kDa nonessential outer membrane protein whose biological function is not entirely known was, however, able to fold in the Bam reconstitution (Figure 2.3). OmpA is thought to play a role in maintaining the structure of the outer membrane and acts as the entry site for multiple bacteriophages.[24] More important, it is distinguished by the presence of a large, soluble periplasmic domain at its C terminus 153 amino acids in length. We believed that we could use this substrate as a tool to investigate the result that BamA did not require a chaperone for its in vitro assembly.

Two variants of OmpA were created: an N-terminally FLAG-tagged full length form of the protein and an N-terminally FLAG-tagged truncated form of OmpA lacking its C-terminal periplasmic domain (FLAG-OmpA(23-193)), a construct that consists solely of the protein's β-barrel domain. Both constructs were created without signal sequences and were therefore expressed as inclusion bodies in the cytoplasm of *E. coli*. The inclusion bodies were purified and

dissolved in 8 M urea. β-barrels are able to refold in detergent solutions, which we used as a positive control for folding in reconstitution experiments. For wild-type OmpA, refolding in detergent produced several unexpected bands at 70 and 22 kDa, which may represent a nonbiologically relevant dimeric form of the protein and an alternative, more compact folded form of OmpA, respectively. Boiling of the refolding reactions fully denatured OmpA and showed that the folded form of OmpA runs at the apparent molecular weight of 25 kDa and the unfolded form runs at 35 kDa. In the case of the truncated form of OmpA, the folded form runs at a higher apparent molecular weight than its unfolded form. For experiments involving liposomes, urea-denatured OmpA was added to Bam complex proteoliposomes directly from 8 M urea or was preincubated with TBS pH 8.0 or the periplasmic chaperone proteins Skp, SurA, or FkpA. After sixty minutes, SDS sample buffer was added to the reactions to quench any folding, the samples were run on semi-native SDS-PAGE, and immunoblotting with α-FLAG was used to visualize the extent of folding.

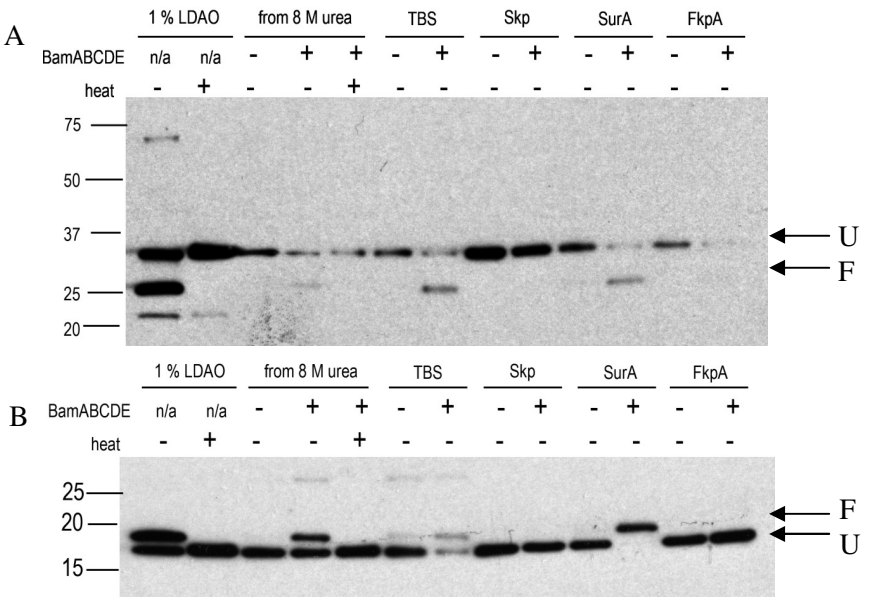

Figure 2.3. The Bam complex refolds OmpA and OmpA lacking its soluble domain in vitro **A.** Wild-type OmpA refolds directly from urea and when preincubated with SurA or TBS, but not when preincubated with Skp or FkpA. **B.** The OmpA β-barrel domain refolds in vitro under the same conditions that lead to wild-type folding in vitro. α-FLAG (U, unfolded OmpA; F, folded OmpA)

These results suggest that when it was preincubated with TBS, enough FLAG-OmpA stayed folding-competent to give rise to a folded band. A similar effect was seen when the substrate was preincubated with SurA. When preincubated with Skp or FkpA, this effect is not seen. This could be due to the chaperone binding too tightly to the substrate, unable to release it to the Bam complex, or the chaperones could somehow be promoting the aggregation of substrate during the preincubation. When the same experiments were done with FLAG-OmpA(23-193), the β-barrel construct of OmpA, we obtained similar results: this construct was folded by the Bam complex with TBS and SurA preincubations, but not when preincubated with Skp or FkpA. Importantly, we observed one striking difference between Bam-mediated folding of the two OmpA constructs.

When the truncated form of the protein is preincubated with SurA, the substrate folded quantitatively, while there was no significant increase in the amount of folding of the wild-type substrate upon preincubation with SurA versus TBS. These observations supported our initial hypothesis that OMPs with large soluble domains have different chaperone requirements than OMPs without periplasmic domains. Deletion of the soluble domain of OmpA led to a folding reaction that was dramatically improved by the addition of chaperones.

2.5: Chaperones assist in the assembly of OmpA on Bam subcomplexes

Based on the result of truncated OmpA folding more readily after a preincubation with SurA, we wondered if these effects translated to its folding on different Bam subcomplexes. Truncated OmpA was added from 8 M urea to different Bam subcomplexes or it was preincubated with a 10-fold molar excess of SurA prior to its introduction to the Bam subcomplexes. Reactions were quenched at 60 minutes (Figure 2.4). As before, some folding of the substrate was observed when it was subjected to the proteoliposomes straight from urea. However, when the substrate was preincubated with SurA, we saw a marked difference in the amount of substrate that gets folded. Whenever BamA was present in the proteoliposomes, SurA greatly increased the amount of substrate that gets folded. The starkest increase in folding occurred in those reactions in which BamAB was present in the proteoliposomes. This result was surprising, as we expected the highest conversion of unfolded to folded OmpA by wild-type BamABCDE proteoliposomes, as had been seen in OmpT and BamA folding reconstitutions. These results suggest that BamC, BamD, and BamE may interfere with the delivery of the OmpA substrate when it is bound to SurA. There is evidence from crosslinking studies that BamA interacts with SurA.[5] Thus, we hypothesize that when BamCDE is removed from the complex, a SurA-bound substrate can more readily access the BamA folding machine.

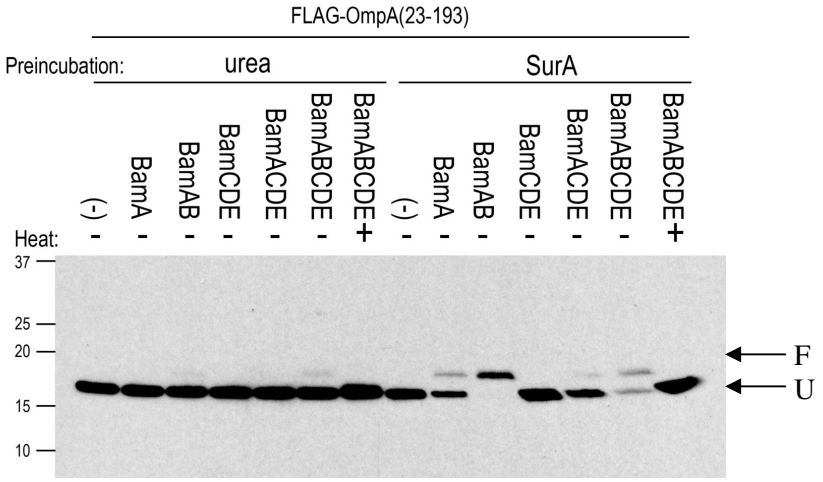

Figure 2.4. The presence of BamA in a proteoliposomes is required for the folding of OmpA's β-barrel domain. Preincubation of OmpA(23-193) with the molecular chaperone SurA drastically increases the extent of refolding in vitro. α-FLAG (U, unfolded OmpA; F, folded OmpA)

To understand how the folding of wild-type OmpA and the β-barrel of OmpA (OmpA(23-193)) proceeds over time, we conducted timecourse experiments using the in vitro reconstitution (Figure 2.5). The two substrates were either preincubated with SurA or pipetted from 8 M urea into empty liposomes or liposomes containing the full BamABCDE complex. A single tube was used for each timecourse (i.e. aliquots were removed from the same reaction mixture at different timepoints) and aliquots were quenched at the desired time points. All samples were run on semi-native SDS-PAGE and analyzed as described above. As expected, we observed no folding of OmpA or the β-barrel domain of OmpA when the folding reactions were performed in the presence of empty phospholipid liposomes.

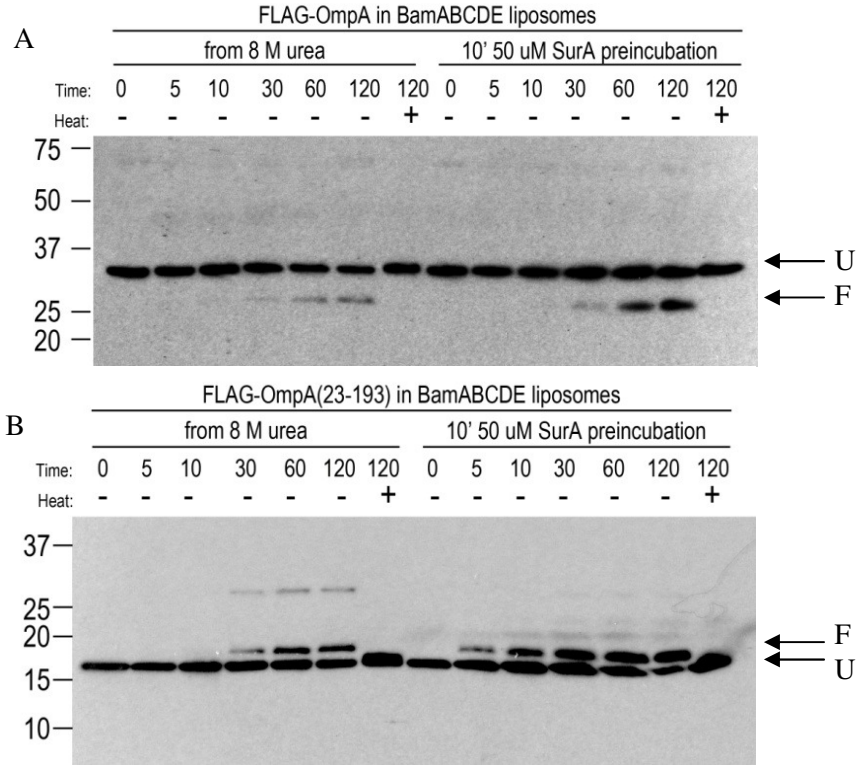

Figure 2.5. The Bam complex assembles the β-barrel domain of OmpA faster than wild-type OmpA **A.** Wild-type OmpA is folded by the Bam complex slightly faster following an incubation with SurA compared to no incubation with the chaperone. **B.** The β-barrel domain of OmpA assembles significantly faster and to a greater extent than wild-type OmpA when it is preincubated with SurA. α-FLAG (U, unfolded OmpA; F, folded OmpA)

As expected based on the results that we obtained in the 60 minute folding reactions (Figures 2.3 and 2.4), wild-type OmpA accumulated over time, but the rate of folding was not significantly increased when the substrate was preincubated with SurA. The first detectable folded material appeared at the 30 minute timepoint independent of OmpA's preincubation with SurA. Conversely, preincubating the β-barrel domain of OmpA with SurA significantly increased the substrate's rate of folding. Like wild-type OmpA, folded β-barrel domain of OmpA was detectable after 30 minutes had elapsed. However, when preincubated with SurA, the folded β-

barrel of OmpA was detected after only five minutes of incubation with the Bam complex. Again, the results with wild-type OmpA suggest a lack of dependence on SurA for proper assembly into membranes, supporting our initial hypothesis that a periplasmic domain can aid in the shuttling of an unfolded substrate to the Bam complex. The faster rate of truncated OmpA folding when preincubated with SurA, relative to the rate of wild-type OmpA without a SurA preincubation suggests that a SurA-bound substrate takes a separate pathway to the Bam complex than a substrate that does not rely on SurA.

2.6: Conclusion

The reconstitution of Bam activity in vitro is a remarkable biochemical tool for investigating the mechanism of OMP assembly. Work with the reconstitution has demonstrated that BamA is the minimal requirement for folding BamA and OmpA and that the presence of BamABCDE in a membrane drastically increases the rate of folding of OMPs compared to background rates of OMP self-assembly. Additionally, these experiments demonstrate that no energy source such as ATP is required for the successful assembly of OMPs, which are assembled in the periplasm where no energy source is present. Likewise, the folding of OmpA in vitro, as demonstrated in this chapter, suggests a role for soluble periplasmic domains in shielding hydrophobic regions of OMPs while they traverse the periplasm. Due to the adaptability of the in vitro assay, the assembly of other OMPs can be explored quite readily using this system. Additions of soluble periplasmic components to reaction mixtures could be used to determine if there are unidentified components necessary for the proper assembly of multimeric OMPs. Ultimately, the readout of the in vitro reconstitution is the presence or absence of a folded substrate and it is so far not possible to track individual assembly steps in vitro. To gain a more detailed understanding of OMP assembly requires a crystal structure of the complex and efforts for obtaining that structure are presented in the next chapter.

2.7: Materials and Methods

2.7.1: Materials

Unless stated otherwise, all chemicals were obtained from Sigma Aldrich and, unless specified otherwise, all cultures were grown in lysogengy broth (LB) obtained from Difco, with antibiotics at a concentration of 50 µg/mL. Cultures were grown in Innova 44 incubators and pelleted using a Beckman Coulter J6-Mi floor centrifuge or a 5810 R desktop centrifuge from Eppendorf. The n-dodecyl-β-D-maltopyranoside (DDM), n-octyl-β-D-glucopyranoside (OG), and lauryldimethylamine-N-oxide (LDAO) were obtained from Anatrace. Ni-NTA resin for protein purifications was obtained from Qiagen. Affinity chromatography was performed in Poly-Prep Chromatography Columns from Bio-Rad. Protein concentrations were determined using a Thermo Scientific NanoDrop 2000 UV/vis spectrometer. Purification of Bam complexes were performed on a GE AKTA Pure FPLC using a Superdex 200 10/30 GL gel filtration column. *E. coli* phospholipids for the formation of proteoliposomes were purchased from Avanti. Proteoliposomes and membrane fractions of lysed cells were pelleted using a Beckman Coulter Optima XE-90 ultracentrifuge. Homogenization of membrane pellets and inclusion bodies was performed using an IKA T18 basic ULTRA-TURRAX homogenizer.

2.7.2: Plasmid construction

Table 2.7.2.1 lists the plasmids that were used in these studies and table 2.7.2.2 lists the primers used to generate the plasmids. Restriction sites and sequence modifications are highlighted by bolding. All genes were amplified from *E. coli* lab strain MC4100.

Table 2.7.2.1. List of plasmids

Name	Description	Construction
pCH103	pET22b-bamA (E22-W810)	PCR with primers: bamA(22-810)-5' and bamA(22-810)-3' and then site directed mutagenesis with primers: bamAstop-5' and bamA-stop-3'
pCH128	pET22b-FLAG-bamA (A21-W810)	Site directed mutagenesis of pCH103 with primers: FLAG-nsbamA-for and FLAG-ns-bamA-rev
pCH024	pET22b-Skp-His_6	PCR with primers: Skp-Nns and Skp-CHis
pSK046	pCDFDuet-bamC-bamD	PCR with primers: bamC-N, bamC-C, bamD-N3, and bamD-C3
pBamE-His	pET22-42-bamE-His_8	As described in Sklar et al.[3]
pSK038	pETDuet-bamB- bamA	PCR with primers: bamB-N, bamB-C, bamA-N, and bamA-C
pSK257	pET28b-His_6-SurA (A21-N428)	PCR with primers: SurA-Nns and SurA-Ce
pSK249	pET22b-ns-OmpA(23-346)	PCR with primers: OmpA-Nns2 and OmpA-Ce2
pDW050	pET22b-FLAG-ns-OmpA(23-346)	Site directed mutagenesis of pSK249 with primers: FLAG-OmpA-N and FLAG-OmpA-C
pDW051	pET22b-FLAG-ns-OmpA(23-193)	Site directed mutagenesis of pDW050 with primers: FLAG-OmpA-trunc-N and FLAG-OmpA-trunc-C

Table 2.7.2.2. List of primers

Name	Sequence
bamA(22-810)-5'	ACCA**CATATG**GAAGGGTTCGTAGTGAAAGATATTCATTTCGA
bamA(22-810)-3'	ATTA**GCGGCCGC**CCAGGTTTTACCGATGTTAAA
bamA-stop-5'	AACATCGGTAAAACCTGG**TAA**GCGGCCG
bamA-stop-3'	GTGCTCGAGTGCGGCCGC**TTA**CCAGGT
FLAG-nsbamA-for	CATATG**GACTACAAAGACGATGACGACAAG**GCTGAAGGGTTCGTAGTG
FLAG-nsbamA-rev	CAGC**CTTGTCGTCATCGTCTTTGTAGTC**CATATGTATATCTCCTTCTT
Skp-Nns	ATGA**CATATG**GCTGACAAAATTGCAATCG
Skp-CHis	ATGA**GCGGCCGC**TTTAACCTGTTTCAGTACG
bamC-N	ACAC**CCATGG**GAGCTTACTCTGTTCAAAAGTCG
bamC-C	ACAC**GCGGCCGC**TTACTTGCTAAACGCAGC
bamD-N3	ACAC**CATATG**ACGCGCATGAAATATCTG
bamD-C3	ACAC**GACGTC**TTATGTATTGCTGCTGTTTGC
bamB-N	ACAC**CCATGG**GACAATTGCGTAAATTACTGCTGC
bamB-C	ACAC**GCGGCCGC**TTAACGTGTAATAGAGTACACGGTTC
bamA-N	GTCCTAGAG**CATATG**GCGATGAAAAAGTTGC
bamA-C	ACAC**GACGTC**TTACCAGGTTTTACCGATGTTAAAC
SurA-Nns	ACAC**CATATG**GCCCCCCAGGTAGTCGATAAAG

SurA-Ce	ACAC**GCGGCCGC**TTAGTTGCTCAGGATTTTAACGTAGG
FLAG-OmpA-N	CATATG**GACTACAAAGACGATGACGACAAG**GCTCCGAAA GATAACACCTGGTAC
FLAG-OmpA-C	AGC**CTTGTCGTCATCGTCTTTGTAGTC**CATATGTATATCTC CTTCTTAAAGTTAAACAAA
FLAG-OmpA-trunc-N	CTACCGTTTCGGTCAG**TAA**GGCGAAGCAGCTCC
FLAG-OmpA-trunc-C	GGAGCTGCTTCGCC**TTA**CTGACCGAAACGGTAG

2.7.3: Preparation of Competent Cells

A 5 mL overnight culture was grown of the desired strain with 50 µg/mL of the required antibiotic added to the culture. The following day, 1 mL of the overnight culture was used to inoculate 100 mL of autoclaved media supplemented with the appropriate antibiotic. This culture was shaken at 37 °C until OD_{600}=0.3, at which point the culture is divided into two ice-cold 50 mL tubes. These tubes were left on ice for 10 minutes and the cells were pelleted at 1,600 g. for 7 minutes at 4 °C. The supernatant was discarded and the pelleted cells were resuspended in 10 mL ice-cold, sterile-filtered 60 mM $CaCl_2$, 15% glycerol, 10 mM PIPES pH 7.0. The cells were spun down for 5 minutes at 1,100 g. at 4 °C, the supernatant discarded, and the cells were resuspended in 10 mL of the ice-cold $CaCl_2$ solution from above. This suspension was kept on ice for 30 minutes and the cells were spun down again at 1,100 g. for 5 minutes at 4 °C. The cells were resuspended in 2 mL of the ice-cold $CaCl_2$ solution and then divided into 250 µL aliquots in ultracentrifuge tubes. These aliquots were immediately flash-frozen in liquid N_2 and stored at -80 °C.

2.7.4: Overexpression and purification of BamAB-His

100 mL 2X YT broth was autoclaved and upon cooling, carbenicillin was added to a concentration of 50 µg/mL. The broth was seeded with BL21(DE3) harboring pSK086 for overnight growth at 37 °C. 6 L of culture was seeded with the overnight culture and shaken at 30 °C until OD_{600}=0.2. The temperature of the incubator was shifted to 25 °C and the culture was grown to OD_{600}=0.6, at which protein expression was induced using IPTG at a concentration of

0.1 mM. The culture was grown for another 3-4 hours, at which point the cells were pelleted for 10 minutes at 5,250 g. at 4 °C. Cell pellets were flash-frozen in liquid N_2 and stored overnight at -80 °C. The following morning, the cell pellet was resuspended in 60 mL 20 mM Tris pH 8.0, 50 µg/mL DNase, 50 µg/mL RNase, 1 mM PMSF, on ice. This suspension was left on ice for 20 minutes and then the cells were disrupted through 3 passes through a cell disrupter at 15,000 psi. The lysate was centrifuged at 5,250 g. for 10 minutes at 4 °C to pellet whole cells. The supernatant of this spin was collected and ultracentrifuged at 100,000 g. for 30 minutes at 4 °C in a 45 Ti rotor. The supernatant of this spin was discarded and the membrane pellet was resuspended in 14 mL TBS pH 8.0, 2% TX-100, 10 mM EDTA, 0.1 mg/mL lysozyme, which was incubated on a rocker at room temperature for 20 minutes. This solution was once more ultracentrifuged for 30 minutes at 100,000 g. at 4 °C to pellet any undissolved membrane fractions. The supernatant from this spin was collected and dialyzed overnight against 3.5 L TBS pH 8.0, 0.5% Triton X-100. 5 mL of Ni-NTA resin slurry was applied to a disposable plastic column and washed 2X with 25 mL wash buffer (TBS pH 8.0, 0.05% DDM, 40 mM imidazole). The dialyzed BamAB-His solution was applied to the column and the flow-through was sent through the column two more times to maximize protein binding to the resin. The resin was washed 2X with 25 mL wash buffer and the protein was eluted from the resin using 15 mL TBS pH 8.0, 0.05% DDM, 200 mM imidazole. The eluate was concentrated to ~10 mg/mL in a 100 kDa molecular weight cut-off filter at 3,000 g. The BamAB-His was further purified by passing it through a Superdex 200 10/30 GL column on the FPLC. An isocratic elution using TBS pH 8.0, 0.05% DDM, 1 mM TCEP was used to elute the protein and the eluate was concentrated to a desired concentration in a 100 kDa molecular weight cut-off filter.

2.7.5: Overexpression and purification of FLAG-ns-BamA

A 15 mL culture of a BL21(DE3) strain containing pCH128 was grown overnight at 37 °C and used to seed a 1.5 L culture the following morning. This culture was shaken at 37 °C until

OD_{600}=0.75, at which point protein expression was induced using IPTG at a final concentration of 100 µM. The culture was grown for an additional 4-5 hours, at which point the cells were pelleted at 5,250 g. at 4 °C for 10 minutes. The cells were resuspended in 25 mL TBS pH 8.0 with 1 mM TCEP and the cells were lysed by 3 passes through a cell disrupter at 15,000 psi. Inclusion bodies were pelleted at 5,000 g. at 4 °C for 10 minutes, the supernatant was discarded, and 10 mL 8 M urea was added to dissolve the inclusion bodies. The inclusion bodies were broken up using a homogenizer, then rocked at room temperature for 15 minutes to dissolve the inclusion bodies fully. Any undissolved material or impurities were pelleted at 6,000 g. for 10 minutes at 4 °C. The supernatant was collected and diluted into 45 mL TBS pH 8.0, 0.5% LDAO, and nutated overnight at 4 °C to refold the protein. This solution was concentrated in a 50 kDa molecular weight cut-off filter the following morning to ~5 mL and injected onto the FPLC using a Superdex 200 column, using 5 1 mL isocratic runs with TBS pH 8.0, 0.03% DDM, 1 mM TCEP as the running buffer. Two overlapping peaks were observed and the fractions corresponding to the second peak were collected and concentrated in a 50 kDa molecular weight cut-off filter to approximately 1 mL. This solution was passed through the Superdex 200 column on the FPLC a second time to purify ns-BamA or its variant further. The fractions corresponding to the folded protein were collected and concentrated to the desired concentration in a 50 kDa molecular weight cut-off filter.

2.7.6: Overexpression and purification of BamCDE-His

Two 15 mL cultures of BL21(DE3) harboring pSK086 and pBamE-His were grown overnight at 37 °C. The following morning, each 15 mL culture was used to inoculate 1.5 LB in a 4 L flask and grown at 37 °C to OD_{600}=0.7. Protein expression was induced with 100 µM final concentration IPTG and grown for an additional 4 to 5 hours. Cells were pelleted at 5,250 g at 4°C for 10 min., then resuspended in 40 mL TBS pH 8.0 with 1 mM final conc. PMSF, 50 ug/mL Dnase, 100 ug/mL lysozyme, and 50 µg/mL RNAse. Cells were disrupted by passing this

suspension three times through a cell disruptor at 15,000 psi. Whole cells and inclusion bodies were pelleted at 5,000 g at 4 °C for 10 minutes. The pellet was discarded and the supernatant containing membrane fragments was ultracentrifuged in a 45 Ti rotor at 100,000 G at 4 °C for 30 minutes. The supernatant was discarded and the brown membrane pellet was resuspended in 10 mL TBS pH 8.0 with 2% Triton X-100, 10 mM EDTA, 0.1 mg/mL lysozyme. A homogenizer at power 3 was used to aid in the resuspension of the pellet. Any undissolved pieces of membrane were pelleted at 100,000 g at 4 °C for 30 minutes in the 45 Ti rotor. The supernatant containing dissolved BamCDE was collected and dialyzed overnight at 4 °C in 3.5 L TBS pH 8.0 with 0.5% Triton X-100. This dialysis step is to remove EDTA from the solution. The concentration of the dialyzed BamCDE solution was assessed, using dialysis buffer as a blank.

2.7.7: Reconstruction of BamABCDE-His for biochemical experiments

Purified BamAB (see 2.7.4) was mixed with purified, dialyzed BamCDE-His (see 2.7.6) in a 1:25 BamCDE-His:BamAB volume ratio. 10 mL Ni-NTA resin slurry was applied to Poly-Prep column and washed with 2X 25 mL wash buffer (TBS pH 8.0, 0.05% n-dodecyl-β-D-maltopyranoside, 40 mM imidazole). The BamABCDE-His mixture was passed through the resin three times. The resin was washed with 2X 30 mL wash buffer and the protein complex was eluted using 15 mL TBS pH 8.0, 0.05% n-dodecyl-β-D-maltopyranoside, 200 mM imidazole. The same volume of BamCDE-His that was added to BamAB in the first step of this protocol was added to the flow-through from the Ni-NTA purification to create more BamABCDE-His complex for purification. A second Poly-Prep column was prepared as described above and the same purification protocol was followed to accumulate more of the protein complex. Eluates from the two column runs were kept separate. The eluates were concentrated to approximately 500 µL in 100 kDa molecular weight cut-off filters at 3,000 g. at 4 °C. This was applied to a Superdex 200 column and eluted using an isocratic run of TBS pH 8.0, 0.03% n-dodecyl-β-D-maltopyranoside, 1 mM TCEP at a flow rate of 0.5 mL/min. Fractions corresponding to the main

peak, at roughly 11 minutes, were collected and concentrated in a 100 kDa molecular weight cut-off filter.

2.7.8: Reconstruction of BamACDE-His for biochemical experiments

Purified, dialyzed BamCDE-His was added to purified, refolded ns-BamA in a 10:1 molar ratio. 10 mL of Ni-NTA resin slurry was applied to a chromatography column and equilibrated with 2X 25 mL wash buffer (TBS pH 8.0, 1% n-octyl-β-D-glucopyranoside (OG), 20 mM imidazole). The BamACDE-His mixture was passed through the resin three times and the resin was washed with 2X 30 mL wash buffer. The Bam complex was eluted with 15 mL TBS pH 8.0, 1% OG, 200 mM imidazole. Eluate was concentrated to about 10 mg/mL in a 100 kDa molecular weight cut-off filter and passed isocratically through a Superdex 200 column on an FPLC using TBS pH 8.0, 1% OG, 1 mM TCEP as the running buffer and a flow rate of 0.5 mL/min. Fractions corresponding to the central, main peak at roughly 11 minutes were collected and concentrated in a 100 kDa molecular weight cut-off filter to the desired concentration.

2.7.9: Preparation of Bam complex proteoliposomes

To form Bam complex proteoliposomes, 40 µL of a 20 mg/mL sonicated aqueous solution of *E. coli* phospholipids was added to 200 µL of a 10 µM solution of protein complex in TBS pH 8.0, 0.03% DDM, and 1 mM TCEP. This solution was incubated on ice for five minutes, then diluted with 8 mL TBS pH 8.0, which reduces the DDM concentration below its CMC and forces the Bam proteins into phospholipid vesicles. This solution was incubated on ice for 30 minutes, at which point it was ultracentrifuged for 2 hours at 300,000 g. at 4 °C. The supernatant was discarded and the pelleted proteoliposomes were resuspended in 200 µL TBS pH 8.0, using gel-loading tips to pipette the proteoliposome suspension up and down. Any proteoliposomes that were not for immediate use were flash-frozen in liquid N_2 and stored at -80 °C.

2.7.10: In vitro reconstitution of OMP folding

2.5 µL of Bam complex proteoliposomes at a concentration of 10 µM was added to 6.5 µL TBS pH 8.0 in a PCR tube. If no preincubation with a chaperone was desired, 1 µL of outer membrane protein substrate, dissolved in 8 M urea and at a concentration of 0.5 µM, was added to the tube. If a preincubation with a chaperone was desired, 1 µL of the outer membrane protein substrate at a concentration of 5 µM in 8 M urea was added to 9 µL of the chaperone in TBS pH 8.0 at a concentration of 50 µM. This was incubated at room temperature for 10 minutes, at which point 1 µL of this mixture was added to a PCR tube containing 2.5 µL of Bam complex proteoliposomes at 10 µM and 6.5 µL TBS pH 8.0. The folding reactions were allowed to proceed at room temperature for the desired amount of time, then quenched with 10 µL 2X SDS sample buffer. Reactions were run on a 4-12% gradient polyacrylamide gel at 150 V for 110 minutes at 4 °C. Proteins were transferred to a PVDF membrane and α-FLAG-HRP antibodies were used to visualize folded and unfolded substrate.

2.7.11: Overexpression and purification of FLAG-OmpA

A 5 mL overnight culture of BL21(DE3) harboring pDW050 (FLAG-ns-OmpA) or pDW051 (FLAG-ns-OmpA(23-193)) was grown at 37 °C with 50 µg/mL and used the following morning to inoculate 500 mL LB media with 50 µg/mL. This culture was grown at 37 °C until OD_{600}=0.4 and protein expression was induced with 0.1 mM IPTG. The culture was grown for an additional 3-4 hours. Cells were pelleted at 5,250 g. at 4 °C for 10 minutes. Cell pellets were resuspended in 15 mL TBS pH 8.0, then lysed by three passes through a cell disrupter at 15,000 psi. Inclusion bodies were spun down at 5,250 g for 10 minutes at 4 °C. The supernatant was discarded and the pelleted inclusion bodies were dissolved in 5 mL 8 M urea, using a homogenizer to disrupt the pelleted inclusion bodies. The 50 mL tube containing this solution was rocked at room temperature for about 20 minutes until the inclusion bodies were fully dissolved. Undissolved

debris was pelleted at 20,000 g. for 20 minutes at 4 °C and the supernatant was collected. This solution was divided into 500 µL aliquots, flash-frozen in liquid N_2, and stored at -80 °C.

2.7.12: Refolding of OMPs in Detergent

In the experiment in Figure 3.2A, the full-length and truncated FLAG-BamA substrates were prepared at a concentration of 5 µM in 8 M urea. They were then diluted ten-fold into a solution of TBS (pH 8), 0.5% LDAO and incubated at room temperature for one hour. The folding reactions were then stopped with 2% SDS sample loading buffer. One-tenth of each reaction was run on semi-native SDS-PAGE, and the products were detected by western blotting as described in the previous section.

2.7.13: Overexpression and purification of His-ns-SurA

A 5 mL overnight culture of BL21(DE3) harboring pCH024 was grown at 37 °C. This culture was used the following morning to seed 500 mL LB media with carbenicillin at 50 µg/mL. The cells were grown at 37 °C until OD_{600}=1.0, at which point IPTG was added at a concentration of 0.1 mM to induce protein expression. The temperature was shifted to 16 °C and the cells were grown overnight. Cells were pelleted the following morning at 5,000 g. for 10 minutes at 4 °C. Cells were resuspended in TBS pH 8.0 with 1 mM PMSF. This solution was then transferred to 50 mL tubes and the cells were lysed by three passages through a cell disrupter at 15,000 psi. Unlysed cells and debris were pelleted at 5,000 g. for 10 minutes at 4 °C, the supernatant was collected, and membrane fractions were pelleted by ultracentrifugation at 100,000 g. for 30 minutes at 4 °C. 10 mL of Ni-NTA resin slurry was applied to a chromatography column and equilibrated with 2X 25 mL TBS pH 8.0, 20 mM imidazole. The supernatant from the ultracentrifugation was passed through the resin twice to enhance the amount of bound protein, then washed with 2X 15 mL TBS pH 8.0, 20 mM imidazole. Bound protein was eluted with 5 mL TBS pH 8.0, 200 mM imidazole, which was then loaded into a 30 kDa molecular weight cut-off

filter and concentrated to roughly 500 µL at 4,000 g. at 4 °C. Protein concentration was assessed by UV/Vis and diluted to the appropriate concentration for biochemical experiments.

2.7.14: Overexpression and purification of ns-Skp-His

The method for the purification of His-ns-SurA was followed, with several exceptions. The BL21(DE3) strain harboring pSK257 was used for SurA expression, which contains a kanamycin resistance cassette instead of a carbenicillin resistance cassette. Because Skp is a smaller protein than SurA, a 10 kDa molecular weight cut-off filter was used to concentrate the eluate from Ni-NTA column purification.

2.8: References

1. Onufryk, Christina, et al. "Characterization of six lipoproteins in the σ_E regulon." *Journal of bacteriology* 187.13 (2005): 4552-4561.

2. Ruiz, Natividad, et al. "Probing the barrier function of the outer membrane with chemical conditionality." *ACS chemical biology* 1.6 (2006): 385-395.

3. Sklar, Joseph G., et al. "Lipoprotein SmpA is a component of the YaeT complex that assembles outer membrane proteins in *Escherichia coli*." *Proceedings of the National Academy of Sciences* 104.15 (2007): 6400-6405.

4. Malinverni, Juliana C., et al. "YfiO stabilizes the YaeT complex and is essential for outer membrane protein assembly in *Escherichia coli*." *Molecular microbiology* 61.1 (2006): 151-164.

5. Vuong, Phu, et al. "Analysis of YfgL and YaeT interactions through bioinformatics, mutagenesis, and biochemistry." *Journal of bacteriology* 190.5 (2008): 1507-1517.

6. Ruiz, Natividad, et al. "Chemical conditionality: A genetic strategy to probe organelle assembly." *Cell* 121.2 (2005): 307-317.

7. Kim, Seokhee, et al. "Structure and function of an essential component of the outer membrane protein assembly machine." *Science* 317.5840 (2007): 961-964.

8. Hagan, Christine L., Seokhee Kim, and Daniel Kahne. "Reconstitution of outer membrane protein assembly from purified components." *Science* 328.5980 (2010): 890-892.

9. Nicchitta, Christopher V., and Günter Blobel. "Assembly of translocation-competent proteoliposomes from detergent-solubilized rough microsomes." *Cell* 60.2 (1990): 259-269.

10. Yakushi, Toshiharu, et al. "A new ABC transporter mediating the detachment of lipid-modified proteins from membranes." *Nature cell biology* 2.4 (2000): 212-218.

11. Görlich, Dirk, and Tom A. Rapoport. "Protein translocation into proteoliposomes reconstituted from purified components of the endoplasmic reticulum membrane." *Cell* 75.4 (1993): 615-630.

12. Brundage, Lorna, et al. "The purified *E. coli* integral membrane protein SecYE is sufficient for reconstitution of SecA-dependent precursor protein translocation." *Cell* 62.4 (1990): 649-657.

13. Akimaru, Jiro, et al. "Reconstitution of a protein translocation system containing purified SecY, SecE, and SecA from *Escherichia coli*." *Proceedings of the National Academy of Sciences* 88.15 (1991): 6545-6549.

14. van der Does, Chris, et al. "Reconstitution of purified bacterial preprotein translocase in liposomes." *Methods in enzymology* 372 (2003): 86-98.

15. Kramer, R. A., et al. "In vitro folding, purification and characterization of *Escherichia coli* outer membrane protease OmpT." *European Journal of Biochemistry* 267.3 (2000): 885-893.

16. Bassilana, Martine, and William Wickner. "Purified Escherichia coli preprotein translocase catalyzes multiple cycles of precursor protein translocation." *Biochemistry* 32.10 (1993): 2626-2630.

17. Kumamoto, Carol A., and J. Beckwith. "Mutations in a new gene, secB, cause defective protein localization in *Escherichia coli*." *Journal of bacteriology* 154.1 (1983): 253-260.

18. Tissieres, Alfred, et al. "Ribonucleoprotein particles from *Escherichia coli*." *Journal of Molecular Biology* 1.3 (1959): 221-233.

19. Nissen, Poul, et al. "The structural basis of ribosome activity in peptide bond synthesis." *Science* 289.5481 (2000): 920-930.

20. Nierhaus, Knud H., and Ferdinand Dohme. "Total reconstitution of functionally active 50S ribosomal subunits from *Escherichia coli*." *Proceedings of the National Academy of Sciences* 71.12 (1974): 4713-4717.

21. Traub, P., and M. Nomura. "Structure and function of *E. coli* ribosomes. V. Reconstitution of functionally active 30S ribosomal particles from RNA and proteins." *Proceedings of the National Academy of Sciences* 59.3 (1968): 777-784.

22. Dalbey, Ross E., Peng Wang, and Andreas Kuhn. "Assembly of bacterial inner membrane proteins." *Annual review of biochemistry* 80 (2011): 161-187.

23. Hagan, Christine L., David B. Westwood, and Daniel Kahne. "Bam lipoproteins assemble BamA in vitro." *Biochemistry* 52.35 (2013): 6108-6113.

24. Morona, Renato, Michael, Klose, and U. Henning. "*Escherichia coli* K-12 outer membrane protein (OmpA) as a bacteriophage receptor: analysis of mutant genes expressing altered proteins." *Journal of bacteriology* 159.2 (1984): 570-578.

Chapter 3: Crystallization of the Bam Complex

3.1: Rationale for the crystallization of the Bam complex

Monitoring the folding of OMPs using the in vitro reconstitution described in Chapter 2 provided valuable information about the requirements for folding several β-barrel substrates by Bam proteins. Despite the progress made using this assay, the reconstitution can provide only limited insight into the mechanistic details of OMP assembly. The readout of these assays is the observation of either a folded OMP or an unfolded OMP; the reconstitution could not provide us with methods to monitor folding intermediates of transmembrane β-barrels. In addition, no general in vivo or in vitro assays had been developed that could provide this detailed level of mechanistic information. Thus, to elucidate the roles of individual Bam lipoproteins and the BamA β-barrel depends not only on developing and executing additional clever in vitro experiments with Bam subcomplexes, but also on elucidating structural information about the Bam complex.

As discussed in Chapter 1, structures of all four lipoproteins, BamBCDE, have been solved in their delipidated forms and a structure of BamA was published fairly recently.[1-4] The structures of individual components of the complex, however, cannot provide structural information about the complex as a whole. Only by crystallizing the whole complex can several important questions be addressed, as biochemical experiments indicate that all five proteins are necessary for optimal activity. Published structures of BamA and BamA's POTRA domains have shown that the POTRA domains can adopt multiple conformations, with a flexible linker between P2 and P3.[5] A structure of the whole complex would reveal which conformation or conformations of the POTRA domains exists when Bam lipoproteins coordinate with BamA. Likewise, it is unknown how the lipoproteins orient themselves with respect to the β-barrel domain of BamA or to the POTRA domain of BamA, information that could be suggestive of a mechanism for OMP assembly. Interestingly, two conformations of the N- and C-terminal β-strands of the BamA barrel have been observed in crystal structures, with one structure showing eight hydrogen

bonding interactions between the strands, the other showing only two hydrogen bonding interactions.[6] These different structures of the β-barrel support a model of β-barrel assembly involving a lateral gate in the β-barrel of BamA, where weakened interactions between the terminal strands of the barrel allow the passage of individual β-hairpins into the lipid environment of the OM. Alternatively, the terminal β-strands of the barrel may allow for β-augmentation between folding β-strands and the BamA β-barrel, a model in which the barrel of BamA expands to accommodate a substrate during its assembly. Obtaining a structure of BamA in complex with the Bam lipoproteins would show the state of this lateral gate when the complex is fully assembled.

Ideally we would crystallize the entire BamABCDE complex, which would provide the clearest picture of how the complex assembles its substrates. At the same time, we were interested in crystallizing BamAD, the two essential components of the complex that are known to bind to one another through POTRA domain P5 of BamA.[7] For several reasons, we decided to focus our efforts on the crystallization of the BamACDE complex. First, this four-protein complex contains the two essential components of Bam, BamA and BamD. Second, the overexpression and purification of this complex was well developed and this isolated complex had been shown to be active in vitro.[8] Third, we decided to omit BamB from this targeted complex because BamB requires POTRA domains P2-5 of BamA to be present for BamA and BamB to copurify, which would have limited the number of BamA POTRA domain constructs that we would have been able to use in screening efforts. Fourth, the purification of BamABCDE requires purifying BamAB from the outer membrane, which yields considerably less BamA than its purification and refolding from inclusion bodies. Fifth, the BamACDE complex is stable in multiple detergents, whereas BamB dissociates from the rest of the complex even in some mild detergents.

3.2: Optimization of the purification of the Bam complex

The purification of the Bam complex reported in Chapter 2 used for biochemical experiments served as a good starting point for crystallization experiments. When BamABCDE, BamACDE, or BamAB are purified by refolding BamA and reconstructing the complex by the addition of Bam lipoproteins, the complex shows considerable activity in vitro. This implies that at least some of the purified proteins are in a physiologically relevant conformation.

Initial screening for crystallization conditions by Christine Hagan and Suguru Okuda produced several interesting crystallization conditions, one of which became a focus of the studies presented in this chapter. Although their method of purification gave crystal-forming protein, those crystals were not reproducible. We believed that this was due to some impurities in the purified proteins: 1) the refolding of BamA reported in Chapter 2 results in about 40% of the protein remaining in the unfolded state, which does not successfully separate from the folded form by gel-filtration and 2) a BamC degradation product predominates in the final preps of a Bam complex (Figure 3.1).

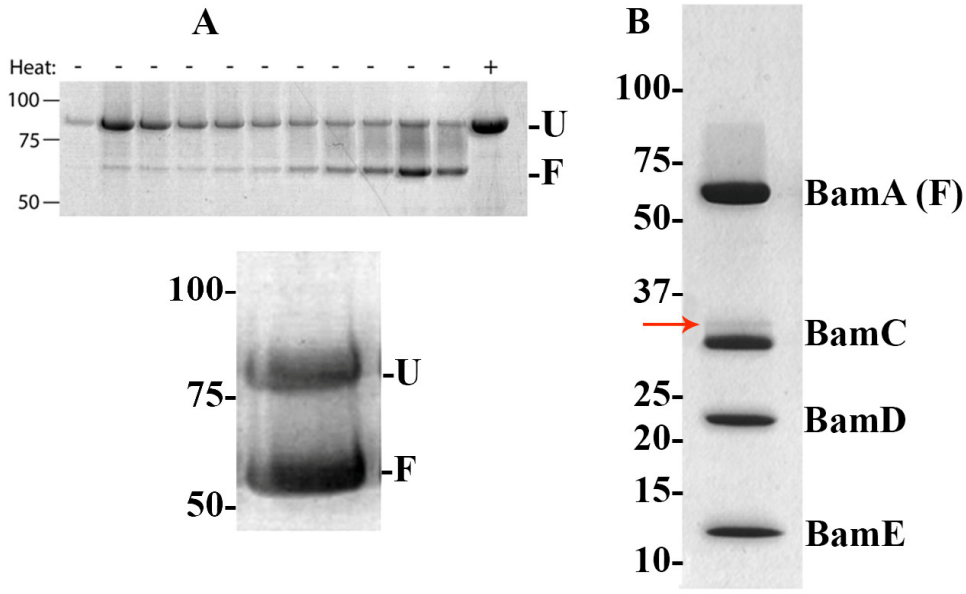

Figure 3.1. Impurities in preparations of BamA and the BamACDE complex. **A.** When BamA is refolded in vitro and purified by size-exclusion chromatography, the folded and unfolded forms coelute (above). None of the fractions contain pure folded BamA. When fractions predominated by folded BamA are concentrated, approximately 40% of the protein stays unfolded. Heat denatures folded BamA. **B.** Purified BamACDE complex contains faint band at 34 kDa that was identified as full-length BamC (highlighted with red arrow). A degradation product of BamC predominates at 32 kDa. Note: this figure is of a BamACDE purification after optimizing the separation of folded from unfolded BamA. (U, unfolded BamA; F, folded BamA) All data are from semi-native SDS-PAGE on 4-12% polyacrylamide gels.

3.2.1: Separation of folded from unfolded BamA

At the outset of this project, we were interested in developing methods for increasing not only the purity of folded BamA, but also the amount of BamA that could be obtained by refolding BamA inclusion bodies in vitro. Because the folded and unfolded forms of the protein are similar in size,

it was not possible to separate them reliably by size-exclusion chromatography—other methods had to be devised.

Several methods exist for refolding inclusion bodies, including diluting the unfolded protein directly into refolding buffer, dialyzing the unfolded protein against a refolding buffer, and diluting the chemical denaturant against a refolding buffer on a microfluidics chip.[9] The method for refolding BamA that is reported in Chapter 2 relies on slow dilution of urea-denatured BamA inclusion bodies into a refolding buffer containing lauryldimethylamine-N-oxide (LDAO), which is incubated overnight at 4 °C. Because this method produced biochemically active BamA, we opted to optimize this method instead of pursuing alternative refolding methods. We began by screening for conditions to increase the amount of folded BamA observed after nutating at room temperature in refolding buffer for 12-16 hours. We hypothesized that refolding BamA at a greater temperature than 4 °C would drive BamA to adopt its thermodynamically more favorable, folded state. Detergents including n-dodecyl-β-D-maltopyranoside (DDM) and n-octyl-β-D-glucopyranoside (OG) were screened and we chemical additives including 500 mM arginine and 400 mM glycerol—reported to improve the refolding of lysozyme and other proteins in vitro—were also screened.[10-12] Lastly, we examined the effects of coincubation of unfolded BamA with refolding buffer containing BamCDE or SurA. We hypothesized that the Bam lipoproteins or a periplasmic chaperone may be able to coordinate with periplasmic loops or the periplasmic face of BamA's β-barrel to assist its refolding. Refolding BamA at room temperature in LDAO increased the proportion of folded material, but none of the other conditions improved the efficiency of BamA refolding.

Next, we screened conditions to improve the separation of folded BamA from unfolded BamA during size-exclusion chromatography. The method reported in Chapter 2 results in a crude separation of unfolded from folded BamA, with TBS pH 8.0, 0.03% DDM, and 1 mM TCEP as

the running buffer (Figure 3.1. A). We screened conditions that we hypothesized could fold additional amounts of BamA on the column, thereby enriching the eluate with the folded form. These conditions included increasing the concentration of DDM in the running buffer, increasing the concentration of NaCl in the running buffer, lowering the concentration of refolded BamA injected onto the column, and co-injected periplasmic chaperones with the refolded BamA. We believed that a higher salt concentration could lead to increased folding by driving hydrophobic regions of unfolded BamA into detergent micelles and that a lower concentration of BamA injected onto the column would increase the resolution of peaks as they came off of the column. Finally, since protein chaperones such as SurA keep unfolded OMPs folding-competent in the periplasm, we hypothesized that co-injection of SurA with the refolded BamA could aid in its on-column refolding. Unfortunately, none of these conditions improved the separation of unfolded BamA from its folded form.

The folded and unfolded forms of BamA run at apparent molecular weights of ~60 kDa and ~85 kDa, respectively. It is not surprising that these two proteins do not separate well by size-exclusion in a Superdex 200 column. We believed that we could exploit other differences in the physical properties of the two forms of BamA to segregate them more effectively. Namely, we believed that the folded and unfolded forms would present different amounts of charged or polar residues to their aqueous surroundings and that this physical difference would be present independent of the protein's location in a detergent micelle. Thus, we explored anion-exchange chromatographic methods to exploit these physical differences. We used a MonoQ 5/50 GL column from GE Life Sciences, which is packed with beads covalently linked to a positively-charged quaternary amine to screen for methods of separating the two species.

Anion exchange relies on a negatively-charged protein binding to the positively charged resin, which is then eluted using a high concentration of salt. If there are anionic small molecules

present in the running buffer, they compete with the protein for binding onto the resin. If they bind tightly enough, they may not elute and will clog the column. For this reason, the LDAO used to refold BamA in vitro had to be replaced with a nonionic detergent. Fortunately, we had found that DDM was able to refold BamA, albeit to a lesser extent than LDAO. Screening of detergent concentrations, salt concentrations, various buffers, and gradients between the running buffer and the elution buffer resulted in a reliable way to separate folded BamA from its unfolded form that does not require any size-exclusion steps (Figure 3.2). BamA is expressed without its signal sequence, the inclusion bodies are purified, dissolved in urea, then added drop-wise to a solution of TBS pH 8.0 and 0.25% DDM in a 1:9 v/v ratio. The refolded material is concentrated the following morning and injected onto a MonoQ column with 20 mM bis-tris pH 6.5, 1% OG as the running buffer and 20 mM bis-tris pH 6.5, 1% OG, 1 mM TCEP, 1 M NaCl as the elution buffer. The pI of BamA is roughly 5.1, so a pH 6.5 buffer was used to keep BamA negatively charged and to exacerbate any charge differences between the folded and unfolded forms of BamA without neutralizing the protein and causing it to aggregate. Likewise, the micelle weight of OG is approximately 17 kDa, which we hypothesized was small enough to expose the maximal amount of charged BamA moieties to the anion-exchange resin for increased differentiation between the folded and unfolded forms.

A

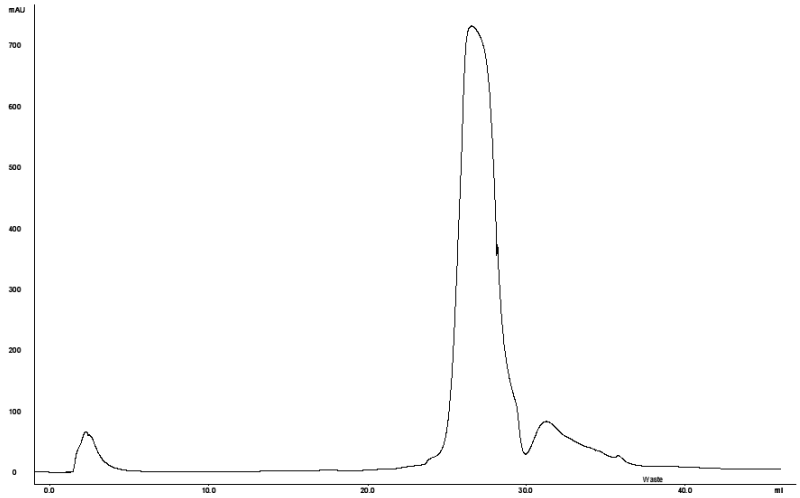

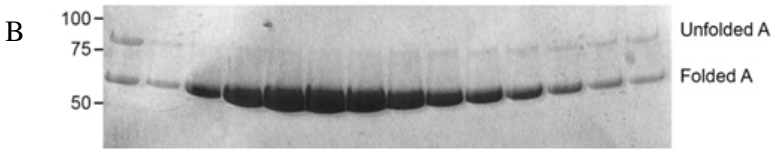

Figure 3.2. Folded BamA is able to be separated from its unfolded form by anion-exchange chromatography **A.** An anion-exchange chromatogram using the method described in 3.6.3. The large central peak is folded BamA. **B.** Semi-native SDS-PAGE of anion-exchange fractions.

3.2.2: Purification of POTRA domain truncations of BamA

Our crystallization efforts focused on the BamACDE subcomplex, which provides more flexibility for creating POTRA domain truncations of BamA. Were BamB to be included in the complex, POTRA domains 2-5 would have to be retained for the BamACDE complex to bind to BamB. BamCDE, on the other hand, only requires P5 to bind to BamA and it is through BamD that BamC and BamE coordinate with BamA.[5] To expand the search space for crystallization conditions, we investigated the generalizability of the refolding and anion-exchange purification methods to POTRA domain truncations of BamA.

An unfolded OMP quickly aggregates in an aqueous environment, which is why macromolecular periplasmic chaperones that sequester hydrophobic regions of OMPs from water in the periplasm are necessary for the trafficking of OMPs to the OM.[13,14] We found that BamA constructs lacking POTRA domains were less soluble than full-length BamA in refolding buffer and that the refolding solution became increasingly viscous when fewer POTRA domains were present on BamA. Because the POTRA domains are soluble and the results presented in Chapter 2 show that soluble periplasmic domains of OMPs may act as chaperones, these observations did not surprise us.[15] Nevertheless, the insolubility of some of these constructs made purification more difficult, if

not impossible, using the method described above. We were able to purify BamAΔP1, BamAΔP1-2, and BamAΔP1-3 successfully, but not BamAΔP1-4 (Figure 3.3).

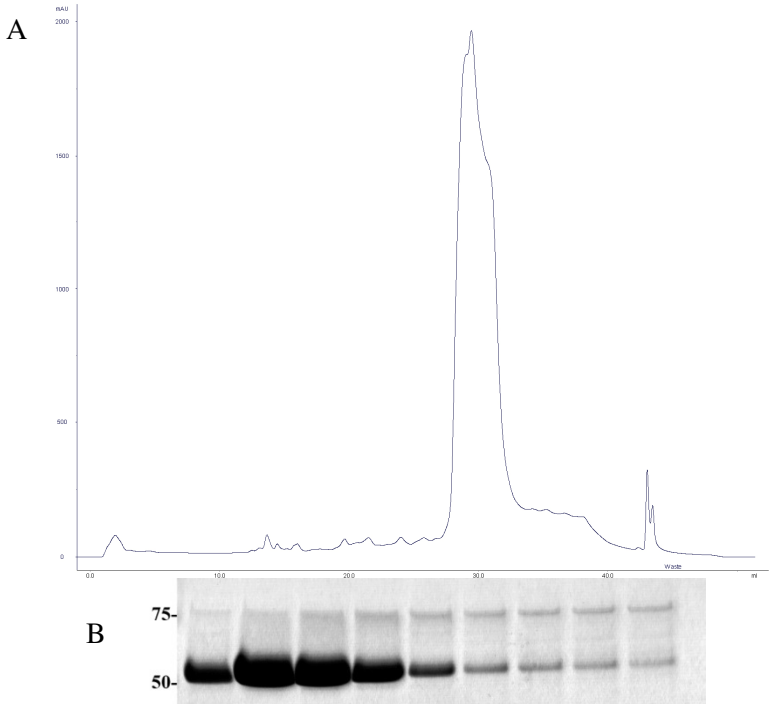

Figure 3.3. (continues on next page). **A.** Anion-exchange chromatogram of BamAΔP1 and **B.** the collected fractions run on semi-native SDS-PAGE. Folded protein runs at a lower apparent molecular weight than the unfolded form. **C.** Anion-exchange chromatogram of BamAΔP1-2 and **D.** a semi-native SDS-PAGE of the collected fractions. **E.** Anion-exchange chromatogram of BamAΔP1-3 and **F.** a semi-native SDS-PAGE of the collected fractions.

C

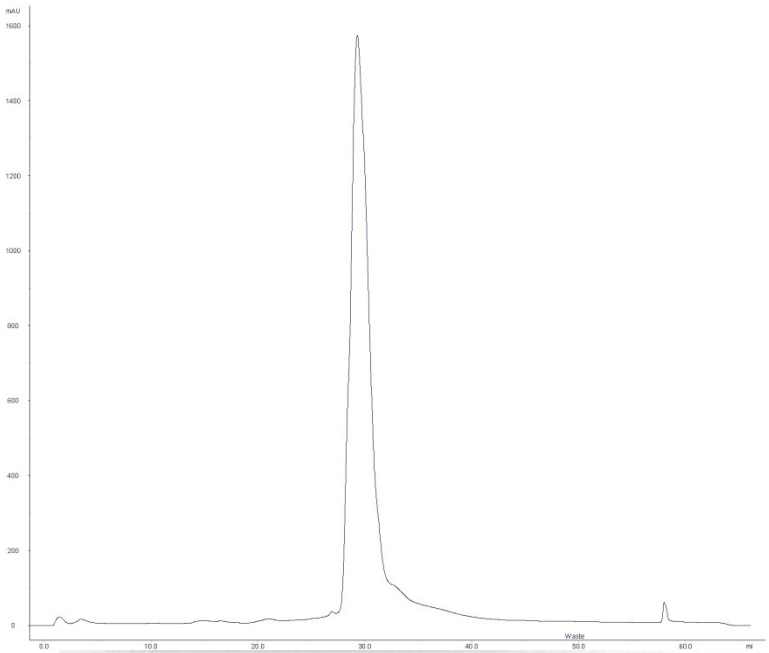
mAU
1600
1400
1200
1000
800
600
400
200
0
0.0
10.0
20.0
30.0
40.0
50.0
60.0
ml
Waste

D

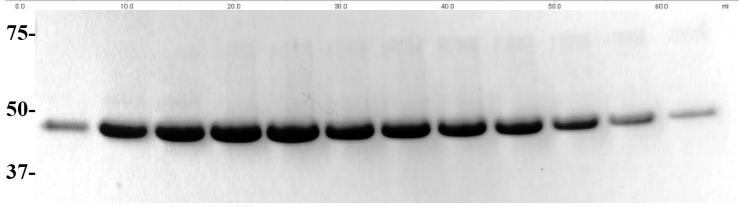
75-
50-
37-

E

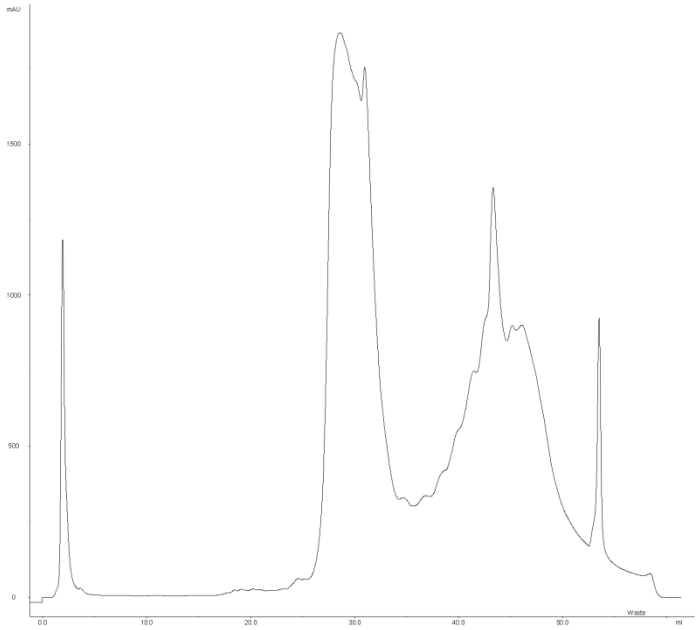
mAU
1500
1000
500
0
0.0
10.0
20.0
30.0
40.0
50.0
ml
Waste

F

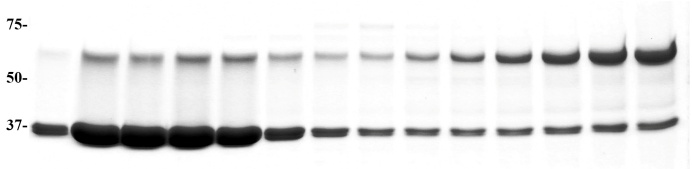
75-
50-
37-

3.2.3: Purification of BamACDE

With pure folded BamA and POTRA domain truncations of BamA in hand, we reconstructed the BamACDE, BamAΔP1CDE, BamAΔP1-2CDE, and BamAΔP1-3CDE subcomplexes in vitro, which is described more fully in 3.6.5. Briefly, folded BamA is mixed with BamCDE in a 10:1 molar ratio. BamCDE are purified from a single strain and past work had established that this method resulted in a 1:1:1 mixture of the lipoproteins.8 Additionally, a polyhistidine tag on BamE is used to pull down the complex, so an excess of folded BamA was used to maximize the amount of BamACDE in the final purification. This mixture was applied to Ni-NTA resin, washed, and eluted. A final pass through a Superdex 200 size-exclusion column was used to remove any impurities from the nickel column eluate and to eliminate imidazole from the buffer. During the washing and elution steps of the nickel column, the OG and Triton X-100 present in the BamACDE mixture was exchanged with the detergent desired for final crystallization screening. Likewise, the running buffer for size-exclusion chromatography contained the detergent that was desired for crystallization screening. Following elution from the size-exclusion column, peak fractions were collected and concentrated for crystallization. A representative semi-native SDS-PAGE analysis of nickel column fractions and concentrated BamACDE eluate from size-exclusion purification in OG is represented in Figure 3.4 below.

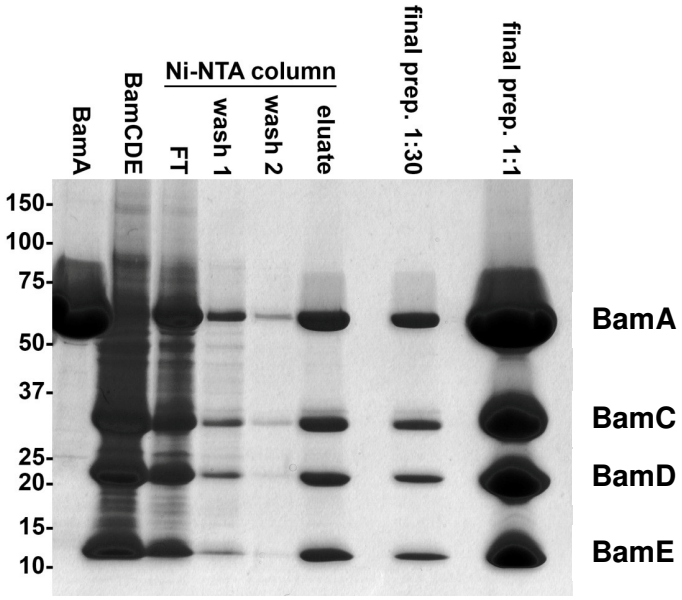

Figure 3.4. Semi-native SDS-PAGE of the purification steps of BamACDE in n-octyl-β-D-glucopyranoside. The four proteins co-elute and show a 1:1:1:1 ratio by gel. BamA stains darker due to its greater size and hydrophobic character. (FT, flow-through)

We screened multiple detergents to determine how stable the BamACDE complex is in varying chemical environments. In total, eight detergents were screened: n-octyl-β-D-glucopyranoside, n-nonyl-β-D-glucopyranoside, n-dodecyl-β-D-maltopyranoside, n-decyl-β-D-maltopyranoside, tetraethylene glycol monooctyl ether (C_8E_4), dimethyldecylphosphine oxide (APO-10), CYMAL 5, and CYMAL 6. With the exception of C_8E_4, the results of which are discussed in the conclusion of this chapter, and DDM, which produced two very closely overlapping peaks by size-exclusion chromatography, the screened detergents did not dissociate lipoproteins from BamA or BamA with truncated POTRA domains and the whole complex eluted in one monodisperse peak (Figure 3.5).

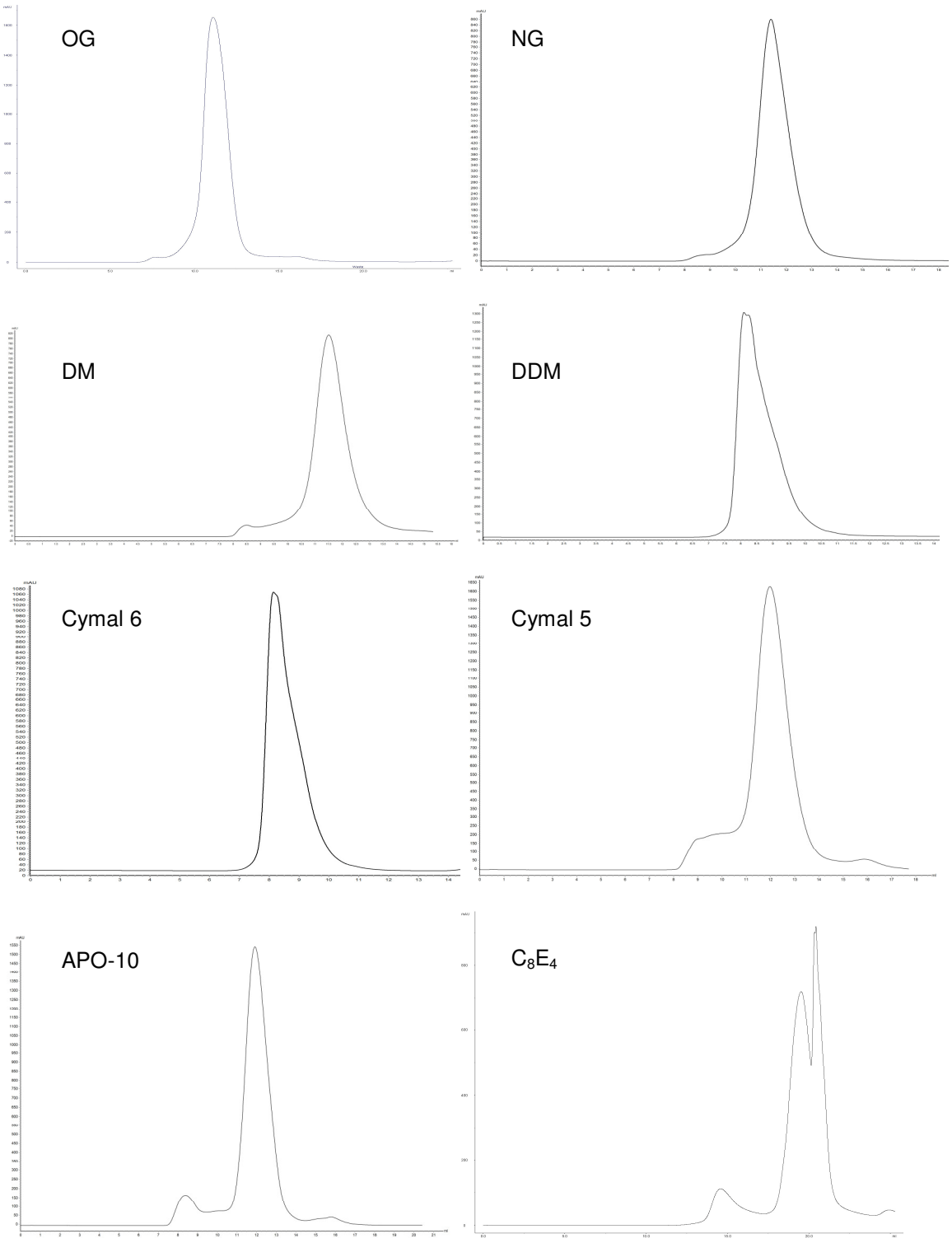

Figure 3.5. BamACDE purifications in various detergents. (OG, n-octyl-β-D-glucopyranoside; NG, n-nonyl-β-D-glucopyranoside; DM, n-decyl-β-D-maltopyranoside; DDM, n-dodecyl-β-D-maltopyranoside, APO-10, dimethyldecylphosphine oxide; C_8E_4, tetraethylene glycol monooctyl ether.)

3.3: Screening of BamACDE crystallization conditions

Although a small amount of full-length BamC remained in preparations of BamACDE and POTRA domain truncations of BamA in complex with BamCDE, early crystal screening produced several promising conditions. Similarly, the condition that Christine Hagan and Suguru Okuda had found became reproducible with the new, purer folded BamA (Entry 1 in Table 3.1). Crystallization conditions were screened extensively using full-length BamA, BamAΔP1, BamAΔP1-2, and BamAΔP1-3 in complex with BamCDE, which were purified in the seven detergents that did not dissociate the complex (Figure 3.5). Crystallization temperature and the ratio between the volume of protein and the volume of reservoir solution added to each drop were two additional variables that were manipulated during initial screening efforts. Finally, we methylated the lysines of the Bam complex according to the protocol described by Walter et al.[16] This technique has been reported to improve crystal contacts in some crystallized proteins by reducing the pI of the crystallized protein. Approximately 20,000 conditions were screened using commercially available block screens MemGold, MemGold 2, ProComplex, ProPlex, MbClass I & II, PEGs I & II, Clear Strategy Screen I & II, Crystal Screen I & II, MemPlus, MemFac, and MemSys, which were purchased from Hampton Research, Molecular Dimensions, or Qiagen. Initial screening was performed in 96-well MRC3 plates and trays were set at 4 °C or 20 °C. The trays were imaged at regular intervals over the course of one month to monitor crystallization.

When purified in most of the detergents listed above, the Bam complex did not form any crystals under screened conditions. N-octyl-β-D-glucopyranoside and n-nonyl-β-D-glucopyranoside produced the most number of hits, which may have been a result of their small micelle size, so efforts became focused on these two detergents as screening progressed. Additionally, the suitability of glucosides for Bam crystallization led us to screen extensively for crystallization using OG- or NG-purified Bam complex in dimyristoyl phosphatidylcholine (DMPC) and (3-[(3-cholamidopropyl)dimethylammonio]-2-hydroxy-1-propanesulfonate) (CHAPSO) bicelles.

Bicelles can be thought of as solubilized lipid bilayer discs wherein a long-chain lipid (DMPC) forms a piece of a bilayer that is encased in a short-chain lipid or detergent (CHAPSO).[17] When a protein that has been purified in a detergent is added to a bicelle solution, it incorporates into the lipid bilayer discs, which more closely resemble the membrane environment that a transmembrane protein would experience in vivo than a detergent micelle. Bicelles are also amenable to use with proteins purified in detergent, so adapting our purification protocols for bicelle crystal screening was not challenging. Finally, the published structure of BamA had been solved from crystals that formed from bicelles, providing evidence that we could obtain hits using bicelles.[2] Table 3.1, below, shows a selection of hits from initial screening efforts.

Table 3.1. Initial crystallization hits

Entry	Construct	Detergent	Crystallization Condition	Crystallization Temperature
1	BamACDE 16 mg/mL	1% OG	100 mM trisodium citrate pH 5.6 1 M ammonium dihydrogen phosphate 50 mM NaF 1:1 protein:reservoir	4 °C
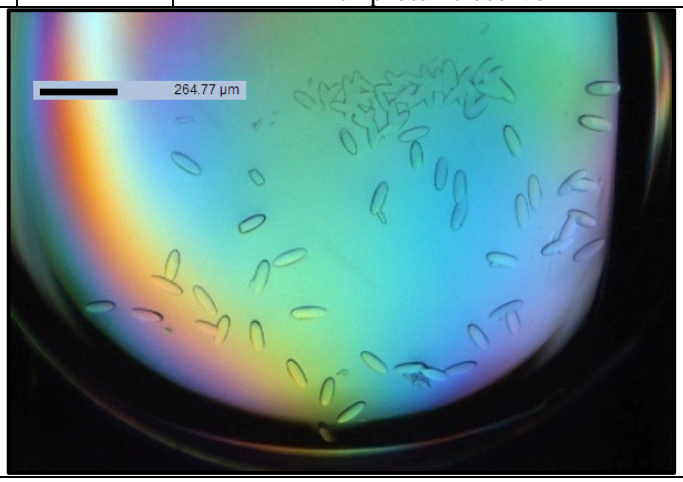				

Entry	Construct	Detergent	Crystallization Condition	Crystallization Temperature
2	BamAΔP1-2CDE 16 mg/mL	1% OG	100 mM tris pH 7.5 30% Jeffamine M-600 1:1 protein:reservoir	20 °C

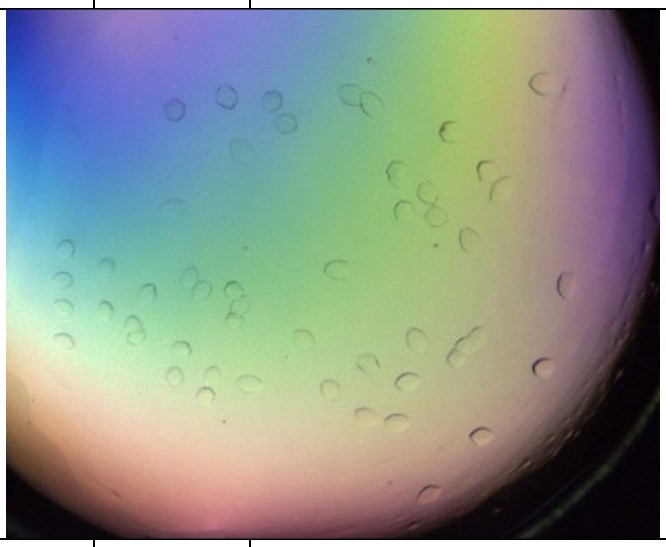

Entry	Construct	Detergent	Crystallization Condition	Crystallization Temperature
3	BamACDE 17 mg/mL	1% OG	100 mM $MgCl_2$ 100 mM tris pH 7.5 22% PEG 400 1:1 protein:reservoir	20 °C

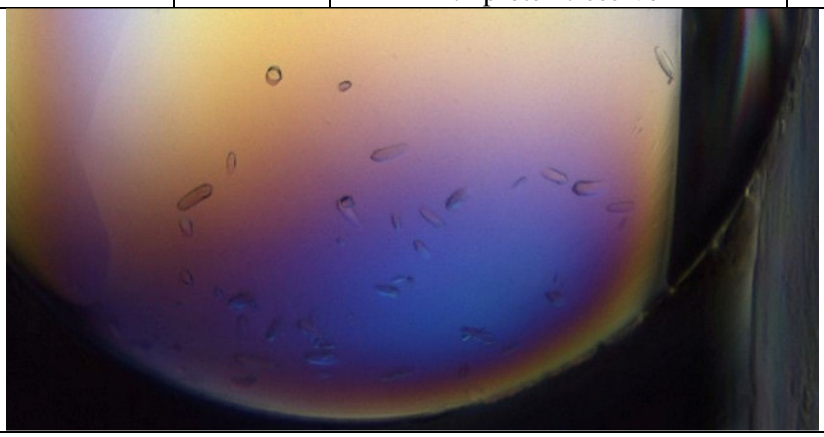

Entry	Construct	Detergent	Crystallization Condition	Crystallization Temperature
4	BamAΔP1CDE 15 mg/mL	1% OG	100 mM NaCl 30% PEG 400 100 mM tris pH 8.5 1:1 protein:reservoir	20 °C

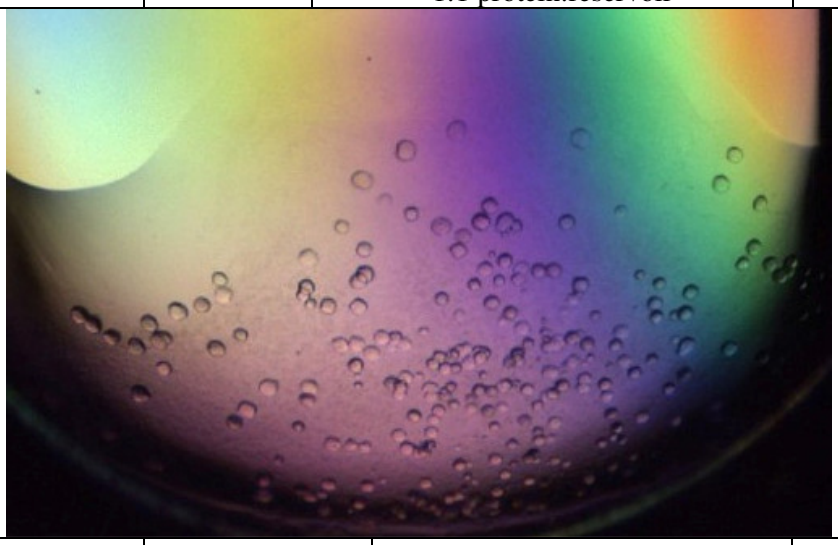

Entry	Construct	Detergent	Crystallization Condition	Crystallization Temperature
5	BamAΔP1CDE 9.4 mg/mL	10 mM NG 5% DMPC + CHAPSO bicelles	100 mM trisodium citrate pH 5.6 1.5% PEG 400 1:1 protein:reservoir	20 °C

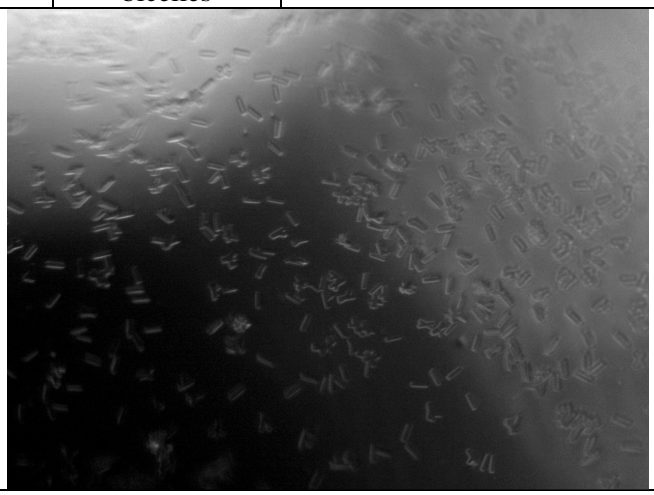

Entry	Construct	Detergent	Crystallization Condition	Crystallization Temperature
6	BamAΔP1-2CDE	1% OG 5% DMPC + CHAPSO bicelles	100 mM NaCl 100 mM trisodium citrate pH 5.6 1:1 protein:reservoir	20 °C
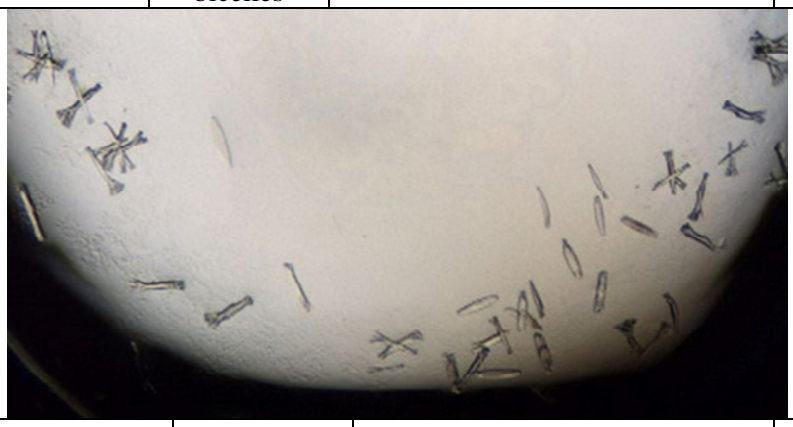				
Entry	Construct	Detergent	Crystallization Condition	Crystallization Temperature
7	BamAΔP1-2CDE 16 mg/mL	1% OG 5% DMPC + CHAPSO bicelles	100 mM sodium acetate pH 5.0 15% MPD 2% PEG 4,000 1:1 protein:reservoir	20 °C
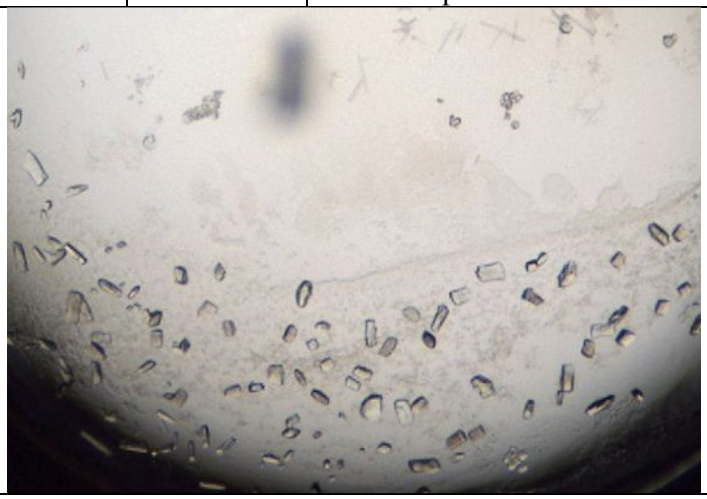				

Entry	Construct	Detergent	Crystallization Condition	Crystallization Temperature
8	BamACDE 16 mg/mL	0.7% OG 7% DMPC + CHAPSO bicelles	100 mM sodium citrate pH 5.5 200 mM KCl 37% pentaerythritol propoxylate 2:1 protein:reservoir	20 °C
	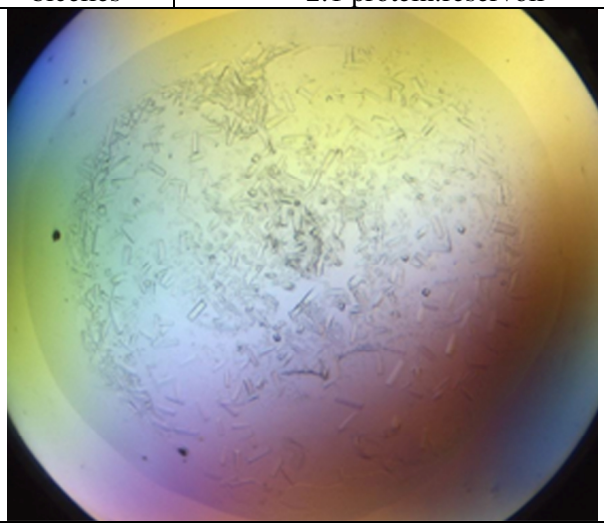			

3.4: Optimization of BamACDE crystals

Reproducing crystals grown under the conditions presented in Entries 2, 4, 5, 6, and 7 of Table 3.1 proved difficult and none of the crystals that were irradiated diffracted to a high resolution. Crystals grown under the Entry 7 condition were not at all reproducible.

The crystallization condition for Entry 2 was not highly reproducible, so we screened fewer conditions for improved crystallization. Grid screens probing the effects of pH, BamAΔP1-2CDE concentration, and Jeffamine concentration did not produce crystals reliably. We also tested the ability of BamAΔP1CDE to crystallize under the initial conditions, but it did not. Finally, we screened cryoprotectants 30% PEG 400, 20% ethylene glycol, various concentrations of Jeffamine, and the CryoOil Fomblin. At best, the crystals diffracted to ~15 Å at APS.

Crystals grown under the Entry 3 condition were reproducible, which allowed for extensive screening for high-resolution crystals. Grid screens were constructed to examine the influence of

pH, the concentration of PEG 400, the concentration of BamACDE, the concentration of magnesium chloride, drop volume, and reservoir volume. We also screened the ratio of protein to reservoir in crystal drops, temperature, alternative PEGS (PEGs 200, 300, 350, 550, and 1000), using 2-methyl-2,4-pentanediol (MPD) as the precipitant, alternative chloride salts ($CaCl_2$, $MnCl_2$, $SrCl_2$, $CrCl_2$, KCl, and NaCl), and the presence of paraffin or silicon oil above the droplets to slow crystal growth. Finally, we tested the abilities of BamAΔP1CDE and BamAΔP1-2CDE to crystallize under these conditions. No screen produced larger crystals or crystals with a different morphology than the original hit. Crystals were picked for collection of diffraction data, using 30% PEG 400 in mother liquor as the cryoprotectant, which was added directly to crystallization drops. Crystals were flash-frozen in liquid N_2, sent to APS, and irradiated at 100 K, but none of the crystals produced measurable diffraction.

Crystals grown under the Entry 4 condition were somewhat reproducible, but screening across pH, PEG 400 concentration, drop volume, and the volume of the reservoir did not produce larger crystals. Of the crystals that did grow, several were cryoprotected by addition of reservoir with 20% ethylene glycol and flash-frozen in liquid N_2 for shipment to the Advanced Photon Source (APS) at the Argonne National Laboratory. At best, these crystals diffracted to ~20 Å.

The crystallization conditions presented under Entry 5 and 6 are quite similar: both contain trisodium citrate at a pH similar to the pI of BamA, which is 5.1. The crystals grown under both of these conditions grew overnight and share similar morphologies. Due to the buffer pH of 5.0 or 5.5, the small size of the crystals, and the fast rate at which the crystals grew, we suspected that the Bam complex was entering a disordered crystalline state. Nevertheless, the crystals were reproducible, which allowed us to screen across pH, concentrations of PEG 400, concentrations of BamAΔP1CDE (Entry 5) and BamAΔP1-2CDE (Entry 6), temperature, reservoir volume, drop size, and larger PEGs as precipitants. Crystals were cryoprotected by serial transfer into mother

liquor containing either 30% PEG 400, MPD, or the CryoOils Foblin Y and Krytox. When irradiated at APS, crystals diffracted to ~20 Å.

3.4.1: Optimizing BamACDE crystals grown in ammonium dihydrogen phosphate

Entry 1 in Table 3.1, the condition that our lab had discovered prior to the work reported here, had only produced several crystals when the purified BamACDE complex contained contaminating, unfolded BamA. Several of these early crystals were cryoprotected using mother liquor with 20% ethylene glycol and screened for diffraction at APS. Crystals diffracted only to ~12 Å, but enough data were collected to place the crystals into the $P6_122$ space group with unit cell dimension a = b = 111.2 Å, c = 755.9 Å with a solvent content of ~70%, as determined by Matthews coefficient. Upon crystallizing BamACDE under this condition with a preparation lacking unfolded BamA, the crystals were robustly reproducible and therefore amenable to extensive optimization screening.

Potential improvements were screened by examining the effects of pH, BamACDE concentration, ammonium dihydrogen phosphate concentration, drop volume, reservoir volume, the ratio of protein to reservoir volume, temperature, the addition of *E. coli* phospholipids to the purified complex, purification of the complex in n-nonyl-β-D-glucopyranoside, as well as additive screening using the Hampton Research 96-well additive screen, the MemAdvantage screen from Molecular Dimensions, the Detergent Screen HT from Hampton Research, and the Silver Bullets additive screen from Hampton Research. No additive screen or adjustment to the crystallization condition resulted in crystals with a new morphology. Likewise, when BamACDE was purified in NG and set in trays under the crystallization conditions, no crystals formed. The same was true when BamA POTRA domains truncations in complex with BamCDE were set in the base crystallization condition. Screening for diffraction of crystals at APS led us to a slightly modified crystallization condition that produced fewer, larger crystals of the complex. This crystallization

condition was 100 mM trisodium citrate pH 6.4, 800 mM ammonium dihydrogen phosphate, 50 mM sodium fluoride. We also screened cryoprotectants PEG 400, ethylene glycol, glycerol, diethylene glycol, xylitol, glucose, $NH_4H_2PO_4$, and a high concentration of trisodium citrate. 20% ethylene glycol produced crystals that froze clear and that diffracted to the highest resolution (Figure 3.6, **C.**).

Several hundred crystals grown under this condition were irradiated at APS, all of which displayed a high degree of anisotropy, diffracting to ~6 Å along the z-axis of the unit cell and to ~9 Å along the other two axes. Two representative frames and a photo of a mounted crystal are presented in Figure 3.6, below. The output from AIMLESS, which is software at the APS beamline that indexes diffraction data, is presented below in Figure 3.7. Indexing of the data in XDS showed that the complex packed into the $P6_122$ space group, just as the original crystals had done. After scaling in XDS, the anisotropy server at UCLA was employed to correct for our highly anisotropic data and molecular replacement attempts were conducted using Phaser in Phenix.[18] We used BamA, POTRA domain truncations of BamA, loop deletions of BamA, BamD, BamC, and the BamCD complex as search models, but no reasonable MR solutions were found. We suspected that this was due to the very large unit cell of these crystals, which implies that multiple BamACDE complexes comprise the asymmetric unit. Our search models were, compared to the total mass of two or more Bam complexes, very small, which may explain why attempts at phasing the data using MR failed.

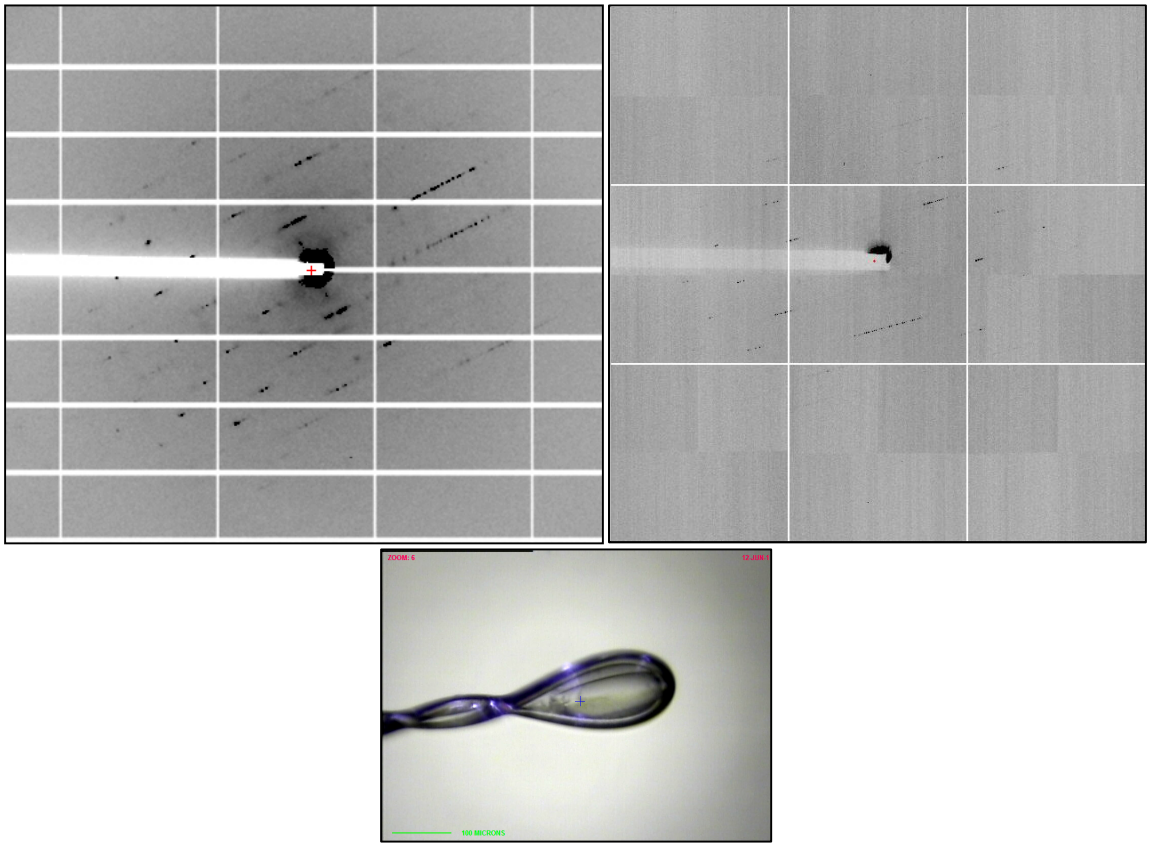

Figure 3.6. A. and **B.** Two representative frames resulting from the irradiation of BamACDE crystals grown in ammonium dihydrogen phosphate, trisodium citrate, and sodium fluoride. **C.** Photo of BamACDE crystal mounted on the 24-ID-E beamline at APS.

SIGMAR (Mosaicity): 0.111°

Asymptotic limit of I/sigma (ISa) = 11.91

	Overall	Inner Shell	Outer Shell
High resolution limit	6.52	20.60	6.52
Low resolution limit	188.97	188.97	6.87
Completeness	99.7	98.7	98.7
Multiplicity	7.4	5.2	7.8
I/sigma	8.6	22.2	1.4
CC(1/2)	0.998	0.997	0.676
Rmerge	0.134	0.066	2.091
Rmerge (anomalous)	0.128	0.064	1.993
Rmeas	0.145	0.073	2.240
Rmeas (anomalous)	0.145	0.074	2.262
Rpim	0.054	0.030	0.790
Rpim (anomalous)	0.068	0.035	1.066
Anomalous completeness	99.5	100.0	97.5
Anomalous multiplicity	4.5	4.7	4.4
Anomalous correlation	0.207	0.361	-0.025
Anomalous slope	1.001	--	--
Total observations	46158	1466	6558
Total unique	6220	280	844

Table 3.2. Crystallographic parameters and statistics associated with crystals grown under the Entry 1 condition in Table 3.1.

Since phasing the data using MR did not work, we prepared a selenomethionine-labeled BamA for experimental phasing. BamA is the largest protein in the Bam complex and contains 14 methionine residues. To obtain a usable signal for phasing requires one selenomethionine per approximately 120 amino acids and the Bam complex as a whole contains roughly 1,400 amino acids, so labeling BamA by itself was expected to be sufficient. SeMet-BamA was overexpressed and purified according to the protocol reported by Van Duyne et al. (see 3.6.7 for the complete method).[19] The BamACDE complex was reconstructed and crystals were grown using the

conditions reported above. Nevertheless, these crystals diffracted to, at best, ~8 Å, which was not high enough resolution to be useful for phasing.

We pursued an additional method in attempts to improve the quality of these crystals. It has been reported that post-crystallization dehydration of crystals can decrease the water content in a crystal, which can improve crystal packing and produce higher resolution data than crystals that had not been dehydrated.[20] Briefly, crystals were removed from their drops and placed into mother liquor in a different well in which the concentration of ammonium dihydrogen phosphate was greater than 800 mM. The new well was sealed and incubated for hours to days, at which point the dehydrated crystal was picked and flash-frozen in liquid N_2. Alternatively, the reservoir solution in a well was removed and replaced with a solution containing ammonium dihydrogen phosphate at a higher concentration than 800 mM, the well was resealed and incubated for hours to several days, and the dehydrated crystals were picked, cryoprotected in mother liquor containing 20% ethylene glycol, and flash-frozen in liquid N_2. None of the crystals that we dehydrated diffracted to a resolution greater than ~12 Å.

While the BamACDE complex had been made purer by enriching the amount of folded BamA in its preparation, A small amount of full-length, undegraded BamC was present in the purified complex (Figure 3.1). In the published structure of a BamCD complex, a large C-terminal loop remained disordered and its structure was unable to be determined.[4] We hypothesized that removal of 10-25 amino acids from the C-terminus of BamC would provide a cleaner purification of BamACDE, removing any full-length BamC (~34 kDa) and leaving only the truncated form (~32 kDa) that appears in preparations of the complex. Constructs lacking 10, 15, 20, and 25 amino acids for the C-terminus of BamC were constructed (Table 3.4) and Bam complexes containing these BamC constructs were purified using the same method as wild-type BamACDE purification. Crystal trays were set using the conditions reported above, but no crystals formed.

3.4.2: Optimizing BamACDE crystals grown in pentaerythritol propoxylate

The shower of crystals depicted in Entry 8 of Table 3.1 formed after 12 hours at 20 °C in a 2:1 protein volume to reservoir volume drop with a total volume of 225 µL. Grid screening across pH, pentaerythritol propoxylate concentration, BamACDE concentration, KCl concentration, drop volumes, ratios of protein volume to reservoir volume, OG concentration, the use of pentarythritol ethoxylate as a precipitant, and additives from the 96-well Hampton Research additive screen gave a reliable crystallization condition that produced fewer, larger Bam complex crystals (Figure 3.7). The newer condition consisted of 100 mM sodium citrate pH 6.2, 35% pentaerythritol propoxylate, and 200 mM KCl, with the Bam complex at 15 mg/mL. Crystals grew after approximately 24 hours.

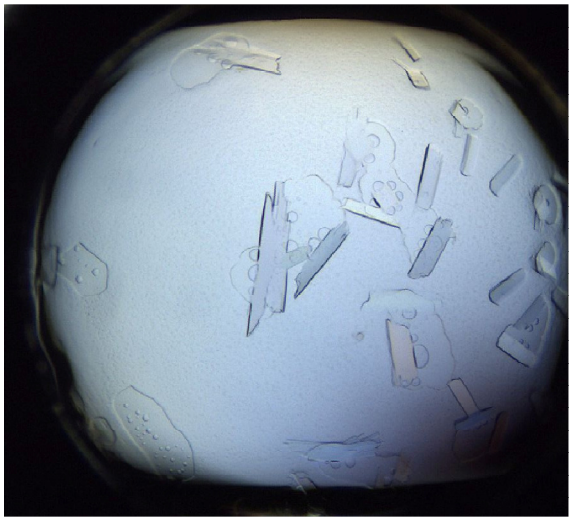

Figure 3.7. Crystals of BamACDE grown in OG bicelles, with reservoir solution consisting of 100 mM sodium citrate pH 6.2, 35% pentaerythritol propoxylate, and 200 mM KCl.

Pentaerythritol propoxylate resembles a branched, short-chain PEG, so we believed that the concentration of this precipitant in the crystallization condition was sufficient to cryoprotect the

crystals during flash-freezing in liquid N_2. Crystals were flash-frozen directly from the drops in which they grew and irradiated at APS (Figure 3.8). Crystals frozen in the fashion described here did not freeze well and diffracted to, at best, ~12 Å. Alternative cryoprotectants such as glycerol, ethylene glycol, and PEG 400 caused the crystals to dissolve in their drops and any crystals that were picked before dissolved did not produce any measurable diffraction.

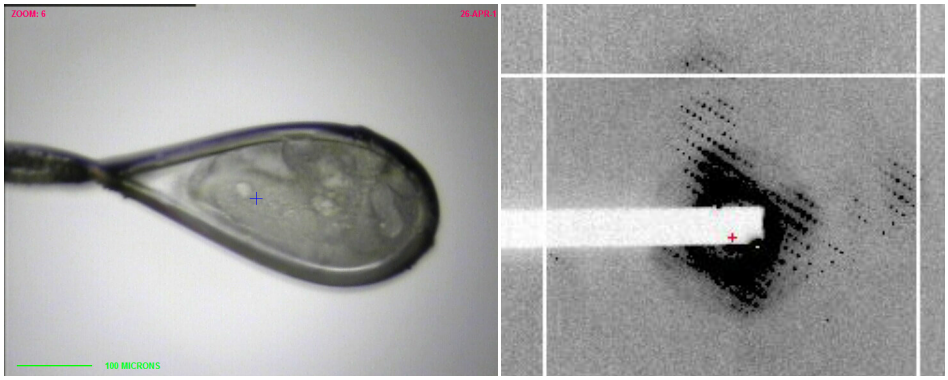

Figure 3.8. Pentaerythritol propoxylate fails to cryoprotect BamACDE crystals grown in 100 mM sodium citrate pH 6.2, 35% pentaerythritol propoxylate, and 200 mM KCl (left). A representative frame from BamACDE crystals grown under these conditions (right).

3.5: Conclusion

While the studies presented in this chapter were being conducted, several groups reported structures of the BamACDE complex and structures of the whole BamABCDE complex from *E. coli* (Figure 3.9).[21,6,22] The expression and purification methods reported by the authors of these papers differ from the protocols that we had employed in several instructive ways. Their procedures relied on the expression of all Bam proteins in one strain of *E. coli* off of a single plasmid. Unlike our method of purification, which relied on three plasmids contained in two *E. coli* strains, the expression of all five Bam proteins in one strain almost ensures that the proteins are expressed in a 1:1:1:1:1 ratio. We pursued the crystallization of BamACDE that was reconstructed from BamA and BamCDE because it could be produced in high yield and it had

been shown to be active in vitro. Our method relied on the refolding of BamA inclusion bodies, which may result in several distinct folding states of BamA that could not be separated from one another. On the other hand, the newly reported methods purify all five Bam proteins from the outer membrane, where their folding state is likely homogenous and active. Along those same lines, the newly reported purification of the BamABCDE complex relied on C_8E_4 in the purification buffer, which we found to dissociate the BamACDE complex (Figure 3.5). Perhaps behavior we observed was due to multiple folding states of BamA following its in vitro refolding, which may have bound more weakly to the Bam lipoproteins than a biologically-assembled BamA.

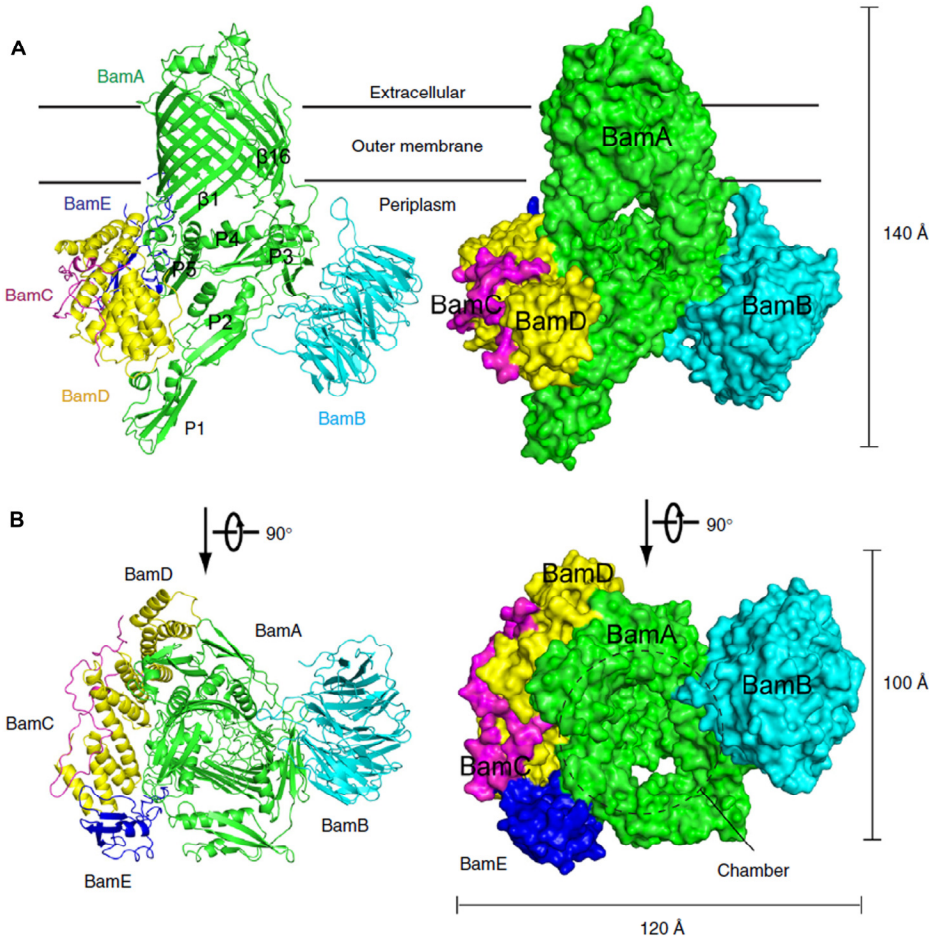

Figure 1.4. The structure of BamABCDE viewed parallel to (**A**) and perpendicular to (**B**) the outer membrane. From ref. 22. pdb:5AYW

The crystal structure of BamABCDE shows that the POTRA domains of BamA form a bent, ring-like structure on the periplasmic face of the complex, which coordinate the Bam lipoproteins and create a cylindrical chamber that may be relevant for the binding of chaperones transporting OMP substrates to the OM. The authors hypothesized that this ring-like structure may rearrange upon a chaperone-OMP complex binding to the Bam proteins, which could cause destabilization of the OM and facilitate the insertion of a folding β-barrel into the outer membrane.[21] Additionally, the BamABCDE complex confirms the unusual arrangement of the N- and C-terminal β-strands of BamA, which demonstrate a misalignment and thus a weaker interaction than other, fully-aligned β-strands in the barrel. Furthermore, POTRA domains 2, 3, and 5 coordinate with the BamA β-barrel at the junction between these terminal strands and form a 16 Å X 42 Å surface hole that may serve as an exit point for OMP substrates. The newly published structures of the Bam complex answer the questions that we had set out to answer: 1) how the POTRA domains of BamA are arranged with respect to the Bam lipoproteins, 2) how the Bam lipoproteins coordinated with respect to the β-barrel of BamA, and 3) if the conformations of the terminal β-strands of BamA suggest a mechanism for OMP assembly. With structures of the Bam complex available, new, structurally-informed biochemical experiments addressing the mechanism of OMP assembly can be devised. Likewise, the detailed understanding of the complex's three-dimensional structure may allow for the rational design of Bam complex inhibitors.

3.6: Materials and Methods

3.6.1: Materials

Unless specified otherwise, cultures were grown in lysogeny broth obtained from Difco, with necessary antibiotics at a concentration of 50 µg/mL and shaken in Innova 44 or New Brunswick Scientific C25KC incubators. n-dodecyl-β-D-maltopyranoside (DDM), n-dodecyl-β-D-maltopyranoside (DM), n-nonyl-β-D-glucopyranoside (NG), tetraethylene glycol monooctyl ether (C8E4), n-octyl-β-D-glucopyranoside (OG), APO-10, Cymal 5, Cymal 6, and lauryldimethylamine-N-oxide (LDAO) were obtained from Anatrace detergents for protein purification were purchased from Anatrace. MbClass I Suite, MbClass II Suite, MemGold, MemGold 2, MemStart, MemSys, MD ProPlex, Nextal ProComplex, Clear Strategy I, Clear Strategy II, MemPlus, and additive screens were obtained from Qiagen, Molecular Dimensions, and Hampton Research. Buffers, salts, and precipitants for crystal growth were purchased from Sigma-Aldrich and Hampton Research. Seeding experiments were performed with a Seed Bead or crystal seeding tool from Hampton Research. ALS pucks for shipping cryo-cooled crystals were purchased from Crystal Positioning Systems. Crystals were grown in 24-well Cryschem Plates or 3-well MRC3 plates from Hampton Research. 3-well trays were set using a Formulatrix NT8 liquid handler and stored at 4 °C or 20 °C in hotels from Formulatrix. Crystals grown in 24-well plates were visualized using a Zeiss Discovery U8 microscope with a Plan S 1.0 X FWD 81 mm objective. An AKTA Pure FPLC system from GE Healthcare Life Sciences was used to conduct size-exclusion and anion-exchange chromatography.

3.6.2: Plasmid construction

Table 3.3 lists the plasmids that were used in these studies and Table 3.4 lists the primers used to generate the plasmids. Any plasmids references in the following methods that do not appear in Table 3.3 can be found and their constructions described in Table 2.7.2.1 in Chapter 2. Restriction

sites and sequence modifications are highlighted by bolding. All genes were amplified from *E. coli* lab strain MC4100.

Table 3.3: List of plasmids

Name	Description	Construction
pSK131	pET22b-bamAΔP1	PCR with primers: p2N2 and bamA-Ce
pSK133	pET22b-bamAΔP1-3	PCR with primers: p4N2 and bamA-Ce
pCH036	pET22b-bamAΔP1-2	PCR with primers: p3N2 and bamA-Ce and then site directed mutagenesis with bamA-G172-5' and bamAG172-3'
pDW053	pCDFDuet-BamC(1-338)-BamD	Site directed mutagenesis in pSK046 with primers: BamC-10aa-for and BamC-10aa-rev
pDW054	pCDFDuet-BamC(1-333)-BamD	Site directed mutagenesis in pSK046 with primers: BamC-15aa-for and BamC-15aa-rev
pDW055	pCDFDuet-BamC(1-328)-BamD	Site directed mutagenesis in pSK046 with primers: BamC-20aa-for and BamC-20aa-rev
pDW056	pCDFDuet-BamC(1-323)-BamD	Site directed mutagenesis in pSK046 with primers: BamC-25aa-for and BamC-25aa-rev
pDW057	pET28b-BamE-His_8	Gibson assembly with empty pET28b and pBamE-His_8 using primers: insert-amp-for, insert-amp-rev, vector-amp-for, and vector-amp-rev

Table 3.4: List of primers

Name	Sequence
p2N2	AGAG**CATATG**GAACGTCCGACCATTGCCAGC
bamA-Ce	ACAC**GCGGCCGC**TTACCAGGTTTTACCGATGTTAAACTG
p4N2	AGAG**CATATG**GATCAGTACAAGCTTTCTGGCGTTG
p3N2	AGAG**CATATG**GTGTCAGCTGAAATCCAGCAAATTAAC
bamA-G172-5'	TATACATATG**GGT**GTGTCAGCTGAAATCCAGCAAATT
bamAG172-3'	GCTGACAC**ACC**CATATGTATATCTCCTTCTTAAAGTT
BamC-10aa-for	CTGGTAGCTGTCTTC**TAG**GCTGCGTTTAGCAAGTAA
BamC-10aa-rev	TTACTTGCTAAACGCAGC**CTA**GAAGACAGCTACCAG
BamC-15aa-for	GTCAGAACGACGCG**TAG**GTAGCTGTCTTCC
BamC-15aa-rev	GGAAGACAGCTAC**CTA**CGCGTCGTTCTGAC
BamC-20aa-for	ATACTCTGACTCAG**TAG**CAGAACGACGCGC
BamC-20aa-rev	GCGCGTCGTTCTG**CTA**CTGAGTCAGAGTAT
BamC-25aa-for	CGATCCGAAAGGT**TAG**ACTCTGACTCAGAG
BamC-25aa-rev	CTCTGAGTCAGAGT**CTA**ACCTTTCGGATCG
insert-amp-for	GGAGATATACCATGCGCTGTAAAACGCTGACTGCTGCAGCAG
insert-amp-rev	GGGCTTTGTTAGTGGTGGTGGTGGTGGTGGTGG
vector-amp-for	ACCACCACTAACAAAGCCCGAAAGGAAGCTGAGTTGGCTG
vector-amp-rev	ACAGCGCATGGTATATCTCCTTCTTAAAGTTAAACAAAATTATTTCT AGAGGGG

3.6.3: Overexpression, purification and refolding of ns-BamA and POTRA truncations of ns-BamA

A 15 mL culture of BL21(DE3) harboring pCH103 (ns-BamA), pSK131 (ns-ΔP1-BamA), pCH036 (ns-ΔP1-2-BamA), or pSK133 (ns-ΔP1-3-BamA) was grown overnight at 37 °C in LB broth with 50 µg/mL carbenicillin. This culture was used to seed 1.5 L of LB with 50 µg/mL carbenicillin, which was grown at 37 °C to OD_{600}=0.7. Protein expression was induced with a final concentration of 100 µM IPTG and the culture was allowed to grow for an additional 4 to 5 hours. Cells were pelleted at 5,250 g. at 4 °C for 10 minutes, then resuspended in 40 mL TBS pH 8.0 with 1 mM PMSF, 50 µg/mL DNAse, 100 µg/mL lysozyme, and 50 µg/mL RNAse. Cells were passed 3 times through a cell disrupter at 15,000 psi. Inclusion bodies were pelleted at 5,000 g. at 4 °C for 10 minutes and the supernatant was discarded. The inclusion bodies were resuspended in 10 mL TBS pH 8.0 to wash them of debris and then repelleted at 5,000 g. at 4 °C for 10 minutes. The inclusion bodies were resuspended and dissolved in 5 mL 8 M urea. To enhance the rate of dissolution, the inclusion bodies were broken up using homogenizer. Any insoluble impurities were pelleted by centrifuging the urea solution for 10 minutes at 20,000 g. at 4 °C. The supernatant was collected and diluted 10-fold into 20 mM Tris-HCl pH 8.0, 0.25% DDM, then nutated overnight at 4 °C to refold the inclusion bodies. This solution was concentrated to a volume of approximately 5 mL in a 50 kDA molecular weight cut off filter. To separate folded from unfolded BamA, this solution was passed through a MonoQ 5/50 GL column on the AKTA pure FPLC in 5 injections of 1 mL, using a 2 mL loop. The loading buffer for the purification consisted of 20 mM bis-tris pH 6.5, 1% octyl glucopyranoside and the elution buffer was composed of 20 mM bis-tris pH 6.5, 1% octyl glucopyranoside, 1 M NaCl, and 1 mM TCEP. At a constant flow rate of 1.3 mL per minute, each run was performed as follows: 5 mL of loading buffer to equilibrate the column, then 5 mL loading buffer to load the sample onto the column, then a 35 mL linear gradient from 0% elution buffer to 35% elution buffer, then 5 mL

100% elution buffer to clean the column of impurities, and then 5 mL of loading buffer to equilibrate the column. Fractions from the main peak were collected and the concentration was measured using elution buffer used as a blank.

3.6.4: Overexpression and purification of BamCDE-His

Two 15 mL cultures of BL21(DE3) harboring pSK046 and pA8H were grown overnight at 37 °C. The following morning, each 15 mL culture was used to inoculate 1.5 LB in a 4 L flask and grown at 37 °C to OD_{600}=0.7. Protein expression was induced with 100 µM final concentration IPTG and grown for an additional 4 to 5 hours. Cells were pelleted at 5,250 g. at 4°C for 10 min., then resuspended in 40 mL TBS pH 8.0 with 1 mM final conc. PMSF, 50 ug/mL Dnase, 100 ug/mL lysozyme, and 50 µg/mL RNAse. Cells were disrupted by passing this suspension three times through a cell disruptor at 15,000 psi. Whole cells and inclusion bodies were pelleted at 5,000 G at 4 °C for 10 minutes. The pellet was discarded and the supernatant containing membrane fragments was ultacentrifuged in a 45 Ti rotor at 100,000 g. at 4 °C for 30 minutes. The supernatant was discarded and the brown membrane pellet was resuspended in 10 mL TBS pH 8.0 with 2% Triton X-100, 10 mM EDTA, 0.1 mg/mL lysozyme. A homogenizer was used to aid in the resuspension of the membrane pellet. Any undissolved pieces of membrane were pelleted at 100,000 g. at 4 °C for 30 minutes in the 45 Ti rotor. The supernatant containing dissolved BamCDE was collected and dialyzed overnight at 4 °C in 3.5 L TBS pH 8.0 with 0.5% Triton X-100. This dialysis step is to remove EDTA from the solution. The concentration of the dialyzed BamCDE solution was assessed, using dialysis buffer as a blank.

3.6.5: Reconstruction of BamACDE-His for crystallographic studies

The dialyzed BamCDE was mixed with the solution of folded BamA in a 10:1 BamCDE:BamA molar ratio in preparation for nickel column purification. 10 mL of Ni-NTA slurry was centrifuged at 10,000 g., the supernatant was discarded and the pelleted resin was washed three

times with 10 mL wash buffer (20 mM tris pH 8.0, 150 mM NaCl, 1% octyl glucopyranoside, 40 mM imidazole, 1 mM TCEP). The BamACDE solution was mixed with the pelleted, washed resin and nutated at 4 °C for 30 minutes to bind the protein complex to the resin. This mixture was poured into a disposable, 30 mL plastic column, then the flow-through was collected and passed through the Ni-NTA resin a second time. The resin was washed twice with 25 mL of wash buffer and the protein complex was eluted using 7.5 mL elution buffer (20 mM tris pH 8.0, 150 mM NaCl, 1% OG, 200 mM imidazole, 1 mM TCEP). The eluate was concentrated to roughly 1 mL in a 100 kDa molecular weight cutoff filter, then passed through a Superdex 200 size-exclusion column at 0.5 mL/minute using 20 mM tris pH 8.0, 150 mM NaCl, 1% OG, 1 mM TCEP in an isocratic elution. Fractions from the main peak were concentrated in a 100 kDa molecular weight cutoff filter.

3.6.6: Limited proteolysis of the Bam Complex

Chymotrypin and trypsin were dissolved in water to concentrations of 1000, 333, 111, 37, 12, and 4 µg/mL. 2 µL of one protease was added to 22 µL of purified BamACDE and incubated at room temperature for 30 minutes. 8 µL 4X SDS loading buffer was added to the sample to quench the reaction, which was then vortexed and incubated at 95 °C. Samples were run in a 4-12% gradient polyacrylamide gel and stained with coomassie to visualize protein fragments.

3.6.7: Overexpression and purification of ns-SeMet-BamA

A 5X concentrated solution of salts for generating minimal M9 media was autoclaved: 64 g sodium phosphate penta-hydrate, 15 g potassium phosphate (dibasic), 2.5 g NaCl, 5 g ammonium chloride were added to 800 mL deionized water and the volume was brought to 1 L with water. After the media was autoclaved and cooled, sterile-filtered reagents were added: 2 mL 1 M magnesium sulfate, 100 µL 1 M $CaCl_2$, and 20 mL 20% glucose. A 10 mL overnight culture of BL21 (DE3) harboring pCH103 was grown in LB with 50 µg/mL carbenicillin. The cells from

the overnight culture were pelleted at 5,000 g. for 10 minutes at 4 °C, then washed with 10 mL minimal M9 media and used to seed 1 L minimal M9 media. This was shaken at 37 °C and grown overnight. The following morning, the culture had grown to OD_{600}=1.2. 50 mg selenomethionine, 100 mg lysine-HCl, 100 mg threonine, 100 mg phenylalanine, 50 mg leucine, 50 mg isoleucine, and 50 mg valine were added to the culture. 15 minutes later, protein expression was induced with 1 mM final concentration IPTG and grown for an additional 8 hours at 37 °C. The cells were pelleted at 5,250 g. for 10 minutes at 4 °C and the pellets were flash-frozen in liquid N_2 for overnight storage at -80 °C. The selenomethionine-labeled ns-BamA was refolded and purified according to the protocol for unlabeled BamA as described in 3.6.3.

3.6.8: Lysine methylation of the Bam complex

BamCDE-His and ns-BamA were purified according to the methods described in 3.6.4 and 3.6.3. 10 mL Ni-NTA resin slurry was applied to a plastic chromatography column and equilibrated with 2X 25 mL wash buffer (1% n-octyl-β-D-glucopyranoside, 50 mM HEPES pH 8.0, 150 mM NaCl, 40 mM imidazole). Purified, refolded ns-BamA was mixed with BamCDE-His in a 1:10 molar ratio and passed through the column two times to enhance the amount of protein complex binding to the resin. 2X 25 mL of wash buffer was passed through the column and the protein complex was eluted using 7.5 mL elution buffer (1% n-octyl-β-D-glucopyranoside, 50 mM HEPES pH 8.0, 150 mM NaCl, 200 mM imidazole. The eluate was concentrated in a 100 kDa molecular weight cut-off filter to a volume of approximately 1 mL, then run isocratically through a Superdex 200 column on an FPLC with a running buffer composed of 50 mM HEPES pH 8.0, 150 mM NaCl, 1% n-octyl-β-D-glucopyranoside to remove imidazole from the sample. Fractions corresponding to the main peak were concentrated to 1 mg/mL in a 100 kDa molecular weight cut-off filter. For every mL of protein solution, 20 µL 1 M dimethylamine-borane complex and 40 µL 1 M formaldehyde were added. The solution was mixed gently and incubated at 4 °C for 2 hours. At that point, an additional 20 µL 1 M dimethylamine-borane complex and 40 µL 1 M

formaldehyde were added for every 1 mL of protein solution and the reaction was nutated at 4 °C overnight. The following morning, the alkylation reaction was quenched using an excess of TBS pH 8.0, 1% n-octyl-β-D-glucopyranoside, 1 mM TCEP. This solution was concentrated to 600 µL in a 100 kDa molecular weight cut-off filter and centrifuged at 4 °C for 10 minutes at 10,000 g. to pellet any precipitated protein. The supernatant was removed and applied to a Superdex 200 column on an FPLC. The protein was eluted using an isocratic method, with the running buffer composed of 20 mM tris pH 8.0, 150 mM NaCl, 1% n-octyl-β-D-glucopyranoside, 1 mM TCEP at a flow rate of 0.5 mL/min. Fractions corresponding to the main peak were collected and concentrated in a 100 kDa molecular weight cut-off filter to the concentration desired for crystallographic experiments.

3.6.9: Preparation of Bam complex bicelles

A 25% w/v solution of 1,2-dimyristoyl-*sn*-glycero-3-phosphocholine (DMPC) and CHAPSO bicelles was prepared by mixing 375.3 mg DMPC with 124.7 mg CHAPSO (a 2.8:1 molar ratio), which was subsequently diluted with water. This suspension was heated at 60 °C and cooled on ice repeatedly, with frequent vortexing, until the lipids had dissolved into solution. At room temperature, this solution forms a gel, while near 4 °C the solution becomes much less viscous. To make the protein bicelles, the bicelle solution was put on ice until the gel became a liquid, at which point the bicelle solution was added to a solution of 12 mg/mL Bam complex in a 1:4 volume ratio, bringing the final bicelle concentration to 5%. This solution was kept on ice for at least 30 minutes and used within several hours to set crystallization trays at room temperature.

3.6.10: Crystallization

Purified Bam complex was concentrated to the appropriate concentration (5-20 mg/mL) in a 100 kDa molecular weight cut-off filter and dispensed into 96-well MRC3 crystallization trays from Hampton Research using a Formulatrix NT8 liquid handler. A reservoir volume of 30 µL was

pipetted and crystallization drops ranged in volume from 200 nL to 1 µL, with variable protein solution:reservoir solution ratios present in the drop. Plates were stored at 4 °C or 20 °C and imaged at regular intervals over the course of a month. When scaling up crystallization conditions, trays were set by hand in CrysChem 24-well trays, using reservoir volumes of 500 µL and drop volumes ranging from 1 µL to 4 µL with various protein volume to reservoir volume ratios.

3.6.11: Collection and analysis of X-ray diffraction data

Crystals were screened for diffraction at 100 K on the 24-ID-E beamline at the Advanced Photon Sources (APS) at the Argonne National Laboratory in Chicago, Illinois. Initial screening for diffraction was done with a 40 µm diameter beam at 40% transmission, taking one pair of exposures for indexing purposes. When crystals did not show significant radiation damage, full 360° datasets were collected. Otherwise, collection recommendations from the beamline software RAPD were followed to obtain datasets. Indexing and scaling of data was performed in XDSGUI and freeR flags were appended to the data using the Import software in the CCP4 software suite. Molecular replacement was conducted using Phaser in Phenix.

3.7: References

1. Kim, Kelly H., et al. "Structural characterization of *Escherichia coli* BamE, a lipoprotein component of the β-barrel assembly machinery complex." *Biochemistry* 50.6 (2011): 1081-1090.

2. Noinaj, Nicholas, et al. "Structural insight into the biogenesis of β-barrel membrane proteins." *Nature* 501.7467 (2013): 385-390.

3. Kim, Kelly H., and Mark Paetzel. "Crystal structure of *Escherichia coli* BamB, a lipoprotein component of the β-barrel assembly machinery complex." *Journal of molecular biology* 406.5 (2011): 667-678.

4. Kim, Kelly H., Suraaj Aulakh, and Mark Paetzel. "Crystal structure of β-barrel assembly machinery BamCD protein complex." *Journal of Biological Chemistry* 286.45 (2011): 39116-39121.

5. Kim, Seokhee, et al. "Structure and function of an essential component of the outer membrane protein assembly machine." *Science* 317.5840 (2007): 961-964.

6. Bakelar, Jeremy, Susan K. Buchanan, and Nicholas Noinaj. "The structure of the β-barrel assembly machinery complex." *Science* 351.6269 (2016): 180-186.

7. Malinverni, Juliana C., et al. "YfiO stabilizes the YaeT complex and is essential for outer membrane protein assembly in *Escherichia coli*." *Molecular microbiology* 61.1 (2006): 151-164.

8. Hagan, Christine L., Seokhee Kim, and Daniel Kahne. "Reconstitution of outer membrane protein assembly from purified components." *Science* 328.5980 (2010): 890-892.

9. Yamaguchi, Hiroshi, and Masaya Miyazaki. "Refolding techniques for recovering biologically active recombinant proteins from inclusion bodies." *Biomolecules* 4.1 (2014): 235-251.

10. Kohyama, Keisuke, Toshihiko Matsumoto, and Taiji Imoto. "Refolding of an unstable lysozyme by gradient removal of a solubilizer and gradient addition of a stabilizer." *Journal of biochemistry* 147.3 (2010): 427-431.

11. Reddy, K., et al. "l-Arginine increases the solubility of unfolded species of hen egg white lysozyme." *Protein Science* 14.4 (2005): 929-935.

12. Tsumoto, Kouhei, et al. "Role of arginine in protein refolding, solubilization, and purification." *Biotechnology progress* 20.5 (2004): 1301-1308.

13. Hagan, Christine L., Thomas J. Silhavy, and Daniel Kahne. "β-Barrel membrane protein assembly by the Bam complex." *Annual review of biochemistry* 80 (2011): 189-210.

14. Vertommen, Didier, et al. "Characterization of the role of the *Escherichia coli* periplasmic chaperone SurA using differential proteomics." *Proteomics* 9.9 (2009): 2432-2443.

15. Hagan, Christine L., David B. Westwood, and Daniel Kahne. "Bam lipoproteins assemble BamA in vitro." *Biochemistry* 52.35 (2013): 6108-6113.

16. Walter, Thomas S., et al. "Lysine methylation as a routine rescue strategy for protein crystallization." *Structure* 14.11 (2006): 1617-1622.

17. Ujwal, Rachna, and James U. Bowie. "Crystallizing membrane proteins using lipidic bicelles." *Methods* 55.4 (2011): 337-341.

18. Sawaya, Michael R. "Methods to refine macromolecular structures in cases of severe diffraction anisotropy." *Structural Genomics: General Applications* (2014): 205-214.

19. Van Duyne, Gregory D., et al. "Atomic structures of the human immunophilin FKBP-12 complexes with FK506 and rapamycin." *Journal of molecular biology* 229.1 (1993): 105-124.

20. Heras, Begona, and Jennifer L. Martin. "Post-crystallization treatments for improving diffraction quality of protein crystals." *Acta Crystallographica Section D: Biological Crystallography* 61.9 (2005): 1173-1180.

21. Han, Long, et al. "Structure of the BAM complex and its implications for biogenesis of outer-membrane proteins." *Nature structural & molecular biology* 23.3 (2016): 192-196.

22. Gu, Yinghong, et al. "Structural basis of outer membrane protein insertion by the BAM complex." *Nature* 531.7592 (2016): 64-69.

Chapter 4: Cocrystallization of *Staphylococcus aureus* PBP2 with Small Molecule Inhibitors

4.1: Introduction

The cell wall of Gram-negative and Gram-positive bacteria is composed of polysaccharide strands that are heavily crosslinked with peptide bridges. This macromolecular mesh, called peptidoglycan (PG), protects the cell from osmotic stress. In Gram-positive bacteria, the PG cell wall resides extracellularly and its thickness ranges from about 20 nm to 50 nm, as revealed by electron micrographs.[1] A set of essential enzymes, peptidoglycan glycosyltransferases (PGTs) and transpeptidases (TP), synthesize PG. Because the cell wall is necessary for cell viability, PGTs and TPs have received considerable attention as antibiotic targets.[2] PGTs are responsible for creating the sugar polymer backbone and TP enzymes crosslink peptide moieties between sugar polymer strands (Figure 4.1). The substrates on which these enzymes act are Lipid II and oligomers of Lipid II, a diphospholipid-linked disaccharide pentapeptide that is synthesized on the intracellular side of the cell membrane and subsequently flipped to the extracellular space before PG synthesis.[3]

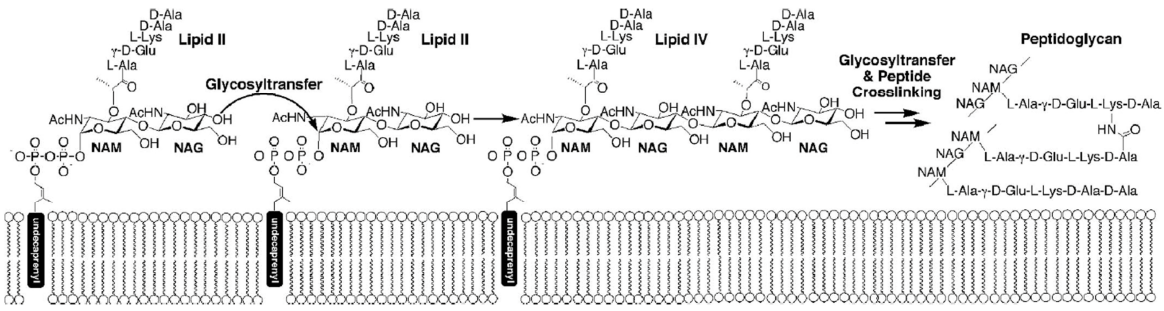

Figure 4.1. Biosynthesis of the cell wall. Lipid II monomers are polymerized by GT enzymes on the extracellular face of the cell membrane into higher-order sugar polymers, consisting of alternating N-acetylmuranic acid (NAM) and N-acetylglucosamine (NAG) sugars. TP enzymes catalyze the crosslinking of these polymers through peptide moieties to form an enormous mesh. Figure is from ref. 11.

PGTs are divided into two classes: 1) bifunctional PGTs consisting of an N-terminal PGT domain that is linked to a C-terminal TP domain, a class of proteins that are known as penicillin-binding proteins (PBPs) and 2) monofunctional PGTs that do not contain a TP domain.[4] An immobilized β-lactam antibiotic such as penicillin pulls down bacterial PBPs, a trait that gave rise to the name of this class of enzymes.[5] β-lactams react with a serine residue in the active site of the TP domain of PBPs, forming a covalent acyl-enzyme adduct that irreversibly inhibits TP function. Although many β-lactam antibiotics have been developed over the last ninety years, bacteria have evolved β-lactamase enzymes, which hydrolyze the β-lactam ring of the antibiotic, rendering it inactive. On the other hand, only one small molecule natural product, moenomycin A (Figure 4.3, top), has been found to bind to the PGT domain of a PBP or a monofunctional PGT.[6] Moenomycin A is an incredibly potent inhibitor of PGT activity with single digit nanomolar affinity, but its poor oral bioavailability prevents it from being a clinically-useful antibiotic.[7]

Staphylococcus aureus expresses only one bifunctional penicillin-binding protein called PBP2. PBP2 consists of an N-terminal cytoplasmic tail, a transmembrane domain, a globular PGT domain, and a C-terminal TP domain. PBP2 is of particular interest because a naturally-occurring mutant form of the protein, PBP2a, renders the organism resistant to β-lactam antibiotics, including methicillin. The active site of PBP2a has a lower affinity for β-lactams than PBP2 and the rate of acylation of PBP2a's active site serine is much slower in PBP2a than in PBP2.[8] The name given to strains of *S. aureus* bearing this mutant allele is methicillin-resistant *Staphylococcus aureus* (MRSA), which can be particularly dangerous. Blood infections with MRSA result in death in 20-40% of patients.[9] Since the TP domain of PBP2a is immune to β-lactam antibiotics and the PGT domains of PBP2 and PBP2a very closely resemble each other, the development of a small molecule inhibitor of the PBP2/PBP2a PGT domain would be invaluable in terms of combating infections with this pathogen.

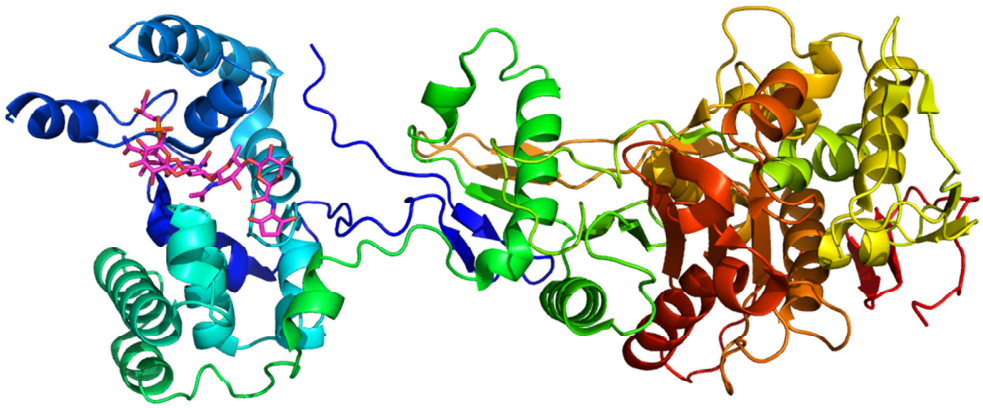

Figure 4.2. Cartoon representation of PBP2(59-716)-His_6, lacking its cytoplasmic and transmembrane domains, bound to moenomycin. The protein in colored from N- (blue) to C- (red) terminus. The PGT domain is depicted on the left and the TP domain is on the right. Moenomycin is represented as sticks. pdb:2olv

Several crystal structures of wild-type PBP2 have been reported and a crystal structure of moenomycin bound to the PGT domain of PBP2 has also been published (Figure 4.2).[10-13] Based on crystal structures of PBP2 in complex with moenomycin A, a former postdoctoral researcher in the Kahne Group, Dr. Christian Gampe, developed a fluorescently-labeled, truncated analog of moenomycin A that bind to the PBP2 PGT domain at the same location as the untagged form of moenomycin A (Figure 4.3).[14] They identified the minimal pharmacophore of moenomycin A (black) and conjugated this molecule with fluorescein. The fluorescently-labeled moenomycin derivative was used in fluorescence polarization assays to identify potential PGT inhibitors. The assay relies on the small molecule probe tumbling slowly in solution when it is bound to a large macromolecule like PBP2 and the unbound probe tumbling at a greater rate. A slowly-tumbling fluorophore will reemit polarized light in the same direction as the incoming light to a greater extent than a quickly-tumbling fluorophore. Thus, small molecules that displace the fluorescent probe from PBP2 are identified by a decrease in polarization.[15]

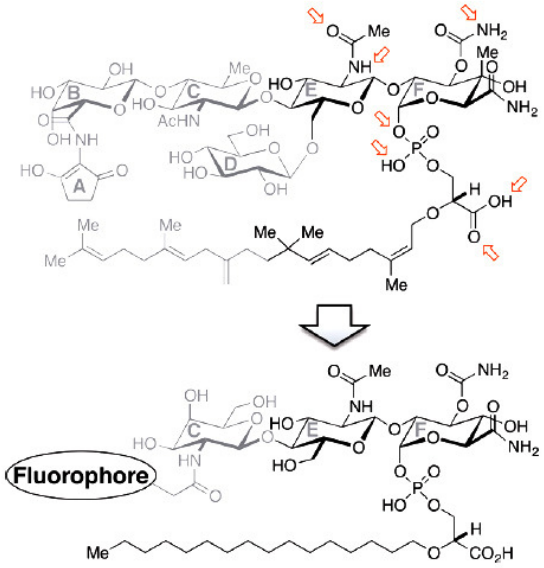

Figure 4.3. Moenomycin A (top) and the small-molecule probe for fluorescence polarization assays (bottom). The pharmacophore of moenomycin is in black, regions of the molecule that do not contribute to PGT binding are in grey, and the red arrows indicate regions of moenomycin that are important for binding to conserved amino acids in the active sites of PGTs. Figure is from ref. 14.

4.2: Crystallization of PBP2 with putative PGT inhibitors

In collaboration with scientists at Evotec, several small molecule inhibitors of PBP2 were found using the fluorescence displacement assay described above (Figure 4.4). Aside from displacing the fluorescent moenomycin probe developed by Gampe et al. in vitro, the molecules had minimum inhibitory concentrations in *S. aureus* between 0.5 µg/mL and 8.0 µg/mL in vivo, suggesting that they could bind to the PGT domain of PBP2, inactivating it and causing cell death. All molecules other than the phosphate-derivatized molecule D in figure 4.4 were very insoluble in water, but all of the molecules were soluble in DMSO.

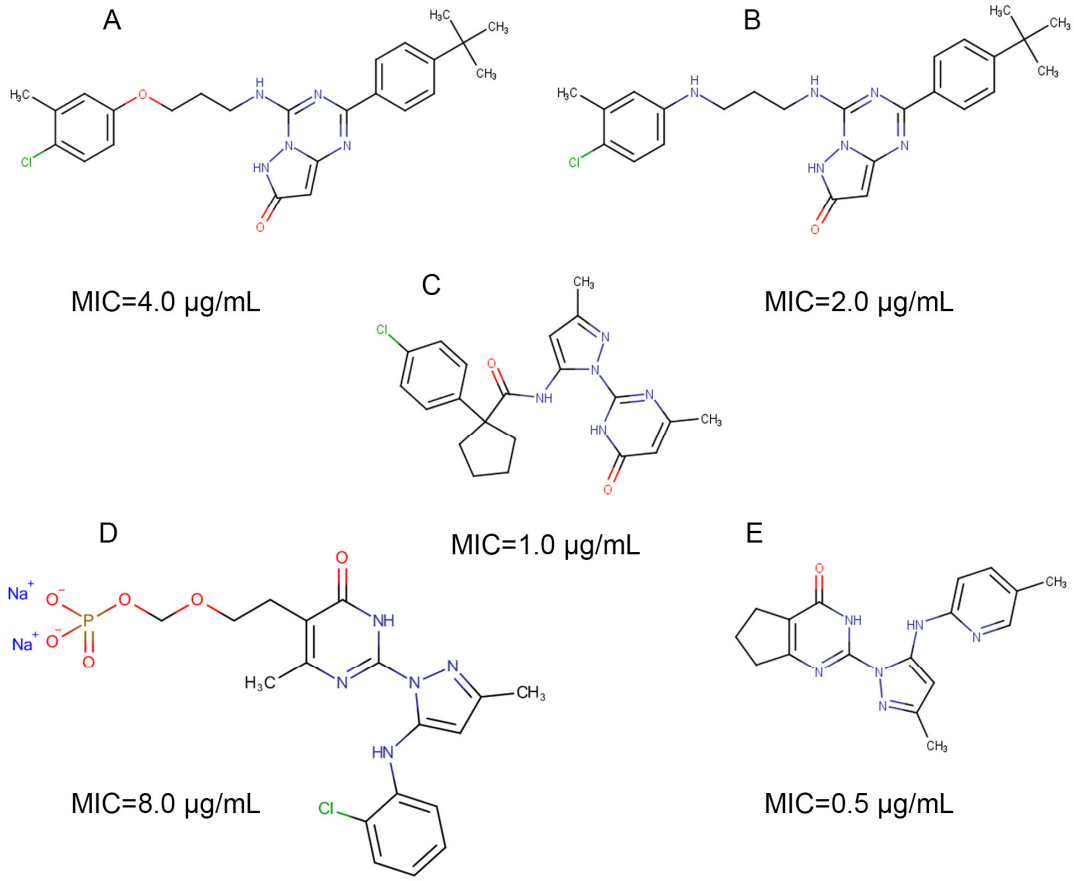

Figure 4.4. Small molecules identified as potential inhibitors of PBP2 PGT activity from a fluorescence displacement assay using a truncated, fluorescein-conjugated moenomycin probe. MIC, minimum inhibitory concentration in *S. aureus*.

We aimed to obtain a crystal structure of PBP2 bound to a small molecule inhibitor identified in this screen. We were interested in recreating the PBP2 crystals reported by Lovering et al. before attempting to cocrystallize small molecules with PBP2. We used the same PBP2(59-716)-His_6 construct that had been reported, which lacks the N-terminal transmembrane domain, resulting in cytoplasmic expression of the protein.[13] In brief, PBP2(59-716)-His_6 was overexpressed at 15 °C in *S. aureus* overnight, cells were lysed, whole cells were pelleted, and the supernatant was passed through Ni-NTA resin. PBP2(59-716)-His_6 was eluted from the nickel column, passed

through a Superdex 200 size-exclusion column, and finally purified by anion-exchange chromatography on a MonoQ column (Figure 4.5). Purified PBP2(59-716)-His_6 was concentrated to 18 mg/mL and pipetted by hand into 0.5 µL protein solution + 0.5 µL reservoir solution (100 mM HEPES pH 7.0, 0.55 M KCl, 9% (w/v) PEG 8000) drops in a ChrysChem 24-well sitting drop crystallization tray. After a couple of days, crystal plates formed in small, circular clusters (Figure 4.6).

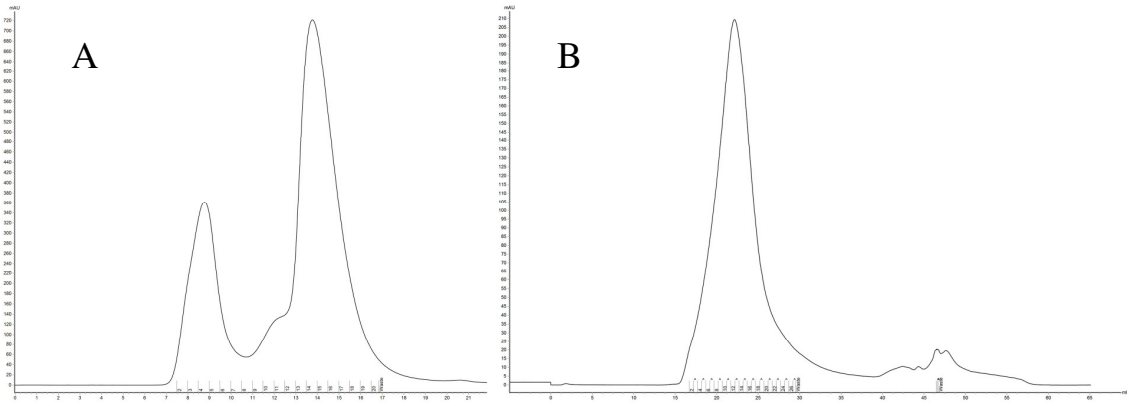

Figure 4.5. A. Size-exclusion chromatogram of PBP2(59-716)-His_6 purification on Superdex 200 column. **B.** Anion-exchange chromatogram of PBP2(59-716)-His_6 purification on MonoQ column.

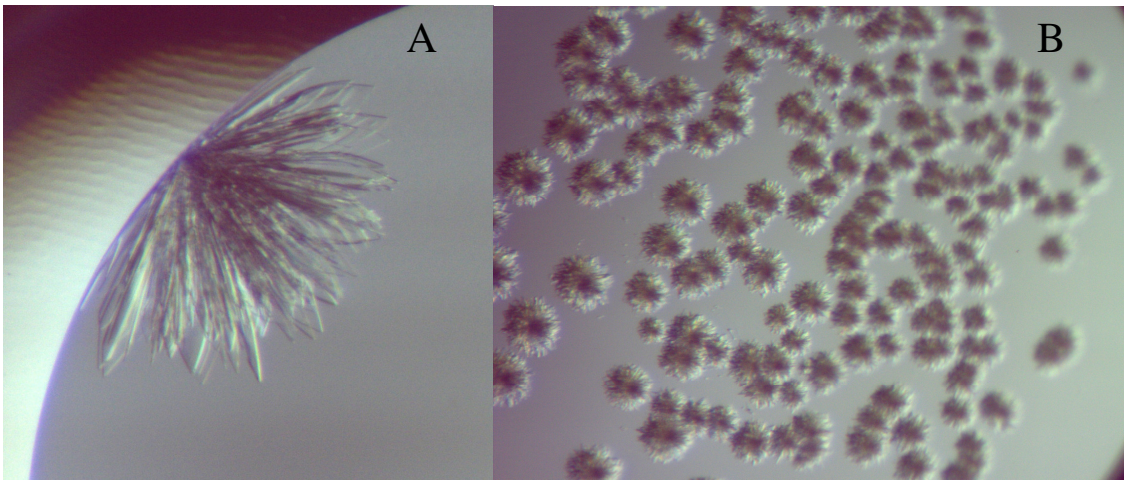

Figure 4.6. PBP(59-716)-His_6 crystals grown in 100 mM HEPES pH 7.0, 0.55 M KCl, 9% (w/v) PEG 8000. **A.** Fanned, overlapping crystal plates rarely grew to the ~75 µm long crystals shown here. **B.** More frequently, a shower of crystal pinwheels formed. Crystals were grown by Jeep Srisuknimit.

Crystals were cryoprotected by serial addition of mother liquor containing 20% ethylene glycol to the crystal drop, through which the PBP2(59-716)-His_6 crystals were picked. Crystals were immediately flash-frozen in liquid N_2 and irradiated at 100 K at APS. Results from a 2.9 Å dataset are presented in Figure 4.7 and Table 4.1, though ice formation during freezing occurred far more frequently than the clear freeze demonstrated below.

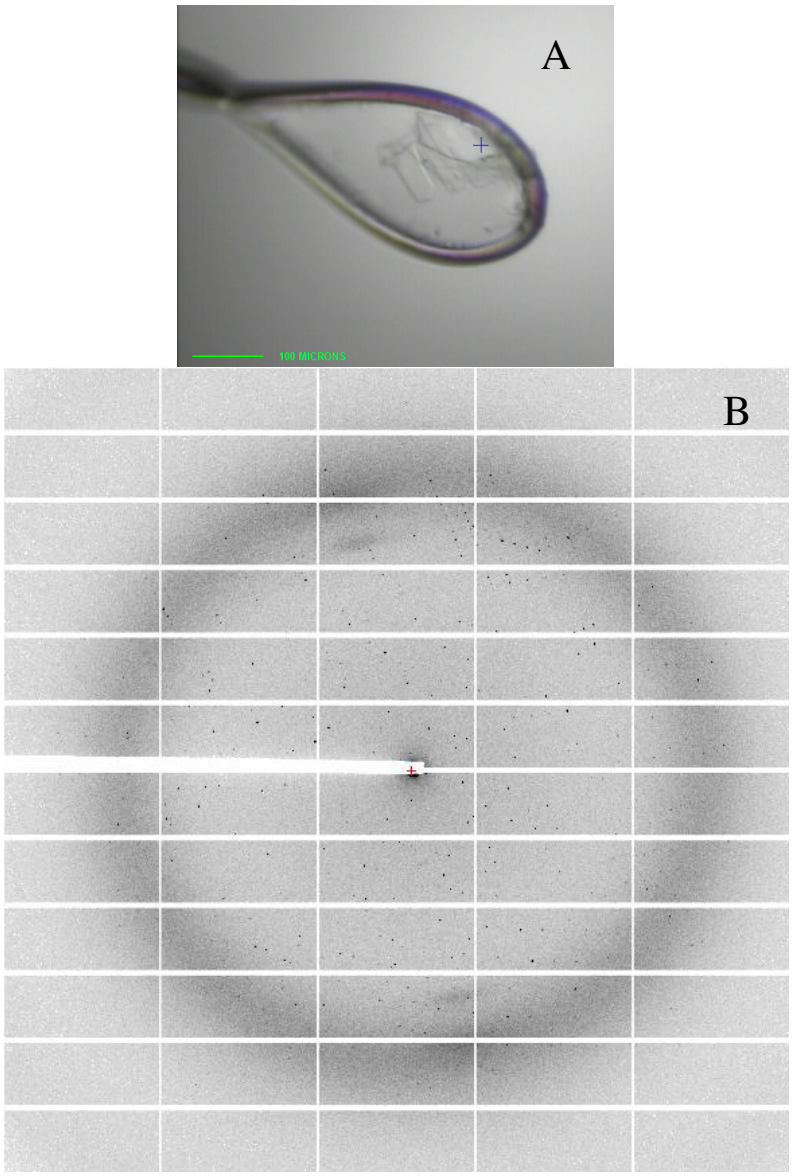

Figure 4.7. A. PBP2(59-716)-His_6 crystals mounted on the 24-ID-E line at APS. Crystals froze clear. **B**. A representative frame from a 2.9 Å dataset. Crystals were grown by Jeep Srisuknimit.

Spacegroup: C 2 2 21
Unit Cell: 70.17 246.8 101.8 90 90 90
SIGMAR (Mosaicity): 0.10969°
Asymptotic limit of I/sigma (ISa) = 23.44

	Overall	Inner Shell	Outer Shell
High resolution limit	2.96	8.88	2.96
Low resolution limit	78.51	78.51	3.14
Completeness	98.0	95.4	97.7
Multiplicity	3.0	2.9	3.0
I/sigma	7.0	21.4	1.5
CC(1/2)	0.981	0.999	0.631
Rmerge	0.170	0.039	0.774
Rmerge (anomalous)	0.139	0.036	0.650
Rmeas	0.205	0.048	0.933
Rmeas (anomalous)	0.188	0.048	0.878
Rpim	0.112	0.026	0.509
Rpim (anomalous)	0.125	0.031	0.585
Anomalous completeness	86.7	89.5	83.8
Anomalous multiplicity	1.5	1.6	1.4
Anomalous correlation	0.139	0.054	0.142
Anomalous slope	1.046	--	--
Total observations	55712	2112	8793
Total unique	18405	722	2937

Table 4.1. Crystallographic parameters and statistics for the dataset from which Figure 4.7 B. was generated.

Because we were recreating the crystallization condition of PBP2(59-716)-His_6 that had been reported previously, APS beamline software was able to solve the dataset presented in Table 4.1 automatically by molecular replacement. The space group into which our protein packed and the unit cell dimensions of the crystal matched those of the apoenzyme structure reported previously.[13] Having reproduced high-resolution crystals of PBP2(59-716)-His_6, we began

cocrystallization and soaking experiments with the small molecules presented in Figure 4.4. and Lipid II monophosphate, which has been shown to inhibit PBP2 in vitro.[16] General methods were informed by work reported by Hassell et al.[17]

All but one of the small molecules provided by the researchers at Evotec were insoluble in water, which made soaking them into crystals or setting up cocrystallization experiments particularly difficult. The addition of DMSO-dissolved compound A, B, C, or E to a solution of protein caused the compound to crash out of solution immediately. Despite these difficulties, we took several approaches to obtain PBP2(59-716)-His_6 cocrystals with the small molecules. 1) Protein solutions were nutated overnight with an inhibitor at a 1:1, 1:2, 1:5, or 1:10 protein:inhibitor molar ratio. Although the putative inhibitors crashed out, we hypothesized that enough of the small molecule would dissolve into solution and associate with the protein. The following morning, undissolved compound was pelleted, the protein was concentrated to 18 mg/mL, and crystal trays were set. 2) We found that the addition of DMSO-dissolved inhibitor to a crystal drop did not disrupt the already-formed crystals, although the added small molecule quickly precipitated. Because the crystals themselves appeared stable, we set up soaking experiments. A putative inhibitor was diluted in DMSO so that a 0.5 µL addition of the solution to a crystal drop would deliver the small molecule in a 10:1 inhibitor:protein molar ratio. These crystallization wells were resealed and incubated for up to 24 hours before crystals were cryoprotected and flash-frozen. 3) Finally, we performed fast soaks by serially transferring a crystal into increasingly concentrated cryoprotectant solutions containing one of the putative inhibitors. This gave the crystal exposure to dissolved compound for less than one minute. Crystals were picked from the final cryoprotectant solution and flash-frozen in liquid N_2. Although many small crystals formed from the screening methods listed above none diffracted to a resolution comparable to that of the published apoenzyme structure and no structures were able to be solved from datasets that were collected from these crystals.

4.3: Conclusion

PBP2(59-716)-His_6 does not reliably crystallize under the conditions reported above. Based on grid screening of PBP2(59-716)-His_6 crystallization conditions, the protein remains stable at high concentrations and may have a greater propensity to form crystals if it is crystallized above 20 mg/mL. Likewise, cryoprotecting the PBP2(59-716)-His_6 crystals using the method reported in section 4.2 nearly always causes ice crystals to form during flash-freezing. Extensive screening of cryoprotectants and alternative methods of cryoprotection are required in order to find conditions that will freeze clear.

The results presented in this chapter represent a small step toward the development of PBP inhibitors that affect the function of the PGT domain of PBP2. Further small molecule screening using the moenomycin A probe in Figure 4.3 could lead to the discovery of additional small molecule inhibitors. Moenomycin A is the only known small molecule to inhibit this essential function of PBPs, but due to its poor pharmacological features, finding an alternative would be of great service to human health. Crystal structures of novel PGT inhibitors bound to PBP2 would show if the inhibitory mechanism of moenomycin A is the preferred binding mode or if there are alternative sites for inhibiting the protein's activity. These studies would enable the development of much needed antibiotics to treat this pathogen.

4.4: Materials and methods

4.4.1: Materials

Unless stated otherwise, all chemicals were obtained from Sigma Aldrich and, unless specified otherwise, all cultures were grown in lysogengy broth (LB) obtained from Difco, with antibiotics at a concentration of 50 µg/mL. Cultures were grown in Innova 44 incubators and pelleted using a Beckman Coulter J6-Mi floor centrifuge or a 5810 R desktop centrifuge from Eppendorf. Ni-NTA resin for protein purifications was obtained from Qiagen. Affinity chromatography was performed in Poly-Prep Chromatography Columns from Bio-Rad. Protein concentrations were determined using a Thermo Scientific NanoDrop 2000 UV/vis spectrometer. Purification of PBP2 was performed on a GE AKTA Pure FPLC using a Superdex 200 10/30 GL gel filtration column and a MonoQ 5/50 GL anion-exchange column. *E. coli* phospholipids for the formation of proteoliposomes were purchased from Avanti. Homogenization of membrane pellets and inclusion bodies was performed using an IKA T18 basic ULTRA-TURRAX homogenizer.

4.4.2: Overexpression and purification of PBP2

12 X 1.5 L LB were autoclaved and a 200 mL culture of LB with 50 µg/mL kanamycin was seeded with an *S.* aureus strain expressing PBP2(59-716) for overnight growth. The following morning, 1.5 mL 50 mg/mL kanamycin was added to each 1.5 L flask, which were each inoculated with 15 mL of the overnight culture. Cells were grown at 37 °C, shaking, until OD_{600}=0.4-0.5, at which point the incubator's temperature was reduced to 15 °C. Once the temperature of the shaker equilibrated to 15 °C, 750 µL of 1 M IPTG was added to each flask to induce protein expression. Cells were grown overnight and pelleted the following morning at 5,000 g. for 15 minutes at 4 °C. Cells were resuspended in TBS pH 8.0 and repelleted at 5,000 g. for 15 minute at 4 °C. Cell pellets were resuspended in 40 mL 10 mM tris pH 8.0, 1 M NaCl, 10 mM $MgCl_2$, 10% v/v glycerol, 40 mM CHAPS, 100 µg/mL DNase, and 1 mM PMSF. Cells were lysed by 3 passes through a cell disrupter at 15,000 psi and any unlysed cells were pelleted by

ultracentrifugation at 37,000 g. for 30 minutes at 4 °C. 3 mL Ni-NTA resin was loaded onto a plastic Poly-Prep column and equilibrated with 2X 25 mL wash buffer (10 mM tris pH 8, 200 mM NaCl, 40 mM imidazole, and 0.28 mM LDAO). The supernatant from the ultracentrifugation run was passed through the Ni-NTA resin twice and the resin was washed with 2X 25 mL wash buffer. Protein was eluted with 30 mL elution buffer (10 mM tris pH 8, 200 mM NaCl, 200 mM imidazole, and 0.28 mM LDAO). This eluate was concentrated to ~7-10 mL in a 50 kDa molecular weight cut-off filter at 4,000 and 4 °C. 1 mL injections onto a Superdex 200 column, with an isocratic run using 20 mM imidazole, 10 mM tris pH 8, 0.28 mM LDAO as the running buffer removed imidazole from the protein solution and any contaminating proteins. Fractions from this size-exclusion run were concentrated in a 50 kDa molecular weight cut-off filter until the protein concentration was ~8 mg/mL. A MonoQ 5/50 GL column was equilibrated with running buffer (10 mM tris pH 8, 0.28 mM LDAO) and the concentrated size-exclusion fractions were injected onto the column 1 mL at a time. Line A was connected to running buffer and line B was connected to elution buffer (10 mM tris pH 8, 0.28 mM LDAO, 500 mM NaCl). The run conditions for anion exchange were as follows, with the flow rate at 1 mL/min.: 1) 5 mL 100% wash buffer, 2) 10 mL of sample application with 100% wash buffer, 3) 3 mL linear gradient to 10% elution buffer, 4) 25 mL linear gradient to 14% elution buffer, 5) 5 mL linear gradient to 40% elution buffer, 6) 5 mL linear gradient to 100% elution buffer, 7) 5 mL 100% elution buffer, and 8) 10 mL 100% wash buffer to reequilibrate the column. The largest peak corresponded to PBP2(59-716), which eluted at ~60 mM NaCl. Fractions corresponding to this peak were concentrated in a 50 kDa molecular weight cut-off filter to the desired concentration for crystallization.

4.4.3: Crystallization

Purified PBP2 was concentrated to 18 mg/mL in a 50 kDa molecular weight cut-off filter and dispensed by hand into CrysChem 24-well trays, using reservoir volumes of 500 µL and drop

volumes ranging from 1 µL to 4 µL with protein volume to reservoir volume ratios of 1:1, 1.5:1, and 2:1. Trays were set at room temperature and crystals were grown for several days.

4.4.4: Collection and analysis of X-ray diffraction data

Crystals were screened for diffraction at 100 K on the 24-ID-E beamline at the Advanced Photon Sources (APS) at the Argonne National Laboratory in Chicago, Illinois. Initial screening for diffraction was done with a 40 µm diameter beam at 40% transmission, taking one pair of exposures for indexing purposes. When crystals did not show significant radiation damage, full 360° datasets were collected. Otherwise, collection recommendations from the beamline software RAPD were followed to obtain datasets. Indexing and scaling of data was performed in XDSGUI and freeR flags were appended to the data using the Import software in the CCP4 software suite. Molecular replacement was conducted using Phaser in Phenix.

4.5: References

1. Shockman, Gerald D., and J. F. Barren. "Structure, function, and assembly of cell walls of gram-positive bacteria." *Annual Reviews in Microbiology* 37.1 (1983): 501-527.

2. Silver, Lynn L. "Challenges of antibacterial discovery." *Clinical microbiology reviews* 24.1 (2011): 71-109.

3. Ruiz, Natividad. "Lipid Flippases for Bacterial Peptidoglycan Biosynthesis." *Lipid insights* 8.Suppl 1 (2015): 21.

4. Goffin, Colette, and Jean-Marie Ghuysen. "Multimodular penicillin-binding proteins: an enigmatic family of orthologs and paralogs." *Microbiology and Molecular Biology Reviews* 62.4 (1998): 1079-1093.

5. Spratt, Brian G. "Properties of the Penicillin-Binding Proteins of *Escherichia coli* K12." *European Journal of Biochemistry* 72.2 (1977): 341-352.

6. Ostash, Bohdan, and Suzanne Walker. "Bacterial transglycosylase inhibitors." *Current opinion in chemical biology* 9.5 (2005): 459-466.

7. Goldman, Robert C., and David Gange. "Inhibition of transglycosylation involved in bacterial peptidoglycan synthesis." *Current medicinal chemistry* 7.8 (2000): 801-820.

8. Peacock, Sharon J., and Gavin K. Paterson. "Mechanisms of methicillin resistance in *Staphylococcus aureus*." *Annual review of biochemistry* 84 (2015): 577-601.

9. Lowy, Franklin D. "Antimicrobial resistance: the example of *Staphylococcus aureus*." *The Journal of clinical investigation* 111.9 (2003): 1265-1273.

10. Sung, Ming-Ta, et al. "Crystal structure of the membrane-bound bifunctional transglycosylase PBP1b from *Escherichia coli*." *Proceedings of the National Academy of Sciences* 106.22 (2009): 8824-8829.

11. Yuan, Yanqiu, et al. "Crystal structure of a peptidoglycan glycosyltransferase suggests a model for processive glycan chain synthesis." *Proceedings of the National Academy of Sciences* 104.13 (2007): 5348-5353.

12. Heaslet, Holly, et al. "Characterization of the active site of *S. aureus* monofunctional glycosyltransferase (Mtg) by site-directed mutation and structural analysis of the protein complexed with moenomycin." *Journal of structural biology* 167.2 (2009): 129-135.

13. Lovering, Andrew L., et al. "Structural insight into the transglycosylation step of bacterial cell-wall biosynthesis." *Science* 315.5817 (2007): 1402-1405.

14. Gampe, Christian M., et al. "Tuning the moenomycin pharmacophore to enable discovery of bacterial cell wall synthesis inhibitors." *Journal of the American Chemical Society* 135.10 (2013): 3776-3779.

15. Kuru, Erkin, et al. "In situ probing of newly synthesized peptidoglycan in live bacteria with fluorescent D-amino acids." *Angewandte Chemie International Edition* 51.50 (2012): 12519-12523.

16. Dumbre, Shrinivas, et al. "Synthesis of modified peptidoglycan precursor analogues for the inhibition of glycosyltransferase." *Journal of the American Chemical Society* 134.22 (2012): 9343-9351.

17. Hassell, Anne M., et al. "Crystallization of protein–ligand complexes." *Acta Crystallographica Section D: Biological Crystallography* 63.1 (2007): 72-79.

Appendix 1: Bam Lipoproteins Assemble BamA in Vitro

The following pages are reprinted (adapted) with permission from

Hagan, Christine L., David B. Westwood, and Daniel Kahne. "Bam lipoproteins assemble BamA in vitro." *Biochemistry* 52.35 (2013): 6108-6113.

BIOCHEMISTRY
including biophysical chemistry & molecular biology

Article

pubs.acs.org/biochemistry

Bam Lipoproteins Assemble BamA *in Vitro*

Christine L. Hagan,[†] David B. Westwood,[†] and Daniel Kahne*[,†,‡]

[†]Department of Chemistry and Chemical Biology, Harvard University, Cambridge, Massachusetts 02138, United States

[‡]Department of Biological Chemistry and Molecular Pharmacology, Harvard Medical School, Boston, Massachusetts 02115, United States

Supporting Information

ABSTRACT: The Bam machine assembles β-barrel membrane proteins into the outer membranes of Gram-negative bacteria. The central component of the Bam complex, BamA, is a β-barrel that is conserved in prokaryotes and eukaryotes. We have previously reported an *in vitro* assay for studying the assembly of β-barrel proteins by the Bam complex and now apply this assay to identify the specific components that are required for BamA assembly. We establish that BamB and BamD, two lipoprotein components of the complex, bind to the unfolded BamA substrate and are sufficient to accelerate its assembly into the membrane.

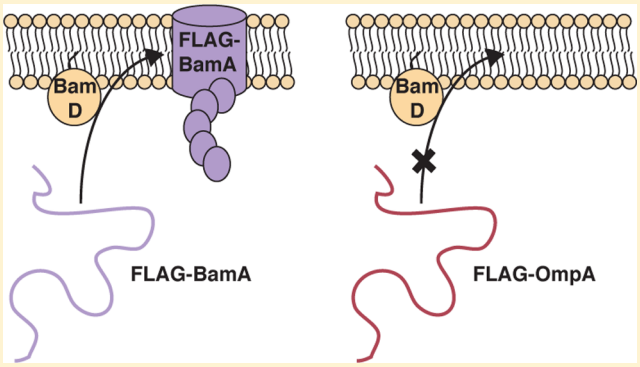

The outer membranes (OMs) of Gram-negative bacteria contain transmembrane proteins with β-barrel structure. These proteins are synthesized in the cytoplasm with N-terminal signal sequences, which target them for secretion across the inner membrane (IM) via the Sec machine.[1−3] They are then transported in complex with chaperones across the aqueous periplasmic compartment between the membranes and are finally assembled in the OM by the β-barrel assembly machine (Bam).[4] The *Escherichia coli* Bam complex contains two proteins that are essential for cell viability: an integral membrane β-barrel, BamA, and an OM lipoprotein, BamD, which is anchored to the membrane by an N-terminal lipid and which binds to the soluble region of BamA that extends into the periplasm.[5−7] Three other lipoproteins, BamB, -C, and -E, associate with these two proteins but are not essential.[5,8−10] The mechanism of β-barrel assembly is believed to be highly conserved because orthologs of BamA are found in all organisms that contain β-barrels.[11−16] However, very little is known about how that mechanism proceeds; it is thought to involve multiple steps, including substrate recognition, folding, and membrane insertion, but it is not clear how the components of the Bam complex accomplish those steps.

We have reconstituted the process of β-barrel assembly *in vitro* from purified components and now make use of this system to dissect the Bam complex and observe the effects of its individual components.[17,18] We chose to study the assembly of BamA because it is an essential outer membrane protein (OMP), and given that its function is to assemble other OMPs, we hypothesized that its assembly mechanism might reveal or reflect aspects of how it functions in the more general OMP assembly process. Through this analysis, we have determined that BamB and BamD bind to unfolded substrates.

EXPERIMENTAL PROCEDURES

Protein Expression and Purification. The methods used to express and purify the proteins used in this study are described in the Supporting Information.

Proteoliposome Preparation. Proteoliposomes containing the Bam complex and Bam subcomplexes were prepared by the detergent dilution methods described previously.[18] Briefly, *E. coli* phospholipids (40 μL of a 20 mg/mL sonicated aqueous suspension) were added to the purified Bam complexes (200 μL of 10 μM solutions) in TBS (pH 8), 0.03% DDM, and 1 mM TCEP and incubated on ice for 5 min. These phospholipid/detergent/protein complex mixtures were then diluted with 8 mL of TBS (pH 8) and incubated on ice for 30 min. They were then ultracentrifuged at 300000*g* for 2 h at 4 °C. The pelleted proteoliposomes were resuspended in 200 μL of TBS (pH 8). Empty liposomes were prepared in parallel with these proteoliposomes by the same detergent dilution method, simply omitting the Bam proteins. Liposomes and proteoliposomes that were not used immediately were flash-frozen in liquid nitrogen and stored at −80 °C.

Folding Assays. *Folding into Bam Proteoliposomes.* The unfolded FLAG-BamA or FLAG-OmpA substrate was prepared at a concentration of 5 μM in 8 M urea and then diluted 10-fold into solutions containing empty liposomes or the Bam proteoliposomes. The proteoliposomes were also diluted 4-fold from their stock concentrations into these reaction mixtures. A typical reaction mixture contained 2.5 μL of liposomes or proteoliposomes, 6.5 μL of TBS (pH 8), and 1 μL

Received: July 2, 2013
Revised: August 6, 2013
Published: August 6, 2013

dx.doi.org/10.1021/bi400865z | *Biochemistry* 2013, 52, 6108−6113

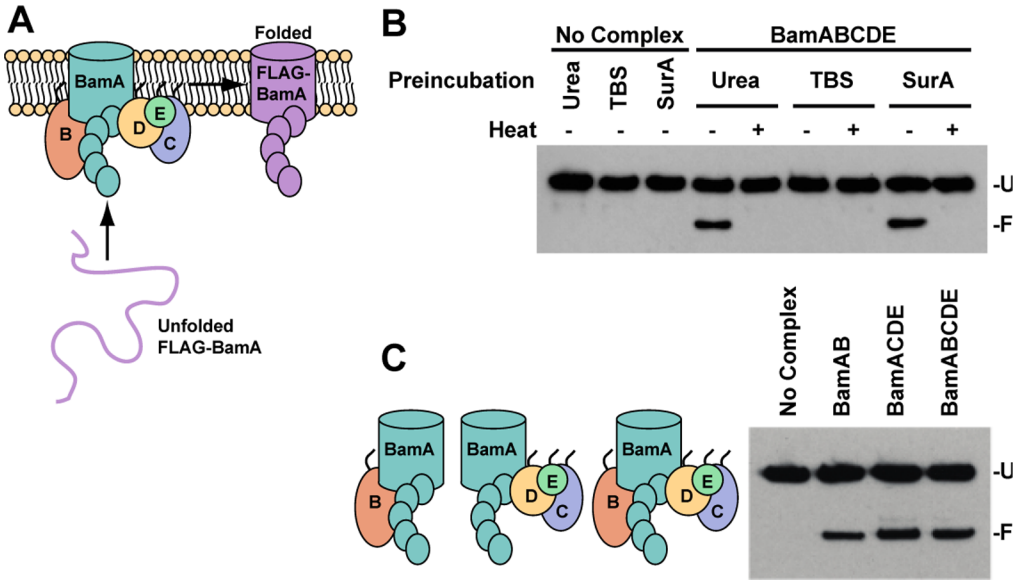

Figure 1. BamA can be folded by a minimal set of OMP assembly components. (A) Schematic of the experimental design. The purified Bam complex is incorporated into liposomes composed of *E. coli* phospholipids, and unfolded FLAG-tagged BamA is added to these proteoliposomes with or without a chaperone. (B) Urea and SurA maintain the folding competence of BamA equally well. FLAG-BamA was prepared in 8 M urea and then diluted directly into empty liposomes or proteoliposomes containing the Bam complex, or the denatured substrate was first incubated in solutions of Tris-buffered saline (TBS) or SurA and then added. The final concentrations of the substrate and SurA were 0.5 and 5 μM, respectively. The reactions were stopped after 60 min, and the products were analyzed by SDS−PAGE and immunoblotting with anti-FLAG antibodies. (C) Bam subcomplexes lacking the lipoproteins demonstrate activity similar to that of the complete complex in assembling full-length FLAG-BamA (U, unfolded FLAG-BamA; F, folded FLAG-BamA).

of 5 μM substrate such that the final concentrations of the substrate and Bam complex were 0.5 and ~2.5 μM, respectively. If the experiment included a preincubation, the substrate was first diluted 10-fold from a 50 μM solution in 8 M urea to a solution of TBS (pH 8) or purified SurA in TBS (pH 8) and incubated at 25 °C for 10 min. These preincubated solutions were then diluted 10-fold into the proteoliposomes. Unless noted otherwise in the figures, the concentrations of SurA and the substrates were 50 and 5 μM, respectively, in the preincubation and 5 and 0.5 μM, respectively, in the final reaction mixtures. Reactions were stopped after incubation at 25 °C for 60 min (unless noted otherwise in the figures) by adding ice-cold 2× SDS sample loading buffer [125 mM Tris (pH 6.8), 4% SDS, 30% glycerol, 0.005% bromophenol blue, and 5% β-mercaptoethanol]. For the time course experiments, aliquots of the reaction mixtures were removed at the indicated time points, quenched by the same method, and kept on ice. All quenched samples were subjected to sodium dodecyl sulfate−polyacrylamide gel electrophoresis (SDS−PAGE) (4 to 20% gel) at 150 V for 110 min at 4 °C. The proteins were transferred from the gel to a PVDF membrane by semidry transfer in 25 mM Tris-HCl and 192 mM glycine (pH 8.3) at 10 V for 1 h. The products of the reaction were detected by immunoblotting with FLAG-HRP antibodies (used at a dilution of 1:200000). The blot images were scanned, and ImageQuant TL was used to calculate the densities of the observed bands. The percent yields of folded protein were determined by comparing the densities of the unfolded and folded bands in each lane.

Folding in Detergent. FLAG-tagged substrate proteins were prepared at a concentration of 5 μM in 8 M urea. They were then diluted 10-fold into a solution of TBS (pH 8) and 0.5% LDAO and incubated at 25 °C for 1 h. The folding reactions were stopped with 2× SDS sample loading buffer. The quenched samples were subjected to SDS−PAGE and immunoblotted as described in the previous section.

Folded Chimeric BamA Affinity Purification. FLAG-tagged wild-type and mutant BamA substrates were prepared at a concentration of 100 μM in 8 M urea. These substrates were then diluted 10-fold into TBS (pH 8) and 0.5% LDAO and incubated at 25 °C for 60 min to allow their β-barrels to fold. Concentrated, purified BamCDE-His$_6$ complex was then added to each of the folded substrates to a final concentration of 10 μM. Aliquots of these mixtures were removed and used as "input" samples for SDS−PAGE analysis. The remainder of each mixture was subjected to Ni-NTA affinity chromatography in TBS (pH 8) and 0.05% DDM. Proteins in the eluates were precipitated with 10% trichloroacetic acid and incubated on ice for 30 min. These samples were then centrifuged at 18000*g* for 10 min at 4 °C, and the pellets were resuspended in 1 M Tris (pH 8) and 2× SDS sample loading buffer. The input and these "eluate" samples were subjected to SDS−PAGE on a 4 to 20% gradient gel at 200 V for 45 min. The proteins were then detected by staining with Coomassie blue.

Unfolded Substrate Affinity Purifications. Urea-denatured FLAG-BamA and FLAG-OmpA were prepared at a concentration of 100 μM and subsequently diluted 10-fold into a solution of soluble BamB-His$_6$, BamD-His$_6$, or BamE-His$_6$ in TBS (pH 8) and incubated at room temperature for 10 min. The final concentrations of the unfolded OMP and the soluble Bam proteins were 10 and 100 μM, respectively. A small aliquot of each of these mixtures was removed for use as an input sample. The remainder of the mixture was subjected to Ni-NTA affinity purification; after the material had been loaded on the column, it was washed with TBS (pH 8) with 20 mM imidazole, and the bound proteins were eluted in TBS (pH 8) with 200 mM imidazole. Proteins in the eluates were precipitated with 10% trichloroacetic acid and resuspended in

dx.doi.org/10.1021/bi400865z | *Biochemistry* 2013, 52, 6108−6113

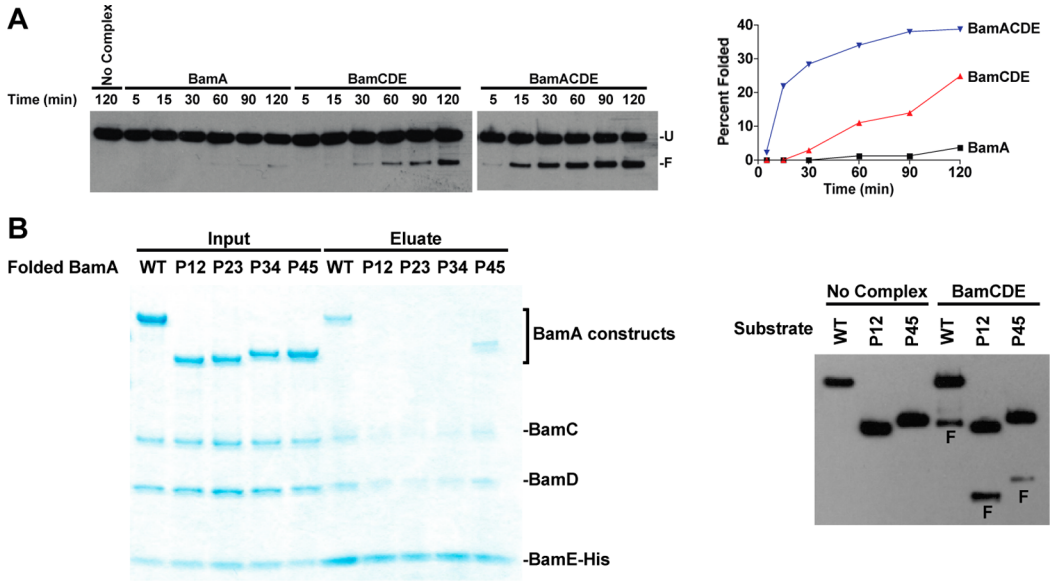

Figure 2. Bam lipoproteins are sufficient to facilitate BamA assembly. (A) The BamCDE lipoproteins facilitate FLAG-BamA assembly more effectively than BamA alone, but BamA and BamCDE function most effectively as a complex. The assembly of FLAG-BamA into proteoliposomes containing BamA, BamCDE, or BamACDE was monitored over the course of 2 h. Reactions were stopped at the indicated time points. Folding yields were determined by comparing the densities of the folded and unfolded bands and plotted. (B) The chimeric $BamA_{P12}$ substrate does not bind to BamCDE after it is folded (left), but these lipoproteins do facilitate its assembly (right). The FLAG-tagged wild-type, chimeric (P12, P23, and P34), and truncated (P45) BamA substrates were folded in detergent (0.5% LDAO) for 60 min; purified BamCDE-His_6 lipoproteins were then added, and the complexes were isolated by Ni-NTA affinity chromatography (left). Unfolded FLAG-tagged BamA substrates were added to empty liposomes or BamCDE proteoliposomes, and the folding reactions were stopped after 120 min (right) (F, folded FLAG-BamA construct).

1 M Tris (pH 8) and 2× SDS sample loading buffer as described in the previous section. The proteins in the input and these eluate samples were separated by SDS−PAGE and stained with Coomassie blue.

RESULTS

We began by identifying the minimal set of components that are required to assemble a BamA substrate *in vitro*. The fact that the OMP chaperones and some of the Bam proteins are nonessential suggests that they are not required for the assembly of all OMPs. We found that BamA can be assembled *in vitro* without a chaperone (Figure 1A,B). We diluted urea-denatured, FLAG-tagged BamA with or without SurA, a major periplasmic chaperone,[19−21] into proteoliposomes containing the Bam complex.[17,18] The reaction products were separated via seminative SDS−PAGE, and the folded and unfolded forms of the proteins were then visualized by immunoblotting with anti-FLAG antibodies. (*β*-Barrels do not unfold in SDS unless they are boiled; therefore, their folded and unfolded forms have different mobilities on SDS−PAGE. The FLAG tag on the substrate BamA distinguishes it from the untagged BamA in the complex.) The substrate did become less foldable in the absence of solubilizing factors (i.e., in Tris-buffered saline), and SurA maintained its folding-competent state. However, SurA could be functionally replaced by urea (Figure S1 of the Supporting Information). These results are consistent with *in vivo* measurements demonstrating that BamA levels do not decrease when *surA* is deleted.[22−25] Therefore, the BamA substrate can be delivered to the Bam complex in different ways without affecting its assembly on the machine. Accordingly, we proceeded with our *in vitro* analysis of the direct effects of the Bam complex components on this substrate in the absence of a chaperone.

We found that no specific Bam lipoprotein is required to assemble BamA *in vitro*; BamAB and BamACDE subcomplexes both assembled BamA into proteoliposomes (Figure 1C and Figure S2A of the Supporting Information).[17] The BamAB subcomplex is less effective, but it appears that BamB can at least partially substitute for BamCDE. Clearly, BamD is essential *in vivo*, while BamB is not; therefore, these proteins must have additional nonredundant functions that may relate to the assembly of other OMP substrates. Given that BamA is the only common component in the subcomplexes, we examined whether the functions of the lipoproteins are critical in the assembly mechanism or whether BamA alone is capable of assembling more BamA. We compared the activities of proteoliposomes containing just BamA or BamCDE to that of BamACDE proteoliposomes to determine if BamA functions cooperatively with the lipoproteins (Figure 2A and Figure S2B of the Supporting Information). Surprisingly, the unfolded BamA substrate assembled into proteoliposomes containing only the BamCDE lipoproteins more efficiently than into proteoliposomes containing only BamA. Therefore, the assembly of an unfolded BamA molecule does not require a preassembled BamA molecule in the membrane.

We considered an alternate explanation for the observed folding in the BamCDE proteoliposomes in which the folded BamA product might form a complex with BamCDE and thereby produce a more active assembly machine. We discounted this hypothesis because a BamA substrate that cannot bind to the lipoproteins after it is folded is assembled equally well by them (Figure 2B and Figure S3 of the Supporting Information). The periplasmic region of BamA contains five polypeptide transport-associated (POTRA) domains. The most C-terminal of these, P5, is adjacent to the *β*-barrel and known to bind to BamCDE.[7] We generated chimeric and truncated BamA substrates containing two

dx.doi.org/10.1021/bi400865z | *Biochemistry* 2013, 52, 6108−6113

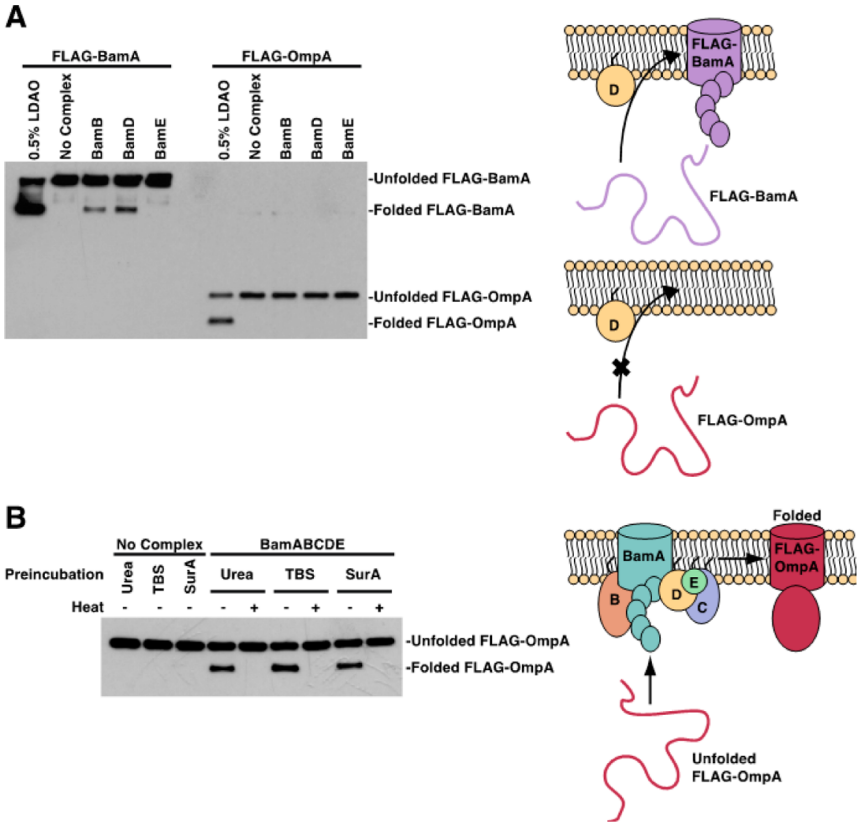

Figure 3. BamB and BamD are individually sufficient to facilitate BamA's self-assembly but are not sufficient to assemble OmpA. (A) Unfolded FLAG-BamA or FLAG-OmpA was added to a detergent solution or to proteoliposomes containing BamB, BamD, or BamE. Reactions were stopped after 120 min. (B) OmpA is assembled by the complete Bam complex without a chaperone. FLAG-OmpA was added directly to proteoliposomes or preincubated in TBS or a 10-fold excess of SurA as described for Figure 1B.

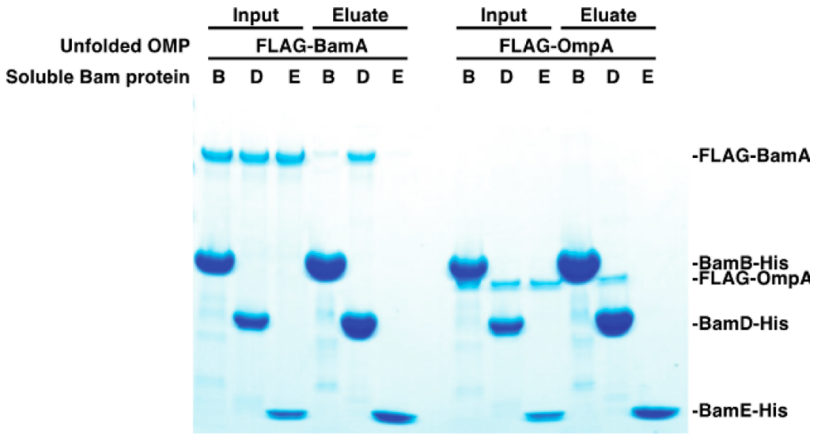

Figure 4. Certain Bam lipoproteins bind unfolded BamA and OmpA. Urea-denatured FLAG-BamA or FLAG-OmpA was diluted into a detergent-free solution containing a 10-fold molar excess of the indicated soluble, His-tagged Bam protein (lacking its N-terminal lipid anchor). Binding of the unfolded OMP to the Bam protein was then assessed by its ability to copurify by Ni-NTA affinity chromatography.

POTRA domains and the β-barrel domain. When the truncated substrate containing POTRA domains 4 and 5 is folded in detergent and then mixed with the BamCDE lipoproteins, it can be copurified with the lipoproteins; the chimeric BamA proteins containing other pairs of POTRA domains (P12, P23, or P34) do not copurify with the lipoproteins. Nevertheless, the BamCDE lipoproteins facilitate the assembly of the chimeric $BamA_{P12}$. We therefore favor a model in which the lipoproteins directly and independently facilitate the assembly of the unfolded BamA substrate (*vide infra*).

In vivo experiments have indicated that BamA assembly is facilitated by the Bam complex.[7,24] Our results do not contradict those studies; the fact that the BamACDE complex was more active than BamCDE clearly demonstrates that when BamA is preassembled in a complex with the lipoproteins it facilitates the assembly of more BamA. Given the difference in the kinetics of the BamABCDE- and BamCDE-catalyzed processes, the latter is unlikely to occur in a wild-type cell. However, by dissecting the Bam complex *in vitro*, we were able to observe the independent function of the BamCDE

dx.doi.org/10.1021/bi400865z | *Biochemistry* 2013, 52, 6108−6113

lipoproteins. It seemed possible that the lipoproteins might perform this same function in the context of the complete complex, and we therefore began to characterize how they assemble BamA to understand their mechanistic role.

We examined whether other OMPs can also be assembled by the lipoproteins alone or if BamA is unusual in this regard. We compared how the individual Bam lipoproteins affect the folding of BamA and OmpA, an abundant but nonessential OMP (Figure 3). Individually, BamB and BamD both facilitated BamA assembly *in vitro*, but BamE did not. (BamC could not be purified individually in a stable form and consequently was not examined.) Clearly, the lipoproteins must have an important, direct effect because BamA does not assemble efficiently into empty liposomes or into BamE proteoliposomes. BamB and BamD must share a common function that has a specific effect on the BamA substrate. In contrast, none of the lipoproteins was sufficient to fold OmpA, but this substrate was assembled if the Bam complex was present in the membrane (Figure 3 and Figure S4 of the Supporting Information).[26] Therefore, OmpA is not inherently unstable in the membranes used here, and we attribute the difference in the ability of BamA and OmpA to assemble to a difference in the properties of the substrates. BamB and BamD have a clear function in the folding process, but it is not sufficient to assemble OmpA.

We hypothesized that the common function of BamB and BamD relates to binding substrates at the OM as has been suggested by some crystal structures and cross-linking experiments.[27−33] We examined whether the lipoproteins interact directly with unfolded OMPs; urea-denatured BamA or OmpA was mixed with an excess of soluble, His-tagged BamB, -D, or -E and then affinity-purified. Soluble constructs of BamB, -D, and -E, which lack their N-terminal lipids, were used so that detergents could be omitted from the experiment to prevent folding of the substrates. BamA copurified with BamD-His, to a lesser extent with BamB-His, and not at all with BamE-His (Figure 4). Therefore, the lipoproteins likely facilitate the assembly of the BamA substrate by binding to its unfolded state. In that respect, they may act like other enzymes by stabilizing a transient or intermediate state in the reaction pathway, and accordingly, their function in assembling the substrate does not involve or require binding to the final product (the folded state of BamA) as indicated by the assembly of the $BamA_{P12}$ substrate described above.

However, this direct interaction between the unfolded substrate and the lipoproteins is not sufficient to produce folding on its own. When soluble BamB or BamD was added to empty liposomes, no folding of BamA was observed (Figure S5 of the Supporting Information), implying that the membrane localization or orientation of the lipoproteins matters. Furthermore, BamD bound unfolded OmpA, but in this case, binding was not sufficient to produce folding of the substrate OMP (Figures 3A and 4). OmpA does not partition into the membrane even if it is bound near it. BamB and BamD are not capable of completing OmpA's assembly alone, but simply binding unfolded BamA near the membrane is sufficient to facilitate this substrate's assembly. BamA may be unusual or unique in its ability to assemble in a manner independent of other components. We were able to exploit this property of BamA to observe the individual functions of BamB and BamD *in vitro*. This is an advantage of our *in vitro* system in that it allows dissection of an essential machine; we do not have to contend with the pleiotropic effects of mutations and deletions *in vivo* and can isolate the effects of individual components.

DISCUSSION

Here we have shown that BamB and BamD can bind unfolded substrates and that this function facilitates the assembly of BamA. These lipoproteins likely interact with the unfolded substrate in different ways, but both are capable of facilitating BamA assembly by localizing the unfolded substrate to the membrane. Although BamD can also bind unfolded OmpA, it is not sufficient to catalyze the assembly of this substrate *in vitro*. We attribute this difference in assembly requirements to the function of BamA. BamA may be able to assemble aided only by the lipoproteins because it performs some of the OMP assembly mechanism; the fact that it is conserved in all organisms may reflect its role in the later folding and insertion steps of β-barrel assembly. BamD alone cannot assemble OmpA because this substrate relies on a preassembled BamA to complete the later steps of its assembly.

Many OMPs have been shown to assemble spontaneously into lipid bilayers *in vitro*, but their ability to do so depends strongly on the lipid content of the artificial membranes.[26,34,35] *In vivo*, however, all OMPs must assemble into the same membrane. The inability of OmpA to assemble under the same conditions as BamA (i.e., into a membrane containing only BamB or BamD) suggests that the BamA substrate may possess some additional or unusual features. We propose that the structure of BamA in some way facilitates its own assembly such that it is less reliant on a preassembled Bam complex than other OMPs. This spontaneous assembly process is clearly much less efficient than the Bam complex-catalyzed process, but it provides an intriguing solution to the "chicken and egg problem". Perhaps in a primitive organism, an ancestral BamA protein assembled itself, and the other complex components later evolved to adapt BamA to assemble more and different types of other OMPs. In turn, BamA became more reliant on the other Bam components for its assembly, and the spontaneous process became comparatively less efficient and important. By creating an efficient catalyst for β-barrel assembly, it also became possible to segregate β-barrels to a single membrane by making the rate of their assembly into the membrane containing the Bam complex dramatically faster than that into an empty membrane.

By dissecting the Bam complex *in vitro*, we have identified a substrate binding interaction that appears to be important in BamA's assembly. Our next step is to establish whether inhibition of this binding event is sufficient to inhibit OMP assembly.

ASSOCIATED CONTENT

Supporting Information

Experimental procedures and five additional figures. This material is available free of charge via the Internet at http://pubs.acs.org.

AUTHOR INFORMATION

Corresponding Author

*E-mail: kahne@chemistry.harvard.edu. Phone: (617) 496-0208.

Funding

This work is supported by National Institutes of Health Grant AI081059.

Notes

The authors declare no competing financial interest.

■ ABBREVIATIONS

Bam, β-barrel assembly machine; OM, outer membrane; IM, inner membrane; OMP, outer membrane protein; DDM, *n*-dodecyl β-D-maltopyranoside; TCEP, tris(2-carboxyethyl)-phosphine; SDS, sodium dodecyl sulfate; LDAO, lauryldimethylamine-*N*-oxide; POTRA, polypeptide transport-associated.

■ REFERENCES

(1) Driessen, A. J., and Nouwen, N. (2008) Protein translocation across the bacterial cytoplasmic membrane. *Annu. Rev. Biochem. 77*, 643−667.

(2) Walter, P., and Johnson, A. E. (1994) Signal sequence recognition and protein targeting to the endoplasmic reticulum membrane. *Annu. Rev. Cell Biol. 10*, 87−119.

(3) Rapoport, T. A. (2007) Protein translocation across the eukaryotic endoplasmic reticulum and bacterial plasma membranes. *Nature 450*, 663−669.

(4) Hagan, C. L., Silhavy, T. J., and Kahne, D. (2011) β-Barrel Membrane Protein Assembly by the Bam Complex. *Annu. Rev. Biochem. 80*, 189−210.

(5) Wu, T., Malinverni, J., Ruiz, N., Kim, S., Silhavy, T. J., and Kahne, D. (2005) Identification of a multicomponent complex required for outer membrane biogenesis in *Escherichia coli*. *Cell 121*, 235−245.

(6) Malinverni, J. C., Werner, J., Kim, S., Sklar, J. G., Kahne, D., Misra, R., and Silhavy, T. J. (2006) YfiO stabilizes the YaeT complex and is essential for outer membrane protein assembly in *Escherichia coli*. *Mol. Microbiol. 61*, 151−164.

(7) Kim, S., Malinverni, J. C., Sliz, P., Silhavy, T. J., Harrison, S. C., and Kahne, D. (2007) Structure and function of an essential component of the outer membrane protein assembly machine. *Science 317*, 961−964.

(8) Eggert, U. S., Ruiz, N., Falcone, B. V., Branstrom, A. A., Goldman, R. C., Silhavy, T. J., and Kahne, D. (2001) Genetic basis for activity differences between vancomycin and glycolipid derivatives of vancomycin. *Science 294*, 361−364.

(9) Ruiz, N., Falcone, B., Kahne, D., and Silhavy, T. J. (2005) Chemical conditionality: A genetic strategy to probe organelle assembly. *Cell 121*, 307−317.

(10) Sklar, J. G., Wu, T., Gronenberg, L. S., Malinverni, J. C., Kahne, D., and Silhavy, T. J. (2007) Lipoprotein SmpA is a component of the YaeT complex that assembles outer membrane proteins in *Escherichia coli*. *Proc. Natl. Acad. Sci. U.S.A. 104*, 6400−6405.

(11) Reumann, S., Davila-Aponte, J., and Keegstra, K. (1999) The evolutionary origin of the protein-translocating channel of chloroplastic envelope membranes: Identification of a cyanobacterial homolog. *Proc. Natl. Acad. Sci. U.S.A. 96*, 784−789.

(12) Voulhoux, R., Bos, M. P., Geurtsen, J., Mols, M., and Tommassen, J. (2003) Role of a highly conserved bacterial protein in outer membrane protein assembly. *Science 299*, 262−265.

(13) Wiedemann, N., Kozjak, V., Chacinska, A., Schonfisch, B., Rospert, S., Ryan, M. T., Pfanner, N., and Meisinger, C. (2003) Machinery for protein sorting and assembly in the mitochondrial outer membrane. *Nature 424*, 565−571.

(14) Paschen, S. A., Waizenegger, T., Stan, T., Preuss, M., Cyrklaff, M., Hell, K., Rapaport, D., and Neupert, W. (2003) Evolutionary conservation of biogenesis of β-barrel membrane proteins. *Nature 426*, 862−866.

(15) Gentle, I., Gabriel, K., Beech, P., Waller, R., and Lithgow, T. (2004) The Omp85 family of proteins is essential for outer membrane biogenesis in mitochondria and bacteria. *J. Cell Biol. 164*, 19−24.

(16) Patel, R., Hsu, S. C., Bedard, J., Inoue, K., and Jarvis, P. (2008) The Omp85-related chloroplast outer envelope protein OEP80 is essential for viability in *Arabidopsis*. *Plant Physiol. 148*, 235−245.

(17) Hagan, C. L., Kim, S., and Kahne, D. (2010) Reconstitution of outer membrane protein assembly from purified components. *Science 328*, 890−892.

(18) Hagan, C. L., and Kahne, D. (2011) The reconstituted *Escherichia coli* Bam complex catalyzes multiple rounds of β-barrel assembly. *Biochemistry 50*, 7444−7446.

(19) Lazar, S. W., and Kolter, R. (1996) SurA assists the folding of *Escherichia coli* outer membrane proteins. *J. Bacteriol. 178*, 1770−1773.

(20) Rouviere, P. E., and Gross, C. A. (1996) SurA, a periplasmic protein with peptidyl-prolyl isomerase activity, participates in the assembly of outer membrane porins. *Genes Dev. 10*, 3170−3182.

(21) Sklar, J. G., Wu, T., Kahne, D., and Silhavy, T. J. (2007) Defining the roles of the periplasmic chaperones SurA, Skp, and DegP in *Escherichia coli*. *Genes Dev. 21*, 2473−2484.

(22) Vertommen, D., Ruiz, N., Leverrier, P., Silhavy, T. J., and Collet, J. F. (2009) Characterization of the role of the *Escherichia coli* periplasmic chaperone SurA using differential proteomics. *Proteomics 9*, 2432−2443.

(23) Bennion, D., Charlson, E. S., Coon, E., and Misra, R. (2010) Dissection of β-barrel outer membrane protein assembly pathways through characterizing BamA POTRA 1 mutants of *Escherichia coli*. *Mol. Microbiol. 77*, 1153−1171.

(24) Tellez, R., Jr., and Misra, R. (2011) Substitutions in the BamA β-barrel domain overcome the conditional lethal phenotype of a Δ*bamB* Δ*bamE* strain of *Escherichia coli*. *J. Bacteriol. 194*, 317−324.

(25) Denoncin, K., Schwalm, J., Vertommen, D., Silhavy, T. J., and Collet, J. F. (2012) Dissecting the *Escherichia coli* periplasmic chaperone network using differential proteomics. *Proteomics 12*, 1391−1401.

(26) Patel, G. J., and Kleinschmidt, J. H. (2013) The Lipid Bilayer-Inserted Membrane Protein BamA of *Escherichia coli* Facilitates Insertion and Folding of Outer Membrane Protein A from Its Complex with Skp. *Biochemistry 52*, 3974−3986.

(27) Noinaj, N., Fairman, J. W., and Buchanan, S. K. (2011) The crystal structure of BamB suggests interactions with BamA and its role within the BAM complex. *J. Mol. Biol. 407*, 248−260.

(28) Albrecht, R., and Zeth, K. (2011) Structural basis of outer membrane protein biogenesis in bacteria. *J. Biol. Chem. 286*, 27792−27803.

(29) Heuck, A., Schleiffer, A., and Clausen, T. (2011) Augmenting β-augmentation: Structural basis of how BamB binds BamA and may support folding of outer membrane proteins. *J. Mol. Biol. 406*, 659−666.

(30) Sandoval, C. M., Baker, S. L., Jansen, K., Metzner, S. I., and Sousa, M. C. (2011) Crystal Structure of BamD: An Essential Component of the β-Barrel Assembly Machinery of Gram-Negative Bacteria. *J. Mol. Biol. 409*, 348−357.

(31) Kim, K. H., and Paetzel, M. (2011) Crystal structure of *Escherichia coli* BamB, a lipoprotein component of the β-barrel assembly machinery complex. *J. Mol. Biol. 406*, 667−678.

(32) Kim, K. H., Aulakh, S., and Paetzel, M. (2011) Crystal structure of β-barrel assembly machinery BamCD protein complex. *J. Biol. Chem. 286*, 39116−39121.

(33) Ieva, R., Tian, P., Peterson, J. H., and Bernstein, H. D. (2011) Sequential and spatially restricted interactions of assembly factors with an autotransporter β domain. *Proc. Natl. Acad. Sci. U.S.A. 108*, E383−E391.

(34) Kleinschmidt, J. H. (2006) Folding kinetics of the outer membrane proteins OmpA and FomA into phospholipid bilayers. *Chem. Phys. Lipids 141*, 30−47.

(35) Burgess, N. K., Dao, T. P., Stanley, A. M., and Fleming, K. G. (2008) β-barrel proteins that reside in the *Escherichia coli* outer membrane in vivo demonstrate varied folding behavior in vitro. *J. Biol. Chem. 283*, 26748−26758.